

A Protocol Towards Simulating an Image-Based, Motion-Capture-Driven Personalized Musculoskeletal Knee Model

By

Omar Mohammed Abdulrahman Bahig (s3067106)

Graduation Committee:

- Prof.Dr.Ir. N.J.J. Verdonschot (UT)
- Dr.Ir. P. Tzanetis (UT)
- Dr. Erik Prinsen (RRD)

To obtain the degree of Master of Science
in BME at university of Twente

July 15th, 2024

**UNIVERSITY
OF TWENTE.**



TABLE OF CONTENT

List of figures	iii
List of tables.....	vi
Abstract.....	vi
1. Introduction	1
1.1 Rationale of the study	2
1.1.1 Personalization of Knee MS Model	2
1.1.2 Contact Forces and FE for Personalized Cartilage	2
2. Methodology	4
2.1 Data collection.....	4
2.2 MRI Scanning.....	4
2.3 MRI Segmentation	5
2.4 Gait lab	6
2.5 Personalizing the MS Model	9
2.5.1 Bone Morphing	9
2.5.2 Subject Specific Reference Frames	13
2.6 Motion Capture.....	15
2.6.1 Static sub-model.....	16
2.6.2 Dynamic sub-model.....	19
2.7 Inverse Dynamic Model.....	21
2.7.1 Contact Model.....	21
2.7.2 Ligament Model	22
3. Discussion	23
4. Conclusion.....	27
References	28
Appendices	37
Appendix A: C3D Files and Respective Activities.....	37
Appendix B: MoCap Markers' label renaming	38
Appendix C: Template Model	39
Appendix D: Femur Landmarks.....	40
Appendix E: Tibia and Patella Landmarks	41
Appendix F.1: Right Knee Morphing.....	43
Appendix F.2: Left Knee Morphing (Mirrored)	47
Appendix G: Rotational Error (MATLAB)	51
Appendix H: Extracting Landmarks.....	52
Appendix I: Morphing Errors	53
Appendix J: Other.....	54
Appendix K: Workflow Tracing	56

List of figures

Figure 1 MRI acquisition techniques (A: fat suppression, B: fat-saturated) of the knee, in coronal plane. Adopted form (9).....	2
Figure 2 General workflow of TopTreat project. It involves Musculoskeletal and Finite Element modelling and integration. In MS modelling, the model is personalized to the subject's bone geometries and movement based on MRI scans and gait lab recorded motion. Knee kinematics and kinetics are evaluated for four groups (healthy, meniscus patients with and without prosthesis, and transtibial bone anchored amputees). The outcomes include knee flexion, tibiofemoral and patellofemoral moments and forces. They then serve as inputs to the finite element model to estimate the cartilage mechanical responses (max principal stress, and shear strain) which to be compared among the four groups.	3
Figure 3 Model workflow towards Musculoskeletal personalization in AnyBody modelling software. The Two blocks in green (knee scans and C3D files) served as the input to the modeling software. MRI knee segmented scans were used to morph the generic model bone to the geometries of the pilot subject's bone while motion capture c3d files were used to drive the MS model and optimize its parameters. The numbered blocks represent the sequence followed in this protocol toward the personalization of the Musculoskeletal model.	4
Figure 4 MRI scans of the pilot subject. The sequence t2_de3d_we (Left) is a T2-weighted, double echo steady state water excitation sequence which was used for segmenting the knee structures as described in 2.3. PD sequence (Right) is a proton density sequence that can identify knee bones. Note that PD sequence was not used for the segmentation because the AI model was not trained with this sequence. However, it was presented here for the purpose of showing what this sequence captures.5	5
Figure 5 Pilot subject's MRI scanning and segmented structures used in the workflow. On the left, the PS lied down inside an MRI machine and underwent partial scanning of her right knee. The scan displayed on the screen is the t2_de3d_we_sag_p2_iso sequence. On the right, the bones (proximal tibia distal femur,) and the cartilages of the tibia, femur, and patella as well as the menisci were extracted and segmented from the MRI scans. Note that the Patella bone was not segmented because the AI model training datasets did not include the patella bone.	6
Figure 6 Retroreflective markers affixed to the pelvis and right lower extremity (Left: Anterior view, right: Posterior view). Four markers were placed on the pelvis, and three-cluster markers on the shank and thigh. Two markers were affixed to the lateral and medial knee epicondyles and malleoli. Finally, five markers were placed on the foot segment.	7
Figure 7 The pilot subject in the motion capture lab (Vicon system) in RRD center. Red circle: infrared high-speed camera, yellow circle: Force plate, white circle: EMG electrodes, blue circle: retroreflective marker.	7
Figure 8 Gait lab activities protocol: After attaching EMG sensors, and markers, IR (infra-red) cameras were used to capture the movement and force plates to record the ground reaction forces. (A) The PS walked at selected pace with the feet falling within the borders of the force plate. (B) Stepping off from a block of 15cm height. PS stood in upright position and landed her right/left foot within the borders of the force plate placed in front of the block. (C) The PS performed a squatting exercise, with hands placed in 90 degrees at the should joint to avoid blocking the markers on the pelvis, to a comfortable depth while maintaining both feet in contact with the force plates.	8
Figure 9 Femur and tibia meshes. (A) illustrates an example of a femur bone mesh with low number of vertices (797 vertices). The edges of this mesh appear blocky and faceted. (B) shows the pilot subject's femur and tibia bone meshes with large number of vertices (66848, and 50508, respectively). The surface details are well captured, and the edges are not blocky or faceted.....	9

Figure 10 Pre-morphing and RBF interpolation morphing scheme for partial femur bone morphing. Blue femur is the original source bone, white femur represents the pilot subject’s distal femur bone. Green points on the blue femur represents the selected landmarks on the source bone while the purple points were selected on the target bone. Red and green femur bones are the morphed source bone with affine and RBF transformations, respectively. The last picture on the right represents the final result of the morphing process (Source bone morphed with RBF transformation). 10

Figure 11 Selected bony landmarks for femur partial morphing (Left: source bone, right: target bone). The distal landmarks were used for morphing the source bone to the pilot subject’s bone while the proximal points on the source bone were used to regulate the morphing at the proximal region and ensure its preservation. Appendix D contains the picked-points file that can be loaded in MeshLab to visualize the landmarks. 11

Figure 12 Tibia partial morphing following the same method used for femur partial morphing (A), and patella morphing with RBF interpolation scheme only (B). Appendix E contains the picked-points files to visualize the landmarks in MeshLab. 12

Figure 13 Distal femur, proximal tibia, and patella subject specific morphing. White bones represent the target bone, and gold bones indicate the morphed source bones. Note that target bones were drawn to visualize how well the morphing was performed by comparing it with the bone morphing performed in the external script as described above in this section. 12

Figure 14 Landmarks with maximum morphing error for each segment. Green bone represents the morphed source bone while white bone represents the pilot subject’s bone. Yellow points represent morphed source landmark while purple points represent target landmark. In A, landmark E (Posterior medial resection) on the femur has the maximum morphing error of 4.248mm. In B, landmark J (Anterior tibia) has the maximum morphing error of 6.404mm on the tibia. Finally, in C, landmark C (Lateral border) has the maximum morphing error of 5.13mm. 13

Figure 15 Knee joint coordinate systems. X axis represents the anteroposterior axis, Y axis denotes the Superioinferior axis, and the z axis represents the mediolateral axis. Blue frame refers to the patella coordinate system, and green frame denotes the femur coordinate system based on the hip center of the generic bone. Red frame represents the coordinate system of the tibia with the generic bone ankle joint center while yellow frame represents the coordinate of the tibia with the use of the malleoli markers’ location. Note that there is an error of 2.96 degrees about z axis between the red and yellow frame while the error is negligible about x and y axes. 15

Figure 16 MS models’ MoCap workflow and studies; Motion and Parameter Identification (MPI) and Inverse Dynamic. MPI study utilized two sub-models (static and dynamic) to optimize segment length, extract markers local coordinates (location relative to the respective segment) and drive the model. The final output from this model is the joint (hip, knee and ankle) angles. These joint angles are then used to drive the inverse dynamic model in the last block of the workflow (inverse dynamic model). Note that each color-coded blocks are inputs to the respective white block. 16

Figure 17 Static Model with morphed knees and the marker dataset used for pelvis, thigh, shank, and foot optimization (Left: anterior view, right: posterior view). These markers were used because of their placement on distinct bony prominences. These markers were used to optimize the pelvis and lower leg bones (Thigh, shank, and foot). Note that there were no markers attached to the upper body. These segments were scaled by the scaling law (Uniform scaling). 17

Figure 18 Optimization of the foot length. (A) The RToe marker. (B) Foot length after the optimization resulted in length of 15.14cm. This did not seem reasonable because the participant foot length was measured at 22cm (C) Foot length after excluding foot length from the optimization which was set to the measured length (22cm). 18

Figure 19 Knee alignment optimization. (A) The neutral posture of the model. (B) the perturbation applied at the knee joint by setting AxisRot to 11 degrees of Valgus (B.1) or 11 degrees of Varus (B.2)

before running the optimization study. (C) The final alignment of the knee after the optimization was performed. AxisRot of the right knee was optimized to 1.38 degrees and 0.39 degrees for the left knee in both cases (varus or valgus perturbation)..... 19

Figure 20 Dynamic trials of the activities recorded in the gait lab that were used to drive the model. (Left) walking at selected pace. (Middle) stepping off from a 15cm-high block. (Right) squatting to a preferred depth. Note that this sub-model contains markers on the thigh and shank and the configuration of the force plate of the left leg..... 20

Figure 21 Contact surfaces configuration on the left knee. (A) Contact surfaces were defined as bone offsets. Bone surfaces for each contact model were defined (colored surfaces). Then, an offset that represented the cartilage thickness was used to scale these bones, so they signify cartilages. (B) Contact surfaces were defined based on the segmented cartilages. Note that the patella cartilage was not used because the patella bone used within this workflow belongs to another subject (as described in 2.3) whose cartilage was not segmented. However, it was used for the purpose of building the workflow. 22

Figure 22 Discrepancy (less overlapping) between generic morphed bone (Gold) and the target bone (transparent white) in tibia bone morphing. Yellow rectangle shows the region where discrepancy was the highest mainly because no landmarks were selected for the morphing process. As a result, the three muscle attachments were not morphed. The red rectangle locates the insertion points of the biceps femoris muscles on the fibula head. This region was not morphed as well because fibula bone was not segmented from the MRI scan. 23

Figure 23 Improving the morphing accuracy with additional landmark. (A) The maximum morphing error was recorded at landmark J at 6.40mm. (B) Adding one landmark (highlighted within the red square) improved the accuracy of morphing. The maximum morphing error (6.40mm) which was observed at landmark J dropped to 5.59mm after adding the landmark. The new maximum error was recorded at 5.72mm but was located at another landmark (landmark H). 24

Figure 24 Contact surfaces configuration over the tibia plateau. (A) Contact surfaces (bone offsets/ cartilages) inconsistency over the lateral tibial plateau due to the limited number of landmarks (11 landmarks). (B) Contact surfaces consistency after adding a marker at the anterior edge of the lateral tibia region. This landmark improved morphing accuracy; thus, may result in better contact surfaces consistency. 24

Figure 25 Glue&Cut method to improve partial morphing. (A) Target bone (green) is glued to the source bone (yellow). In a software like 3D slicer, both bones can be loaded. The target bone is then transformed to the proximal end of the source tibia bone. Once both bones are aligned properly (Glue), the user can identify where to cut the source bone. (B) After gluing the target bone, the user can cut the source bone with the help of the target bone edges. The result of this method is two bones having the same topology. Then the user can use STL_Vertices in AnyBody modelling system to extract the corresponding landmarks. 25

Figure 26 Scanning the regions of interest of the lower leg. A localizer sequence can be used to select the field of view (the lower leg). Then, femur head can be scanned first, the femur shaft can be skipped, and the knee joint can be scanned. Note that it is important to maintain the same scanning setup and field of view; otherwise, scans will be distorted. The anthropometric distance can be maintained between, for instance, the femur head and the distal femur bone with the same setup and localizer sequence. Finally, the tibial shaft can be skipped, and the distal tibia can be scanned similar to the femur head. Eventually, the regions within the yellow rectangles will be output of the MRI scan which captures the missing data needed in this study's protocol. 26

Figure 27 Tibia landmarks used for partial tibia morphing. Left: Landmarks selected on the source bone, right: landmarks selected on the target bone..... 41

Figure 28 Patella landmarks for patella morphing; left (anterior view), right (posterior view)..... 42

List of tables

Table 1 Biomechanical Phenotypes of KOA.....	1
Table 2 MRI sequences that capture the structures of interest: bones, cartilages, and meniscus.	5
Table 3 Min, max, and mean morphing errors between the morphed bone landmark to the corresponding target bone landmark for the femur, tibia, and patella bones.....	13
Table 4 Rotational error of the tibia coordinate systems between the rotational matrices of the coordinate systems created with the malleoli marker's location (A) and the one with created with the generic bone the ankle joint center (B).....	14
Table 5 Marker location and the respective name it should be assigned with for AnyBody software integration.	38
Table 6 List of landmarks used for partial femur morphing based on Figure 9	40
Table 7 List of landmarks used for partial tibia morphing.	41
Table 8 List of landmarks used for patella morphing.....	42

Abstract

There remains no established treatment for knee osteoarthritis (KOA), underscoring the necessity for personalized musculoskeletal models to tailor treatment approaches. In this assignment, a workflow that would enable simulating an image-based, motion-capture-driven personalized musculoskeletal (MS) knee model to estimate knee joint contact forces is presented, as the initial stage of the TopTreat project, which then can be integrated with a Finite Element model for personalized cartilage testing and treatment. Initially, a healthy female underwent a partial MRI scanning exclusively at her right knee (proximal tibia, distal femur, and patella) and subsequently three gait activities (walking, stepping off, and squatting) were assessed in a motion capture lab. Bones, cartilages, and menisci were segmented from the MRI images, and the generic bone and muscle architecture of the MS model were morphed into the segmented bones. Coordinate systems of the femur, tibia and patella were defined and personalized to the subject's bone geometries to estimate knee rotational and translational kinematics after driving the model with the recorded gait lab motion. Finally, three contact models were defined using either bones as offsets or the segmented cartilages to estimate the contact forces at the medial and lateral tibiofemoral and patellofemoral compartments. It was found that the maximum morphing error between the source morphed vertex and the target vertex were reported at 6.404mm, 5.130mm, and 4.248mm for the tibia, patella and femur, respectively. Additionally, an error of about 3° was found between the tibia coordinate systems created with the ankle center of the generic model and with the malleoli markers' location. The optimization process appeared sensitive to the marker's location on the model especially at the foot segment as it was optimized to 15cm while the subject's foot length was measured at 22cm. The realization of this workflow revealed the difficulty and complexity of using partial bones to personalize musculoskeletal models mainly due to the absence of the proximal femur and distal tibia scans. Ideally, information at these two regions are required for more reliable personalization. Eventually, it is crucial to validate the model produced by this workflow before utilizing it for the TopTreat project.

Keywords

Medical imaging, motion capture, musculoskeletal personalization, joint and muscle forces, and knee kinematics

1. Introduction

Osteoarthritis (OA), also termed deteriorating joint disease, primary OA, wear-and-tear arthritis, stands as a significant contributor to disability on a global scale (1,2). The knee emerges as the most impacted joint by OA (3). This condition leads to a gradual onset of pain, stiffness, instability, and declining joint function and mobility, all of which can profoundly affect an individual's quality of life and their ability to participate in physical and societal activities (4). Knee OA (KOA) predominantly affects individuals aged 65 and above, with a prevalence rate in the US reaching 33.6% (equivalent to 12.4 million people) (5). Women exhibit a higher prevalence rate at 42.1% compared to men at 31.2% (6). A study examining the impact of OA in the Nordic region revealed a 43% increase in prevalent OA cases between 1990 and 2015 (7). KOA represents a degenerative joint ailment (1,2,8), resulting in joint discomfort and constraints in functionality which collectively exert considerable detrimental impacts on an individual's quality of life (2,4,9,10). While inflammatory and biomechanical processes affecting the entire organ play significant roles, KOA is also influenced by a combination of factors (11). These encompass innate immune responses, systemic inflammatory agents, synovitis, lower limb alignment such as genu valgum and genu varum, joint morphology etc. (12–14). Additionally, excessive weight placed on the knee can detrimentally impact the functional capability of the knee joint (2). Irrespective of the underlying mechanism, KOA entails damage to articular cartilage, the formation of bony osteophytes, and sclerosis of the subchondral bone (15).

It is worth noting that several biomechanical variables have been investigated in the literature as patients with KOA exhibit altered biomechanics. **Table 1** shows that most of the studies have demonstrated that individuals with tibiofemoral KOA typically exhibit increased knee adduction angles and, moreover, a femur that is positioned more medially relative to the tibia (16). As patients with KOA often deviate from the norm in terms of biomechanics, and with increasing focus on phenotyping these patients, there arises a greater demand for personalized musculoskeletal (MS) models that account for individual anatomy and gait characteristics. These models aim to accurately capture variations in kinematics and kinetics, thereby facilitating investigations into pathologies such as the progression and treatment of KOA (9).

Table 1 Biomechanical Phenotypes of KOA

Biomechanical Variable	Parameters	Studies
Knee Adduction Moment (KAM)	Peak KAM	(3,17–19)
	KAM Impulse	(17,20,21)
	Cumulative Knee adduction load (CKAL)	(20,21)
Knee Abductor Moment (KADM)	KADM	(22)
Medial Contact Force (MCF)	Peak MCF	(3,23,24)
	MCF impulse	(3,25)
	Max MCF loading rate	(24)
Knee Flexion Moment (KFM)	KFM	(20,26–28)
	Peak KFM impulse	(29–31) (31)
Knee Extension Moment (KEM)	KEM	(22,28)
Internal & External Rotational Moment (IERM)	IERM	(22)
Knee Flexion (Excursion)	Excursion	(22,28)
Quadriceps Weakness (QW)	QW	(19,24)
Knee Alignment	Varus/Valgus	(32–34)

The extent of MS personalization attainable varies relying on the quantity of subject data accessible (17). For instance, bone geometrical dimensions can be modified linearly based on the subject's anthropometric measurements or by segmenting bone geometry from medical imaging data (19). CT scans and various MRI sequences are being developed to optimize visualization of the distinct structures within the lower limb and knee (23,29). For example, to effectively differentiate between cartilage, and bone, it is necessary to utilize fat suppression (**Fig. 1.A**) or fat-saturated (**Fig. 1.B**). Such scans have been instrumental in subject-specific musculoskeletal development, which are utilized to estimate joint loads (9). In the context of MS modelling, it is recognized that the outcomes of such models are highly sensitive to input variables, particularly concerning tendon slack length, nominal muscle fiber length, muscle-tendon moment arm, and maximal isometric muscle force (30).



Figure 1 MRI acquisition techniques (A: fat suppression, B: fat-saturated) of the knee, in coronal plane. Adopted from (9)

MS knee joint models offer a method to explore the kinematics, kinetics of the knee joint, and soft tissue stresses, avoiding the ethical considerations associated with invasive measurements (32). These models involve personalizing bones, soft tissues and estimating the internal loading conditions experienced by body structures during specific movements (15). Eventually, they enable the estimation of contact forces and kinematics at the knee joint, which may be impractical to achieve within a Laboratories setting (35). However, given that many methods and models have been applied to total knee arthroplasty (TKA) patients (36,37) and/or healthy subjects (38–42), there exists a gap in knowledge regarding the customization of MS models for those in the early to advanced stages of KOA that needs to be addressed.

1.1 Rationale of the study

1.1.1 Personalization of Knee MS Model

Each patient with knee osteoarthritis (OA) presents distinctive characteristics that are challenging to fully understand when applying regular clinical protocols (43,44). There remains no definitive intervention for this disease. It is widely believed that personalized methods to diagnosis and treatment could significantly enhance the quality of healthcare services, leading to better treatment outcomes and increased patient satisfaction (45). Patient-specific MS models can bridge the gap between diagnosis and treatment of MS diseases by providing quantitative and objective means to accurately determine the underlying biomechanical conditions. These models can also lead to the development of modified treatment plans without the need to consider invasive methods (9). In the TopTreat project, continuous investigations of KOA will be conducted intermittently, necessitating a safe imaging method. CT scan deemed unsuitable given the high radiation doses associated with it. A study reported that limiting improper use of CT scanning and reducing the level of radiations are the key component for patient safety (46); instead, MRI scans are preferred due to their safe application. However, full scanning of the lower limb compromise the resolution of the scan. Consequently, this study is considering MRI scans focused solely on the knee region, specifically the proximal tibia, distal, femur and patella, to personalize the musculoskeletal (MS) model. Additionally, the study examines the feasibility of utilizing motion capture markers placed exclusively on the lower extremity.

1.1.2 Contact Forces and FE for Personalized Cartilage

MS and finite element (FE) modelling are effective tools for studying how joints move and bear weight (8). They also help understand the mechanical effects on the cartilage, like stress and strain (47–57). Research indicates that specific mechanical reactions at the tissue level are crucial in the occurrence and progression of KOA (50,58–60). Therefore, at the tissue level, precise assessments of mechanical reactions are crucial for anticipating disease progression and formulating plans for rehabilitation (61–63). In recent years, various integrated approaches combining musculoskeletal (MS) and finite element (FE) modelling pipelines (**Fig. 2**) have emerged (47,55,56,64). Within a multiscale MS-FE modelling workflow, as the endpoint goal was of this study, the initial step involves estimating muscle forces, and joint kinetics (i.e., contact forces), and joint kinematics (8) utilizing MS modelling software (i.e., AnyBody). Subsequently, the estimates serve as inputs to the FE model for cartilage testing. The ultimate application is to feed FE with contact forces of the knee for cartilage for personalized cartilage testing. However, in this study, we only focused on the personalization and not FE. This step will be carried out in the future.

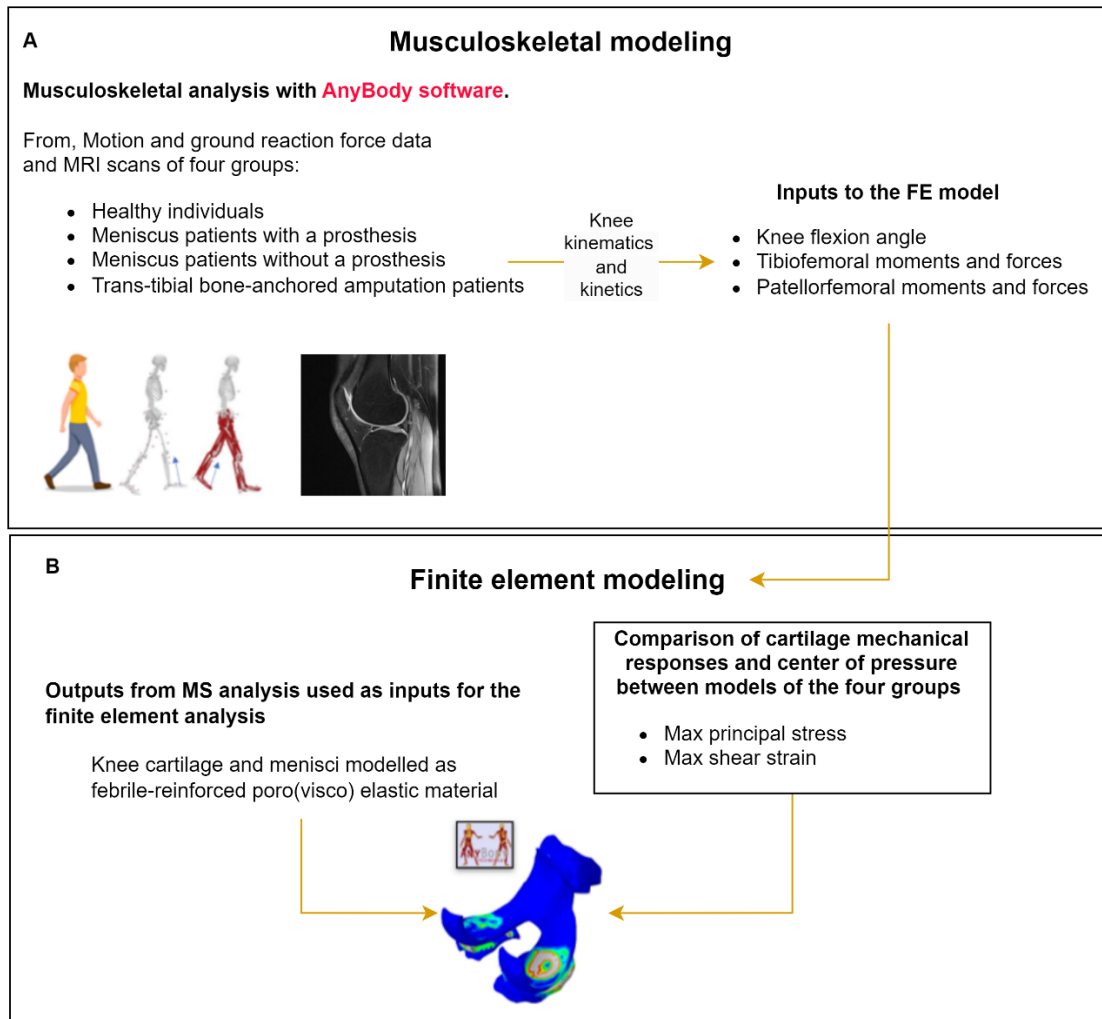


Figure 2 General workflow of TopTreat project. It involves Musculoskeletal and Finite Element modelling and integration. In MS modelling, the model is personalized to the subject's bone geometries and movement based on MRI scans and gait lab recorded motion. Knee kinematics and kinetics are evaluated for four groups (healthy, meniscus patients with and without prosthesis, and transtibial bone anchored amputees). The outcomes include knee flexion, tibiofemoral and patellofemoral moments and forces. They then serve as inputs to the finite element model to estimate the cartilage mechanical responses (max principal stress, and shear strain) which to be compared among the four groups.

Therefore, the main objective of this assignment is to critically describe the various steps of the workflow that would enable simulating an image-based, motion-capture-driven personalized musculoskeletal knee model based on partial femur and tibia MRI bone scans as the initial stage of the TopTreat project.

2. Methodology

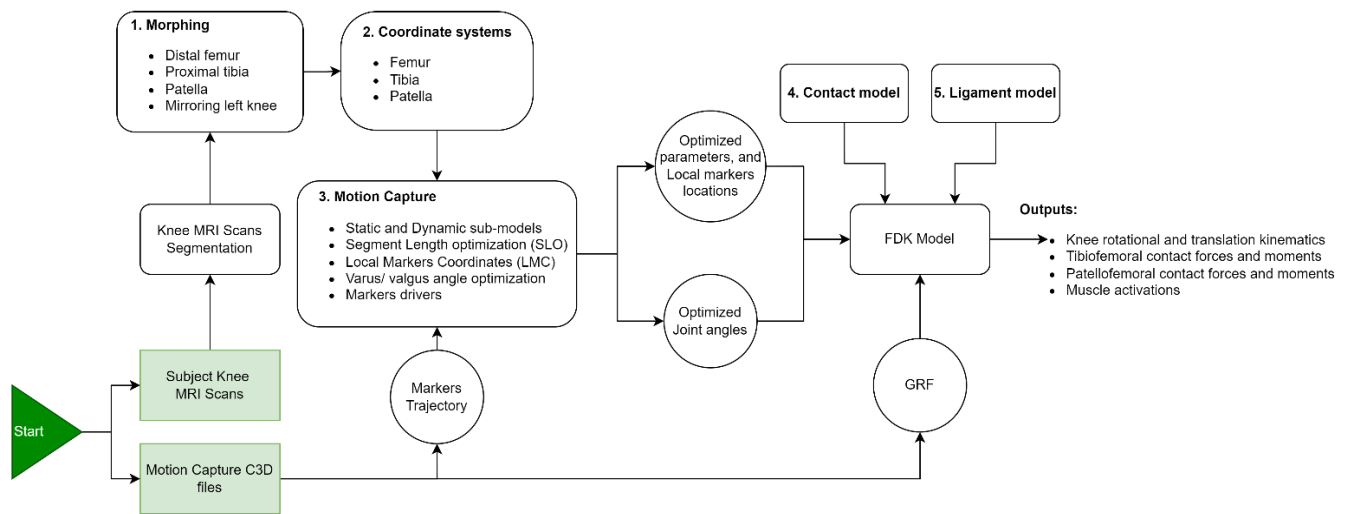


Figure 3 Model workflow towards Musculoskeletal personalization in AnyBody modelling software. The Two blocks in green (knee scans and C3D files) served as the input to the modeling software. MRI knee segmented scans were used to morph the generic model bone to the geometries of the pilot subject's bone while motion capture c3d files were used to drive the MS model and optimize its parameters. The numbered blocks represent the sequence followed in this protocol toward the personalization of the Musculoskeletal model.

2.1 Data collection

A healthy pilot subject (PS) with no knee injuries or complains (body mass 70 kg, height 1.75m, age 28 years) was voluntarily recruited for this feasibility study. Permission for the study was granted by the BMS ethical committee affiliated with the University of Twente (UT), located in the Netherlands. A consent form that contains information about the study, what measurements to be performed, the risks involved and how her data will be processed and stored was signed by the participant and saved in OneDrive/TopTreat/ Inform consent file).

2.2 MRI Scanning

The participant had MRI scanning of her right knee, conducted using a Siemens Magnetom Aera 1.5T MRI machine at the TechMed facility, University of Twente. Detailed knee joint MRI scanning requires knee recoil. The recoil enables a high-resolution scanning of the knee and provides a comprehensive view of the internal and external structures (e.g., cartilage and bone). However, this tool was not available in TechMed Center. Therefore, for the purpose of finding out the best MRI sequence(s) that captures the structures of interest (proximal tibia, distal femur, and patella bones, their cartilages, medial and lateral meniscus), nine sequences were visually explored. The sequences, their settings, can be found in the log file available in the "OneDrive/TopTreat/Dataset/Pilot study (healthy subject)/jgreve-20240315_083447" folder. The OneDrive can be accessed through the following link [TopTreat](#).

Eventually, three main sequences (**Table 2**) and their respective scans were saved. They can be found in the same folder as the log file. The localizer sequence was initially performed to identify the planes and the field of view for the other sequences. The t2_de3d sequence appeared to be effective at detecting cartilage and meniscus, while the Pd_space sequence seemed to be particularly good at detecting bones (**Fig. 4**). However, t2_de3d_we_sag_p2_iso sequence only was used for the segmentation by Radboud UMC as described in 2.3. The given name t2_de3d_we had indications of the type of sequence used; t2 signifies T2 weighted magnetic value of the tissue (the liquid appears bright); de3d specified the sequence type; de is an abbreviation for DESS (Double Echo Steady State), 3d implies 3D-volume acquisition; and _we indicated water excitation where fat is suppressed in the image.

Table 2 MRI sequences that capture the structures of interest: bones, cartilages, and meniscus.

Settings	Localizer_tra	t2_de3d_we_sag_p2_iso	PD_Space_Sag_P2_iso_256
Voxel size	0.7×0.7×6.0mm	0.6×0.6×0.6 mm	0.6×0.6×0.6mm
Slice thickness	6.0mm	0.64 mm	0.60mm
TR (Repetition time)	7.7ms	19.44 ms	1200ms
TE (Echo time)	3.28ms	7.02 ms	33.0ms



Figure 4 MRI scans of the pilot subject. The sequence t2_de3d_we (Left) is a T2-weighted, double echo steady state water excitation sequence which was used for segmenting the knee structures as described in 2.3. PD sequence (Right) is a proton density sequence that can identify knee bones. Note that PD sequence was not used for the segmentation because the AI model was not trained with this sequence. However, it was presented here for the purpose of showing what this sequence captures.

2.3 MRI Segmentation

A network, nnUNetv2 (65), was developed by Radboud UMC and trained based on 2 datasets, OAI-ZIB and imorphics. The two datasets can be found in "OneDrive/TopTreat/Dataset/Segmentations/nnUNet_predictions". The scans in these datasets were all based on DESS (Double Echo Steady State) sequence. The dataset involved data that was manually segmented by specialists which then was used to train the model. For the segmentation, de3d_we_p2_iso sequence was used because the trained data contained de3d (DESS) sequences only. This sequence was utilized for segmenting tibia bones, the femur and the cartilages of the tibia, femur, and patella, and the menisci; however, the patella bone could not be segmented due to its absence in the training datasets (**Fig. 5**). Another patella bone (i.e., patella bone of the Grand challenge model) was used for the purpose of completing the workflow. Therefore, manual segmentation should be carried out for patella segmentation. It is important to note that Pd_space sequence was tested, but it did not yield any useful results.

To start with the segmentation, the DICOMs files of the de3d_we_p2_iso sequence were transformed to .mha files before being processed by the network, which output a .mha mask containing the structures it found. The segmentation process followed a pipeline that is able to segment knee bones and cartilages (66). The pipeline involves a series of CNN (Convolutional Neural Networks) and SSM (Statistical Shape Models) steps that produces 3D segmentation masks for the femoral and tibial bones. Although the DESS sequence is not dedicated to bone segmentation, the model's pipeline was powerful to detect bones masks and successfully segment them. These masks then outline the desired region(s) for subsequent segmentation of the cartilage through 3D CNNs. The detected structures were exported in STL format and saved in "OneDrive/ TopTreat/ Datasets/ Segmentations/ STLs".

In the future, it would be advantageous to expand the model to perform segmentations using additional sequences. The T1 fat suppressed (T1FS) and/ or Proton Density (PD) sequences are particularly promising, as each highlights different structures more effectively to the human eye. Although an AI model may not require multiple sequences to detect body structures, incorporating PD and T1 sequences alongside de3d is beneficial if automatic segmentation fails and manual checks or adjustments are necessary. This was realized in the current workflow because the model did not detect the patella bone, necessitating manual segmentation. Therefore, integrating data

from PD and T1 sequences to retrain the model could enhance its segmentation capabilities. For example, sequences that clearly visualize bone structures can be used to segment all bony structures, including the patella. Similarly, sequences like de3d can be employed to segment cartilages and the meniscus, as the model is already trained to do so.

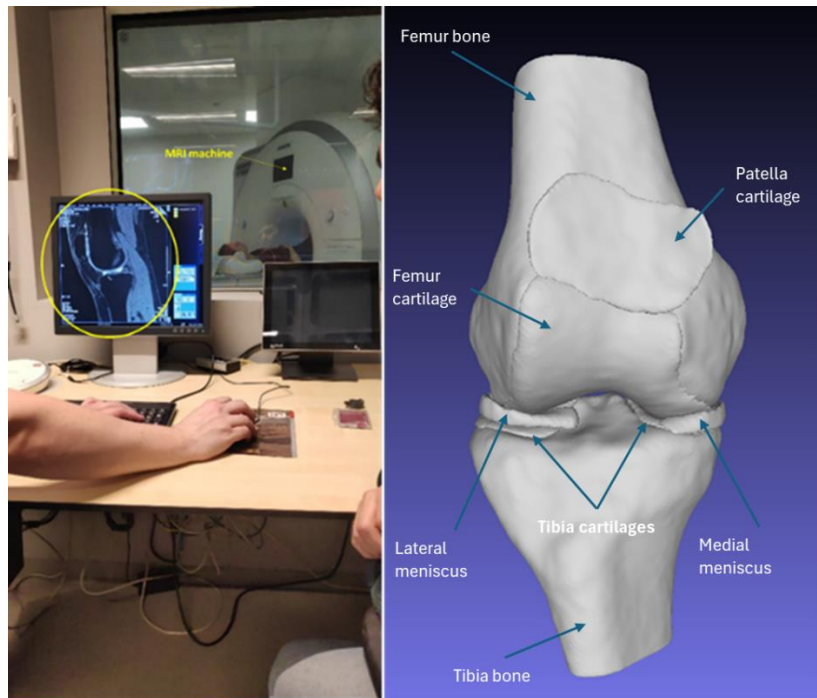


Figure 5 Pilot subject's MRI scanning and segmented structures used in the workflow. On the left, the PS lied down inside an MRI machine and underwent partial scanning of her right knee. The scan displayed on the screen is the t2_de3d_we_sag_p2_iso sequence. On the right, the bones (proximal tibia distal femur,) and the cartilages of the tibia, femur, and patella as well as the menisci were extracted and segmented from the MRI scans. Note that the Patella bone was not segmented because the AI model training datasets did not include the patella bone.

2.4 Gait lab

Thirty-four retro-reflective markers were affixed to various anatomical landmarks exclusively on the lower extremities: four on the pelvis, three on each thigh, two on each knee, three on each shank, two on each malleolus, and five on each foot, totaling 34 markers (**Fig. 6**). The main purpose of limiting the markers to the lower extremity was to enhancing participant comfort during motion capture sessions, potentially leading to more natural movement patterns as well as eventually reducing the burden on individuals with knee OA during data collection. These markers were tracked by eight infrared high-speed cameras operating at a 100 Hz sampling rate. The motion capture system was operated within the Vicon System framework at Roessingh Research and Development (RRD) Centre in Enschede (**Fig. 7**). Two force platforms were embedded in the gait lab to simultaneously capture ground reaction force (GRF) and moments from the foot. The data were recorded at 1000 Hz frame rate.

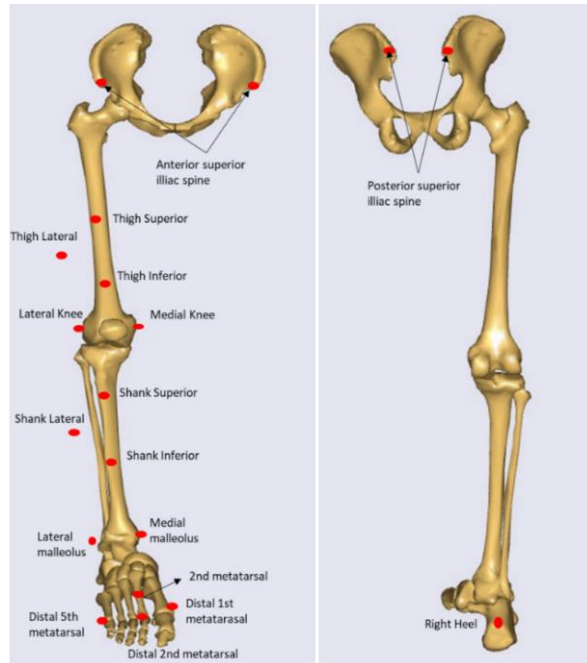


Figure 6 Retroreflective markers affixed to the pelvis and right lower extremity (Left: Anterior view, right: Posterior view). Four markers were placed on the pelvis, and three-cluster markers on the shank and thigh. Two markers were affixed to the lateral and medial knee epicondyles and malleoli. Finally, five markers were placed on the foot segment.

Furthermore, a total of 16 EMG-electrodes were placed on both the right and left extremities, with 8 electrodes on each side (**Fig. 7**). These electrodes were strategically placed to monitor muscle activation during the activities. The targeted muscles included the Vastus medialis, Rectus femoris, Vastus lateralis, medial Hamstring (Semitendinosus), lateral hamstring (Biceps femoris), Gastrocnemius medialis, Gastrocnemius lateralis, and Soleus. The positioning of the electrodes adhered to the widely recognized Seniam Guidelines (67), ensuring consistent and accurate placement for reliable data acquisition. This step was undertaken with the intention of facilitating future validation of the model created with this workflow.



Figure 7 The pilot subject in the motion capture lab (Vicon system) in RRD center. Red circle: infrared high-speed camera, yellow circle: Force plate, white circle: EMG electrodes, blue circle: retroreflective marker.

After that, the participant engaged in a series of activities that were monitored by a motion capture system (Vicon). The session which spanned for 2 hours encompassed the following: Explaining the Vicon system to the participant, setting up the lab environment (i.e., cameras calibration), attaching motion capture markers and EMG electrodes, instructing the participant of the activities, and recording the trials. The protocol included four activities. Firstly, an upright standing static trial was captured. This trial was important for optimizing the model's parameters and calculating the markers positions relative to the body segment local frame as described in 2.6.1. Secondly, the participant was instructed to walk at a self-selected speed (**Fig. 8.A**). Five successful trials were obtained, with an attempt deemed successful if the subject's feet landed within the borders of the force plates. Thirdly, the participant performed a stepping-off maneuver from a block 15 cm in height (**Fig. 8.B**). Starting from an upright standing position, she was instructed to take one step on the block with one foot (e.g., right foot), and step off with the other foot (left foot) and land it on the force plate placed in front of the block. Three successful trials were recorded, with a trial considered successful if the foot landed within the borders of the force plate. Finally, the participant performed a squatting exercise. Initially, she stood upright with both feet in contact with the force plates. She was instructed to position her arms at a 90° angle at the shoulder joint (**Fig. 8.C**). She then squatted to a preferred depth while maintaining straight arms. Three successful attempts were tracked, with a trial deemed successful if she maintained both feet in contact with the force plate throughout the squatting activity.

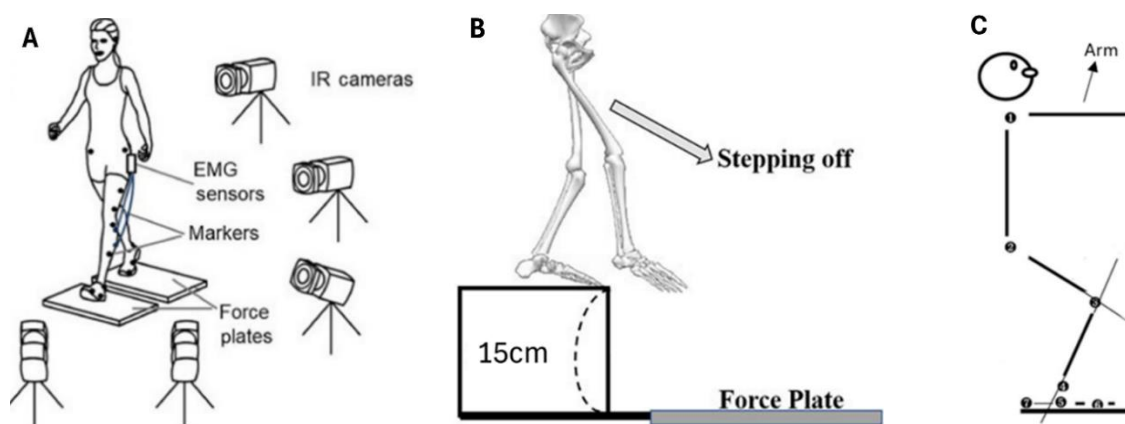


Figure 8 Gait lab activities protocol: After attaching EMG sensors, and markers, IR (infra-red) cameras were used to capture the movement and force plates to record the ground reaction forces. (A) The PS walked at selected pace with the feet falling within the borders of the force plate. (B) Stepping off from a block of 15cm height. PS stood in upright position and landed her right/left foot within the borders of the force plate placed in front of the block. (C) The PS performed a squatting exercise, with hands placed in 90 degrees at the should joint to avoid blocking the markers on the pelvis, to a comfortable depth while maintaining both feet in contact with the force plates.

After recording the activities, preprocessing of the markers data was performed in Vicon Nexus software. First, the marker data was reconstructed using a pipeline predefined within the software. This process was necessary to visualize the markers in the software. After that, markers were labelled automatically using a labelling template; each marker was given a unique name. For instance, a marker placed the anteriorly and superiorly on right iliac was labelled as RASI while the marker placed on the left iliac was labelled as LASI. Then, markers trajectory with maximum of 10 frames gap (missing trajectory) were filled with a Spline function which is predefined in the software. Finally, the data was saved in C3D format. The files were saved in "OneDrive/TopTreat/Datasets/TopTreat test measurement 20240327". The name of the C3D files and the respective activities are highlighted in **Appendix A**. More information about how to generate C3D files is available in Vicon Nexus User Guide (68).

To facilitate the integration of the markers from the C3D file into AnyBody software, it is advisable to rename them to correspond with the labels specified in AnyBody's software marker protocol. **Appendix B** contains the marker locations (as depicted in **Fig. 6**) alongside the corresponding labels they should be assigned. This adjustment can be easily carried out using Mokka software. This step helps prevent errors, particularly since the markers are referenced in other scripts. By matching the marker labels with AnyBody's marker's protocol, the user can facilitate the workflow and eliminate the need for changing the marker names in the other scripts which otherwise would be an overwhelming process. AnyBody software then recognizes the labels automatically.

A patient-specific MS model was made using AnyBody Modelling System v.7.4 (AMS, Anybody Technology A/S, Aalborg, Denmark) (69). The foundational framework for this model was originated from the work of Marra et al. conducted during the grand challenge competition of 2014 (32); that model (**Appendix C**), was originally constructed upon the generic model from the AnyBody Model Repository (AMMR version 1.6), encompassed

components such as the head, trunk, pelvis, and bilateral upper and lower extremities. The primary workflow and the specific modifications implemented in the model are shown in **Fig. 3**.

2.5 Personalizing the MS Model

2.5.1 Bone Morphing

Morphing was the first most important step in building a subject-specific model. "SubjectSpecificScaling.any" file was the starting point. Morphing was needed to adjust muscles attachments, and other nodes. The segmented bones (Target Bones) were utilized to adapt the model (TLEM 2.0) generic bones (Source bones) in AnyBody Modelling System (AMS) to align with the specific anatomical geometries of the participant through an advanced RBF interpolation scheme (RBF scheme) as described below. To assist with the morphing procedure, pre-processing of the segmented bones meshes can be performed in MeshLab v.2016.12 (ISTI-CNR, Pisa, Italy) (27). The main purpose of the preprocessing step is to increase the number of the vertices of the STL file; there is no standardized number. This step can be considered to enhance the details and smoothness of the STL surface and acquire a better resolution in areas with a high curvature. It is worth mentioning that this step is only needed if the surface has low vertices number that does not capture the surface details and makes it look blocky or faceted (**Fig. 9.A**). The STL files received from Radboud UMC have relatively large number of vertices (**Fig. 9.B**); thus, no need for this step. The femur and tibia bones have 66,848 and 50,508 vertices, respectively.

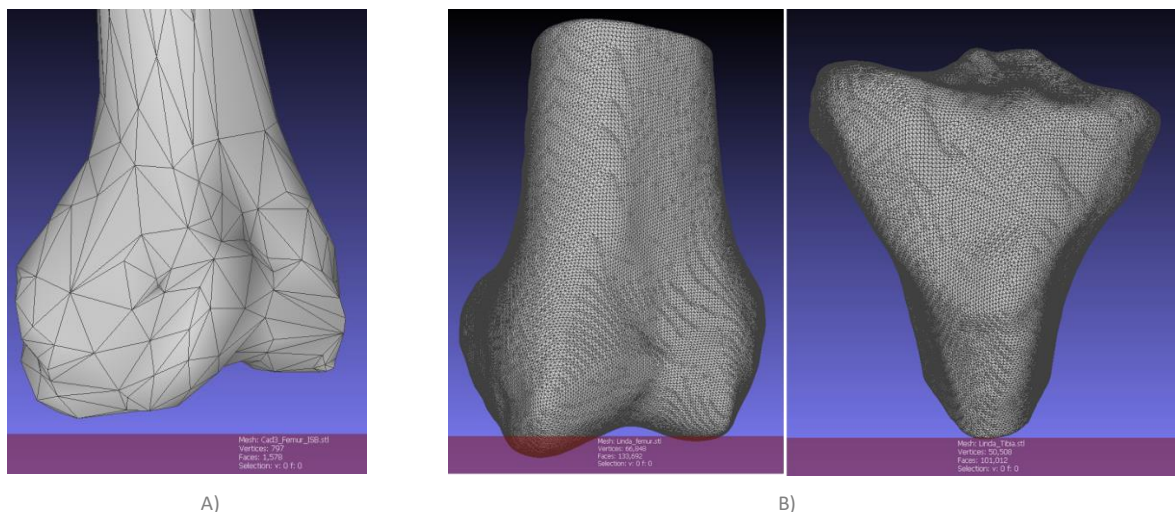


Figure 9 Femur and tibia meshes. (A) illustrates an example of a femur bone mesh with low number of vertices (797 vertices). The edges of this mesh appear blocky and faceted. (B) shows the pilot subject's femur and tibia bone meshes with large number of vertices (66848, and 50508, respectively). The surface details are well captured, and the edges are not blocky or faceted.

Unlike the straightforward process of fully scanned bone morphing implemented in the adopted model, achieving partial bone morphing possessed greater complexity, necessitating additional preparatory steps prior to applying the RBF scheme elaborated below. In fact, no study has yet considered this method for MS personalization. Additionally, since it was unfeasible to visualize each stage of the partial morphing process within the model's framework, partial femur morphing is explained below for the purpose of simplicity (**Fig. 10**). This was done in an external script; same as what is used in the AnyBody tutorial (70). First, given the dissimilarity in topology and orientation between the target femur bone and the source bone, an initial registration of the target bone onto the anticipated anthropometrically scaled femur source bone was indispensable. To accomplish this, a set of distal landmarks that exist in both bones (**Fig. 11**) were chosen to facilitate reverse registration of the target femur onto the source femur. The selection of the landmarks was performed manually in MeshLab using "PickPoints" feature. The coordinates of the chosen points are expressed in millimeter. Therefore, it is important to convert these points into meter when used in AnyBody modelling software. Additionally, it is worth highlighting that there is no specific protocol for the selection of these landmarks. Some of these landmarks were based on the tutorial from AnyBody modelling system (70) and some were subjectively chosen. However, all of them represent a bony landmark. To subjectively select landmarks, both bones can be visualized in MeshLab and a common bony landmark that exists in both bones (source and target) can be selected. For instance, medial and lateral epicondyles

can be observed in the femur bones. **Appendix D** contains a table with the name of the landmarks selected for femur morphing.

Initial registration step was essential for governing the morphing process at both extremities of the bone. After that, a distinct set of proximal landmarks located on the source bone (**Fig. 11**) were chosen to regulate the morphing process at the proximal region of the femur bone, ensuring its preservation. These landmarks were augmented to the source bone distal landmarks as well as the target bone distal landmarks. Eventually, the source's set of landmarks that was used in the scheme consisted of distal femur source landmarks, and proximal femur source landmarks. On the other hand, the target's set of landmarks consisted of the registered distal target femur landmarks (target points at the source position), and anthropometrically scaled proximal source femur landmarks (Fake landmarks).

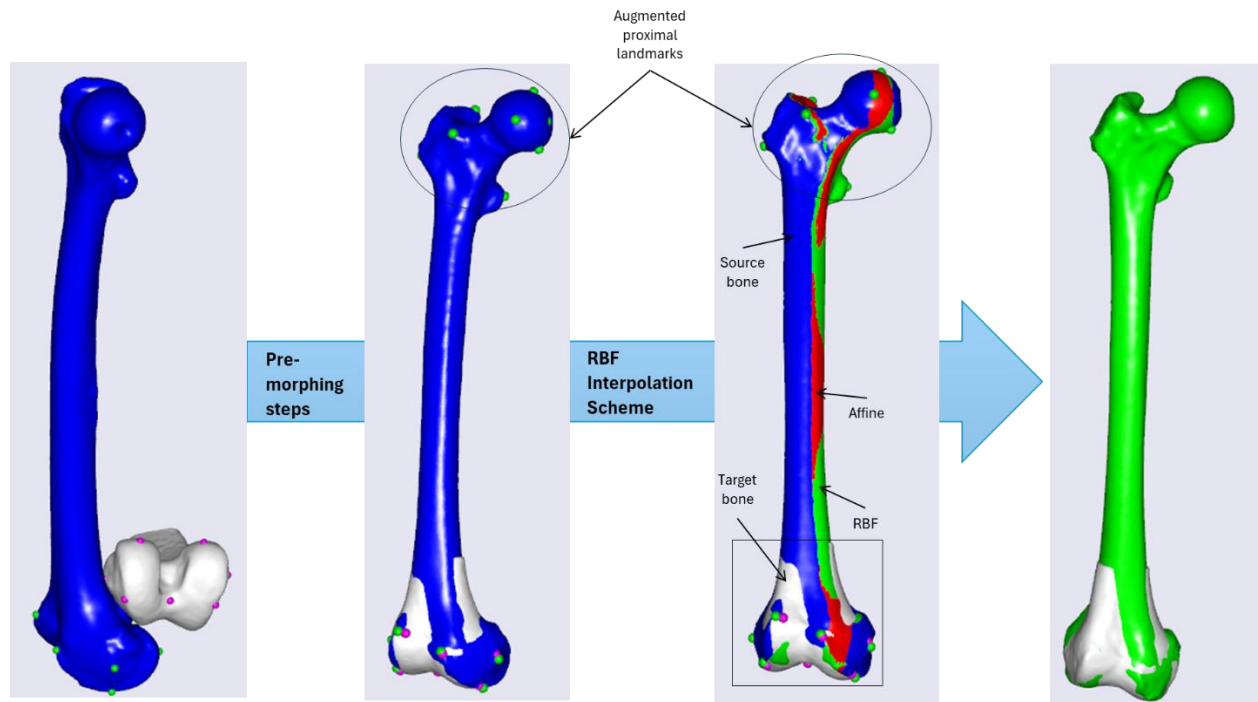


Figure 10 Pre-morphing and RBF interpolation morphing scheme for partial femur bone morphing. Blue femur is the original source bone, white femur represents the pilot subject's distal femur bone. Green points on the blue femur represents the selected landmarks on the source bone while the purple points were selected on the target bone. Red and green femur bones are the morphed source bone with affine and RBF transformations, respectively. The last picture on the right represents the final result of the morphing process (Source bone morphed with RBF transformation).

Following the preparatory steps, the RBF scheme was implemented. Initially in the scheme, the affine transformation was applied with each bone's set of landmarks, preceded by the anthropometric scaling law (Uniform Scaling Law) as a pre-transform. This step was essential for controlling the bone length because the proximal part of the femur was not scanned. Then, a non-linear transformation (RBF) was implemented with the same sets of landmarks utilized in the affine transformation. This transformation deformed related attachments of the soft tissue accordingly. The behavior of the RBF function was controlled using the bounding box property defined in its definition in the software. Lastly, a rigid-body transformation was applied based on the same landmarks to transform the morphed MS bone to the model reference frame from the MRI local frame.

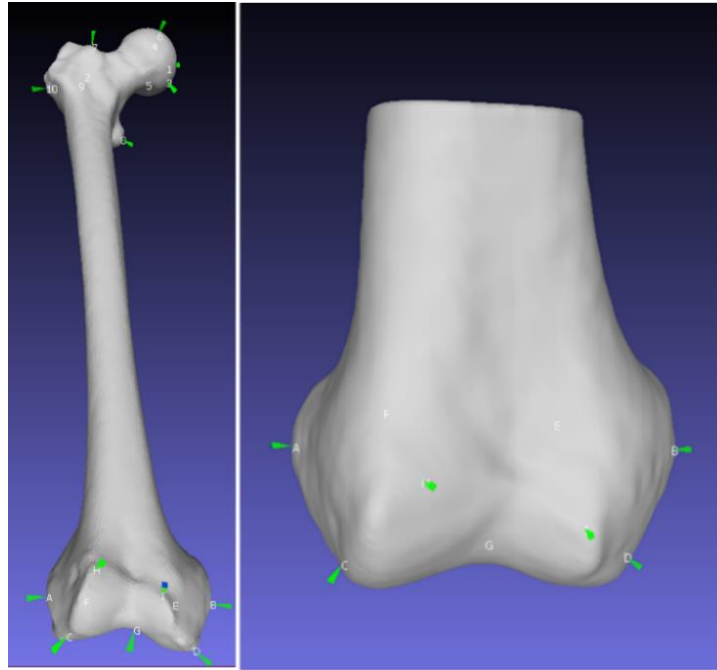
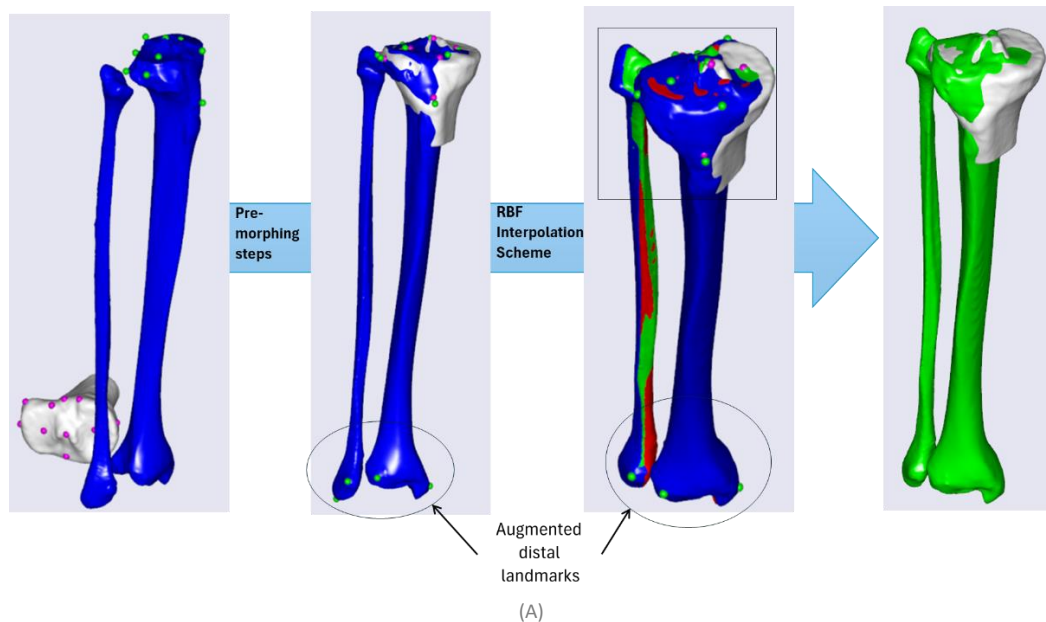


Figure 11 Selected bony landmarks for femur partial morphing (Left: source bone, right: target bone). The distal landmarks were used for morphing the source bone to the pilot subject's bone while the proximal points on the source bone were used to regulate the morphing at the proximal region and ensure its preservation. Appendix D contains the picked-points file that can be loaded in MeshLab to visualize the landmarks.

Partial tibia morphing was conducted like the approach used for partial femur morphing (**Fig. 12.A**). The proximal part of the shank, however, was the region of interest and subsequently was morphed. In contrast, the patella bone underwent a full scan, enabling the direct implementation of the scheme using a designated set of corresponding landmarks (**Fig. 12.B**). The landmarks used for the tibia and patella can be found in **Appendix E**.



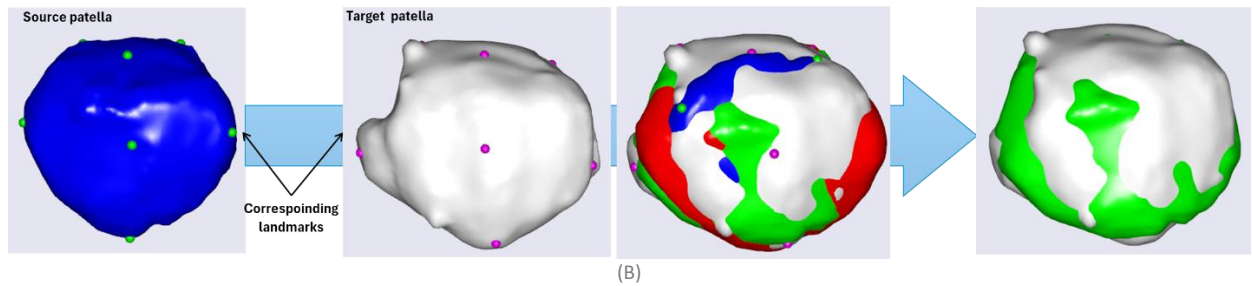


Figure 12 Tibia partial morphing following the same method used for femur partial morphing (A), and patella morphing with RBF interpolation scheme only (B). Blue, white, red and green represent source, target, affine-transformed source and RBF-transformed source bones. Appendix E contains the picked-points files to visualize the landmarks in MeshLab.

After implementing the abovementioned steps in the external script, which was mainly considered to visualize the whole morphing process, the algorithm was applied in the model script “SubjectSpecificScaling.any”. The algorithm pertaining the femur and the tibia were adjusted to partially morph them. The implementation of the partial morphing into the model is depicted in (Fig. 13) and highlighted within the developed algorithm (Appendix F.1).

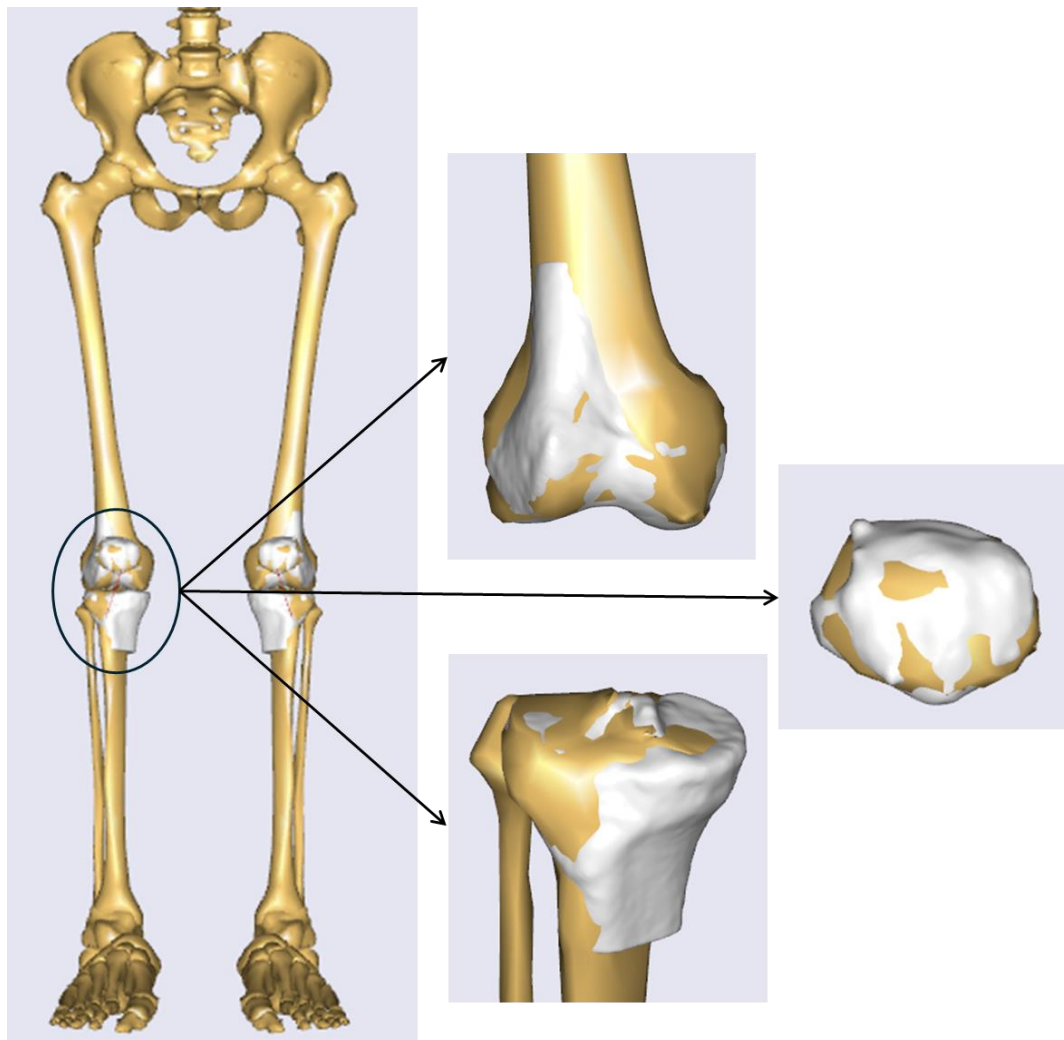


Figure 13 Distal femur, proximal tibia, and patella subject specific morphing. White bones represent the target bone, and gold bones indicate the morphed source bones. Note that target bones were drawn to visualize how well the morphing was performed by comparing it with the bone morphing performed in the external script as described above in this section.

Obviously, the bones were positioned like the MRI scans which indicates that morphing and bone registration were performed properly. However, due to the limited number of landmarks (11 for the tibia, 9 for the femur, and 9 for the patella), the morphed source bone did not fully match the subject's bone. The morphing accuracy can be assessed by the Euclidean distance between each vertex on the subject's mesh to the corresponding the vertex on the morphed bone (71). The highest morphing errors were 4.248 mm, 6.404 mm, and 5.13 mm, for the femur, tibia and patella, respectively (**Table 3**) after the affine transformation but 0 mm for all bones after RBF transformation. This was actually expected because RBF function deformed the bone; thus, the points overlap/coincide on top of each other. **Fig. 14** displays the landmarks where the maximum error occurs. Overall vertex to vertex errors are provided in **Appendix I**.

Table 3 Min, max, and mean morphing errors between the morphed bone landmark to the corresponding target bone landmark for the femur, tibia, and patella bones.

Segment	Min error [mm]	Max error [mm]	Mean \pm SD [mm]
Femur	0.312	4.248	1.915 \pm 1.022
Tibia	0.417	6.404	2.492 \pm 1.543
Patella	1.452	5.130	3.396 \pm 1.331

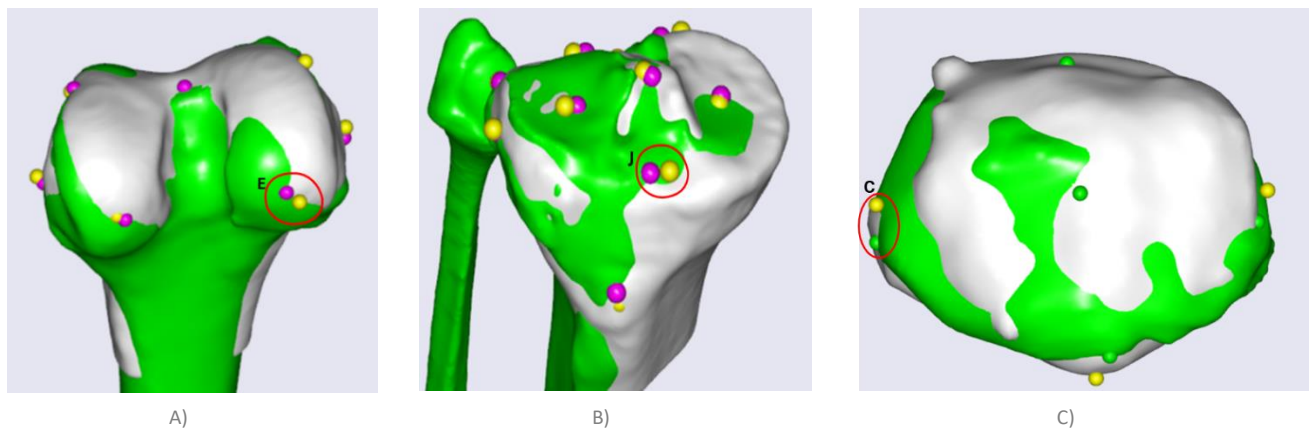


Figure 14 Landmarks with maximum morphing error for each segment. Green bone represents the morphed source bone while white bone represents the pilot subject's bone. Yellow points represent morphed source landmark while purple points represent target landmark. In A, landmark E (Posterior medial resection) on the femur has the maximum morphing error of 4.248mm. In B, landmark J (Anterior tibia) has the maximum morphing error of 6.404mm on the tibia. Finally, in C, landmark C (Lateral border) has the maximum morphing error of 5.13mm.

Additionally, as scans were solely accessible for the right knee, the left knee's geometry underwent morphing by mirroring the bone geometries of the right knee. The same steps applied on the right knee were implemented to the left knee, but the landmarks were mirrored about z axis (**Appendix F.2**). This means that each landmark selected on the right knee was reflected (mirrored) on the left knee. Therefore, both knees were symmetrically morphed. Finally, the morphing function was used to align any designated target node or surface within the musculoskeletal (MS) model's reference frame. This particular step was crucial for tailoring additional nodes or reference frames to match specific target landmarks, such as those derived for tracking frames based using Grood and Suntay method.

2.5.2 Subject Specific Reference Frames

The anatomical local coordinate systems (LCS) for the tibia, femur and patella were established in line with Grood and Suntay method (72), and depicted in **Fig. 15**. This was done in "SubjectSpecificJoints.any" file. The local coordinate systems of the three bones were defined using bony landmarks, which were selected manually in MeshLab software. Certainly, this manual selection process is inherently susceptible to human error. For instance, the medial epicondyle, defined as the most prominent point on the medial condyle, may be subjectively and inconsistently selected due to the fact that the epicondyle has a relatively large region. When a landmark exists in a broad area, it can be challenging to pinpoint an exact location, leading to variability in the selection. Different individuals might choose slightly different points within this large region based on their interpretation, further adding to the inconsistency.

The femoral LCS was established with its origin located between the lateral and medial epicondyles which are defined as the most projecting point on the lateral and medial epicondyle of the femur, respectively. The origin was located between the two points and calculated as the arithmetic mean distance between them and given as $0.5 * (\text{medial epicondyle} + \text{lateral epicondyle})$. This LCS was aligned such that the Y-axis extended from this origin to the center of the hip joint (HJC). Note that the hip center of the model template was utilized here due to the absence of a femoral head in the MRI scan. The Z-axis was defined as perpendicular to the Y-axis and directed medially (defined by medial and lateral epicondyles), while the X-axis was defined as the cross product of Y and Z axes and pointing anteriorly (Green coordinate system).

The tibial LCS center was established between the lateral and medial tibial condyles which are defined as the most prominent point on the lateral and medial condyle of the proximal end of the tibia. Similarly, the origin was located between these two points and calculated as the arithmetic mean distance between them and given as $0.5 * (\text{medial tibial condyle} + \text{lateral tibial condyle})$. The tibial LCS orientation was established with the Y-axis pointing from the joint center of ankle (AJC) to the origin and directing proximally. The center of the ankle joint was defined as the arithmetic mean distance between lateral and medial malleoli. As with the HJC, the AJC of the generic model was utilized because the distal part of the shank was not scanned. The Z-axis was orthogonal to the Y-axis and pointing towards the medial tibial edge (defined by medial and lateral condyles/ intercondylar eminences), while the X-axis was perpendicular to Y and Z axes and directed anteriorly (Red coordinate system).

It is noteworthy that using the location of the lateral and medial malleoli markers from the c3d file to define the tibial tracking LCS was possible (Yellow coordinate system). However, there remains uncertainty, probably, because the distal region of the tibia does not match the patient's geometries as it was not morphed. The error between the two coordinate systems (red and yellow) of the tibia can be described by the rotational error between their rotational matrices (ARel in AnyBody software). Following the calculation steps below, the rotational error was found to be 2.96° around the z axis while the error around the x and y axes was negligible. This means that the coordinate system created with the generic bone ankle center introduced an error about 3° with respect to the coordinate system created with the malleoli markers' location. Although the tibia LCS was possibly obtained through subject's malleoli markers, femoral LCS remains the issue because it was not possible to detect the femur head/ hip center through the available marker's dataset.

Table 4 Rotational error of the tibia coordinate systems between the rotational matrices of the coordinate systems created with the malleoli marker's location (A) and the one with created with the generic bone the ankle joint center (B).

Rotational matrices	A= {{0.9945709, 0.03602191, 0.09762719}, {-0.03219507, 0.9986609, -0.04049478}, {-0.09895516, 0.03713181, 0.9943989}}	B= {{0.9951051, -0.01531953, 0.09762719}, {0.01935221, 0.9989923, -0.04049478}, {-0.09690845, 0.04218586, 0.9943989}}
Rotational error about x axis	-1.889e-07°	
Rotational error about y axis	2.807e-07°	
Rotational error about z axis	2.956°	

Rotational error calculation steps (**Appendix G**):

1. Compute relative rotation matrix R between the two frames:

$$\mathbf{R}_{rel} = \mathbf{A}^T \cdot \mathbf{B} \quad (1)$$

where \mathbf{A}^T is the transpose of matrix A.

2. Converting Rotational matrix to Euler angles, assuming z-y-x convention according to (73):

$$\theta_x = \arctan2(\mathbf{R}_{rel_32}, \mathbf{R}_{rel_33}) \quad (2)$$

$$\theta_y = \arctan2(-\mathbf{R}_{rel_31}, \sqrt{\mathbf{R}_{rel_11}^2 + \mathbf{R}_{rel_21}^2}), \text{ or } \theta_y = \arcsin(-\mathbf{R}_{rel_31}) \quad (3)$$

$$\theta_z = \arctan2(\mathbf{R}_{rel_21}, \mathbf{R}_{rel_11}) \quad (4)$$

The LCS for the patella was defined with its center positioned between nodes chosen at the extreme medial and lateral protuberances (borders) of the patella and given as $0.5 * (\text{medial border} + \text{lateral border})$. The Z-axis extended from the origin and pointed to the medial edge, while the Y-axis was defined orthogonally to the Z-axis and pointed towards the node located superiorly. The X-axis was defined as the cross product of Y and Z axes and oriented anteriorly (Blue coordinate system).

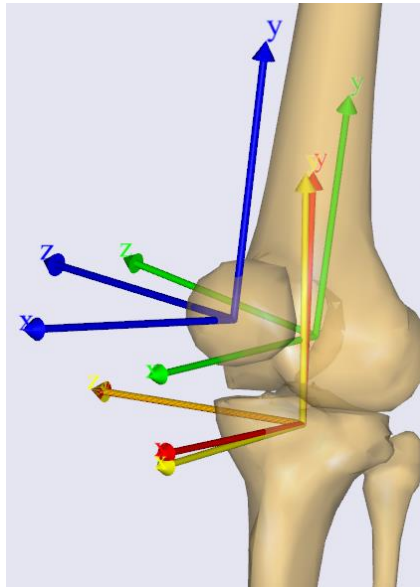


Figure 15 Knee joint coordinate systems. X axis represents the anteroposterior axis, Y axis denotes the Superioinferior axis, and the z axis represents the mediolateral axis. Blue frame refers to the patella coordinate system, and green frame denotes the femur coordinate system based on the hip center of the generic bone. Red frame represents the coordinate system of the tibia with the generic bone ankle joint center while yellow frame represents the coordinate of the tibia with the use of the malleoli markers' location. Note that there is an error of 2.96 degrees about z axis between the red and yellow frame while the error is negligible about x and y axes.

2.6 Motion Capture

Motion capture, or mocap, was pivotal in accurately replicating the gait lab activities (walking, stepping off, and squatting). The model employed in this study encompassed two primary studies: Motion&Parameter Identification and Inverse Dynamic. Both studies adhered to a consistent configuration. Initially, the arms were deliberately excluded from the model. This was done to simplify the model by reducing the computational load. It is considered acceptable because the protocol's primary focus was at the lower extremity, specifically the knee joint, and the configuration was utilized in other studies (17,32). It was not possible to exclude the trunk because hip flexor bundles (i.e., Psoas Major muscle) have attachment points on the lower spine. Additionally, markers were not affixed to the trunk, back, and head segments. Instead, soft drivers were employed on these segments to synchronize with the movement rhythm and adapt to the absence of markers on the upper extremity (described in 2.6.2). Since the angles of the upper extremity joints (e.g., PelvisThorax, neck, etc.) are not important for the inverse dynamic model, utilizing soft drivers for rhythmic motion was sufficient (74).

In general, in the Motion and Parameter Identification study, as illustrated in **Fig. 16**, two MoCap sub-models were integrated: static and dynamic. The folder "...\\MoCapModel GC5\\ Input\\ Subjects\\ PS\\ StaticTrials\\ PS_staticfor2" contains the static model. The static model incorporated the scaled musculoskeletal (MS) model and used a static C3D file (static trial) mainly to optimize segment lengths. The recorded trial can be found in "OneDrive/TopTreat/Dataset/TopTreat /test measurement" folder. The optimization problem was performed locally to the segments where markers were attached. It reduces the difference between the experimentally observed marker positions and model markers within a single frame of a static trial. For instance, the length of the shank was optimized based on the markers attached on the medial and lateral malleoli. Conversely, the dynamic model utilizes dynamic C3D files of the activities mentioned earlier in this section. The folder "...\\MoCapModel GC5\\ Input\\ Subjects\\ PS_PreOp\\Overground Gait Trials\\ PS_ngait_og_ss1" contains the dynamic model. The outputs (optimized segment lengths and markers local coordinates files) from the static model were inputted into the dynamic model, from which joint angles (hip flexion, hip abduction, and hip external rotation, knee flexion, subtalar eversion, and ankle plantarflexion) were obtained. Consequently, these joint angles are utilized in the inverse dynamic model. Each sub-model is explained extensively below.

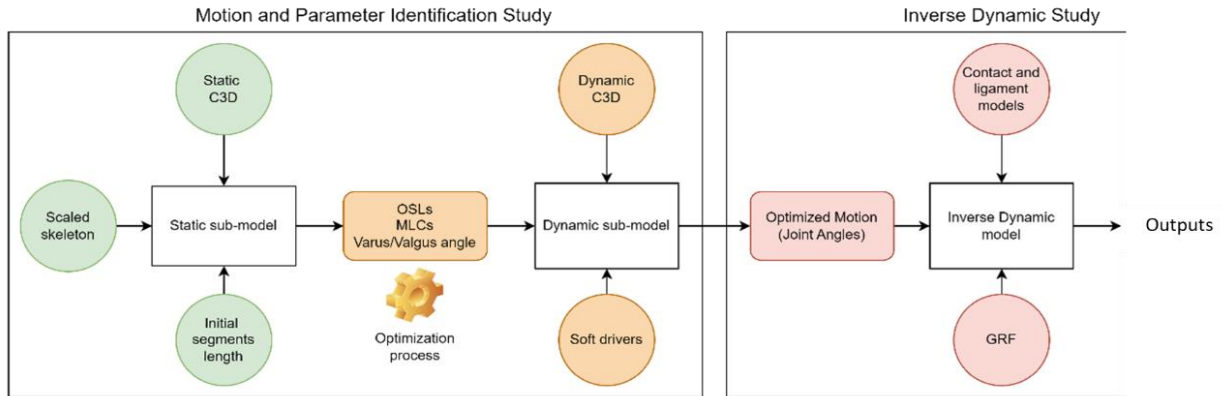


Figure 16 MS models' MoCap workflow and studies; Motion and Parameter Identification (MPI) and Inverse Dynamic. MPI study utilized two sub-models (static and dynamic) to optimize segment length, extract markers local coordinates (location relative to the respective segment) and drive the model. The final output from this model is the joint (hip, knee and ankle) angles. These joint angles are then used to drive the inverse dynamic model in the last block of the workflow (inverse dynamic model). Note that each color-coded blocks are inputs to the respective white block.

2.6.1 Static sub-model

The primary objective of the static sub-model (**Fig. 17**) was to optimize segment lengths, knee alignment (Varus/Valgus angle), and calculate markers location. In AnyBody Modelling System software, Varus/ Valgus alignment is exclusively modelled; no other knee alignments are modelled. The C3D file of the static trial served as the input for this model. Segment lengths were initially expressed as a function of body height, as outlined in (75). This can be found in "SubjectSpecificData.any" file. In this file, the weight and the mass of the subject were also defined. The static trial C3D file should be added to the following folder "...\\MyModels\\ MoCapModelGC5\\ Input\\ Subjects\\ PS\\ Static Trials\\ PS_staticfor2" and defined in "TrialSpecificData.any" file.

To achieve the objective of the static model, Uniform Scaling (US) was initially implemented to scale the femur, patella, and tibia bones because of the implementation of partial morphing. This was implemented automatically after defining the segment lengths. This law is located in "HumanModel.any" file under "..\\ScalingUniform.any" subscript. The morphing scheme could not control the length of these bones; thus, it was necessary to apply this scaling law as a pre-transform (as discussed in 2.5.1) to regulate their lengths. Additionally, the bones of the upper body (i.e., trunk and head), feet, and talus were similarly scaled. Mainly, the purpose of this scaling law was to serve as an initial guess to the optimization problem to better estimate the length of the participants segment length based on the makers data and control the length of the morphed bones while implementing the partial morphing (i.e., femur, and tibia). US scales the segment up/ down based on a scaling factor which is represented by the ratio of the anthropometric segment length/ pelvis width to the default model's segment length/ pelvis width (Anthro.Seg. Length/ Standard.Seg. Length).

After that, Segment Length Optimization (SLO) was executed. It was restricted to the pelvis, thigh, shank, and foot segments. It was only feasible for these segments due to the absence of motion capture markers on the upper body segments (e.g., the trunk). In "ModelSetup.any" file, the lengths of these segments were configured as design variables (AnyDesVar) with their initial length (after being uniformly scaled) serving as the first guess for the optimization algorithm. The optimization function is designed to minimize the least-square differences between the modelled markers (Red) and experimental markers (Blue) during one timeframe of a standing reference trial (33). In AnyBody Modelling system software, AnyDesVar links design variables with the parameter optimization study embedded in the model allowing automatic optimization of the defined variables (i.e., segment lengths). This is quite powerful feature in the software because the user can add any variable in the optimization problem. This can be found in "OptimizeAnthropometricsOnOff" class in "ModelSetup.any" file. The user, then, can use switches (On/ Off) to specify which model parameter (e.g., segment length) to be optimized. These switches are also defined in "ModelSetup.any" file. In our case, pelvis, thigh, shank, and foot lengths were defined in the optimization algorithm by defining them as AnyDesVar and involved in the optimization process. Markers on the pelvis, knee, ankle, and foot were only utilized in this sub-model for the optimization algorithm (**Fig. 17**) because they were placed on distinct bony prominences.

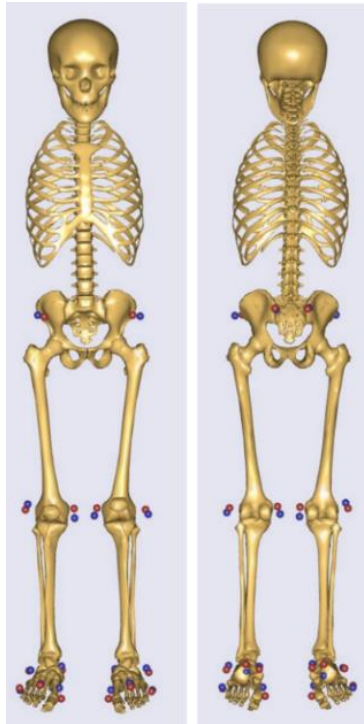


Figure 17 Static Model with morphed knees and the marker dataset used for pelvis, thigh, shank, and foot optimization (Left: anterior view, right: posterior view). These markers were used because of their placement on distinct bony prominences. These markers were used to optimize the pelvis and lower leg bones (Thigh, shank, and foot). Note that there were no markers attached to the upper body. These segments were scaled by the scaling law (Uniform scaling).

Optimizing segment length remains crucial because applying a uniform scaling law scales the segment's length linearly based on the ratio (scaling factor) of the subject's bone length, which is defined as a function of height (75), to the generic model bone length. This definition may not always adhere to the assumption that body proportionality holds uniformly across all individuals. Individuals of the same height may exhibit varying body proportions, such as having a long torso and short legs or the opposite proportion (76). Additionally, it was observed that using markers data to optimize the segment length was quite sensitive to the marker's placement. For instance, the lengths of the pelvis, thigh, and shank were optimized from 17.7cm, 41.22cm, 42.35cm, to 16.32cm, 41.47cm, and 42.52cm, respectively. However, the foot length was optimized at 15.14cm from 25.86cm. Although, markers data remains a better way of estimating segment lengths, within this protocol, it was realized that foot length optimization was not reasonable because the optimized foot length has about 10cm difference from the initial length. To investigate this, the participant was asked to measure her foot length (the distance between two most prominent points (from back of the heel to the end of the longest toe)) which turned out to be about 22cm. One valid explanation to this big difference is the placement of the marker (RToe) located on the 2nd metatarsal head, which was placed on the mid-foot side of the equinus break between the mid-foot and forefoot (**Fig. 18.A**). The marker in the lab might have been placed a bit posteriorly while the model marker was configured at the equinus break; thus, the optimization resulted in a shorter length. Since X axis represented the anteroposterior axis, one can think of optimizing the model's marker on the X direction to compensate for this malplacement. As this is possible, it would compromise the optimization of the foot length. This is because optimizing model marker in the x direction will move it to the location of the experimental marker, but the foot segment would not catch the movement, meaning it would not be optimized. This concludes that the issue remains quite dependent on how trustful the marker data is and how well the markers were placed (77). Nevertheless, a direct solution to this issue was to measure the foot length (i.e., 22cm), exclude the foot length from the optimization process and assign the measured length to the foot segment directly instead of defining its length as a function of the height (**Fig. 18.B&C**). Additionally, for future perspectives, it is better to place this marker on the tip of the 2nd distal phalanges because it is a consistent and easily identifiable anatomical landmark. It is also recommended to measure segment lengths in the lab as well in case the optimization failed or was not realistic.

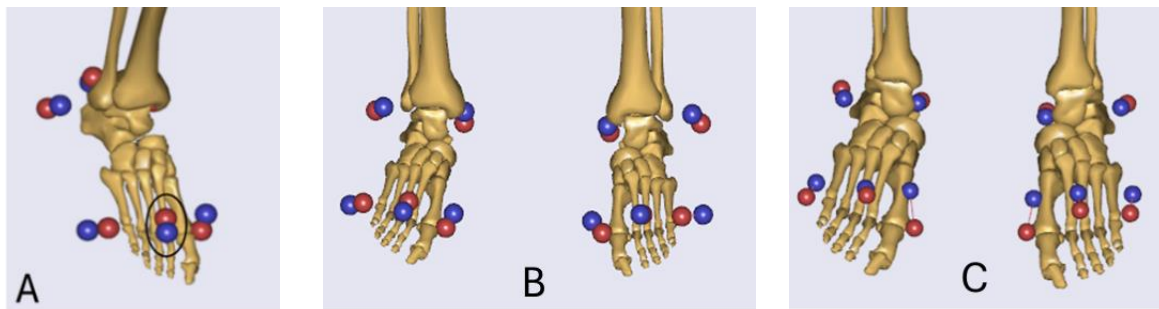


Figure 18 Optimization of the foot length. (A) The RToe marker. (B) Foot length after the optimization resulted in length of 15.14cm. This did not seem reasonable because the participant foot length was measured at 22cm (C) Foot length after excluding foot length from the optimization which was set to the measured length (22cm).

Varus/ Valgus alignment was taken into consideration by the optimization algorithm as well (**Fig. 19**). In Seg.any file, there is a variable called AxisRot that applies a rotation on the knee joint, at the thigh reference frame, in the frontal plane. Like segment lengths optimization, this parameter was added to the optimization by defining it as AnyDesVar; thus, the parameter optimization study predefined in the model automatically considered it in the optimization process. To visualize how this variable was optimized, the neutral posture of the model (**Fig. 19.A**) was perturbed at the knee joint by setting AxisRot to 11 degrees valgus (**Fig. 19.B.1**) or 11 degrees of varus (**Fig. 19.B.2**). This illustration method was considered because the pilot subject has neutral alignment and to check if the optimization could correct this perturbation and achieve the subject's true alignment. After running parameter optimization study in both cases (valgus or varus), AxisRot variable was optimized at 1.38 degrees at the right knee and 0.39 degrees at the left knee in both perturbation cases (**Fig. 19.C**); as the optimization algorithm minimized the difference between the markers of the model (red) and the gait markers (blue), the variable AxisRot value was optimized correspondingly. Interestingly, this variable at each knee was optimized at different values which indicates that the knees have slightly asymmetrical degree of alignment. It also implies that knee alignment of the subject was captured by the markers data as the perturbation was eliminated. Nonetheless, it is important to acknowledge that relying solely on this method is a simplistic and limited approach. Luckily, morphing is also able to capture the knee alignment especially since shank and thigh bones were both morphed. This is because the knee joint axis is established using control points projected onto the standard knee axis, which are subsequently passed through the scaling function automatically; thus, capturing the knee alignment (78). Nevertheless, capturing knee alignment remains imperfect in this protocol because the proximal femur region was not scanned and considered. Although it is currently believed that varus of the tibia is the primary reason of varus alignment in the knee, it was found that abnormal morphological structures of the femur, including irregular shape of the femoral neck and head, and the level of femoral shaft curvature, impact lower limb alignment (79). The same study reported that the morphological characteristics of the proximal end of the femur in the frontal plane influence the shape of the distal end of the femur in both the frontal and transverse planes, subsequently impacting lower limb alignment. For instance, femoral neck anteversion level (a condition in which the femoral neck leans forward with respect to the rest of the femur), and the morphological characteristics of the proximal femur influence the shape of trochlea at the distal femoral. This concludes that in order to capture the knee alignment, it is ideal to scan the entire bones of the subject and morph the generic bones throughout the entire surface.

Finally, following the optimization problem, the markers local coordinates (MLCs) of markers cluster positioned on both the thigh and shank were calculated within their respective segment reference frames. This is mainly because these markers were placed on soft tissues, and it is very difficult to determine their location on the model marker protocol. In "Kinematics.any" file, there is a subscript called "ComputeMarkerPositions.any" where the local coordinates of the markers of interest (i.e., thigh and shank clusters) were computed. These computed coordinates were subsequently stored in files, along with the optimal segment lengths and optimized AxisRot angle and utilized in the dynamic sub-model. These files were generated and saved in the directory path of the static model ("...\ Input\ Subjects\PS\ StaticTrials\ PS_staticfor2") after running the "MotionAndParameter Optimization Model" study of the static model.

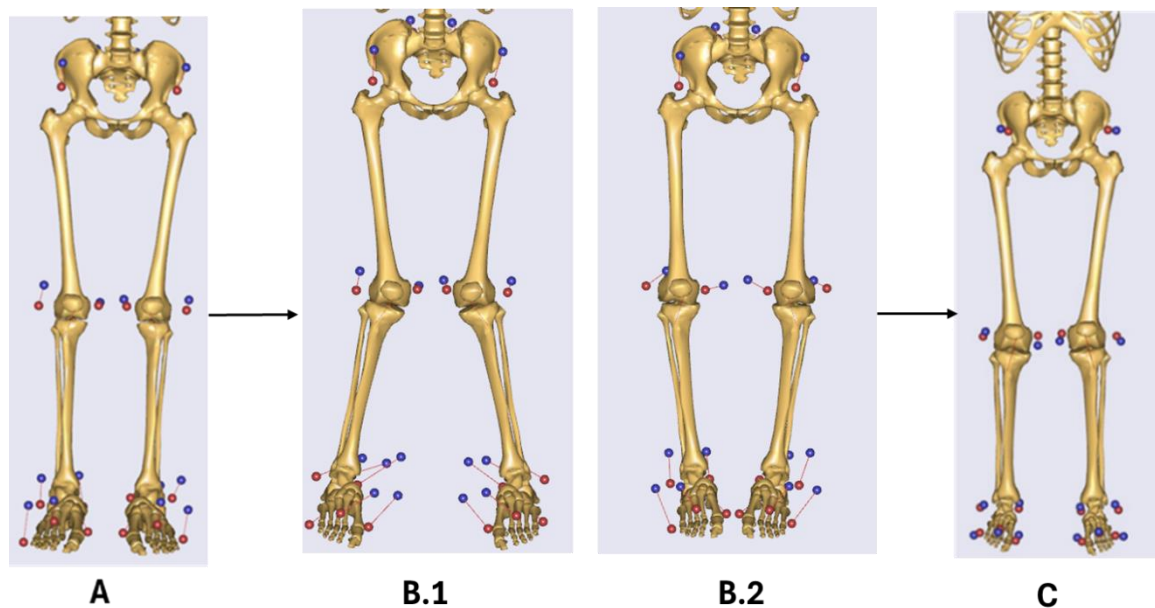


Figure 19 Knee alignment optimization. (A) The neutral posture of the model. (B) the perturbation applied at the knee joint by setting AxisRot to 11 degrees of Valgus (B.1) or 11 degrees of Varus (B.2) before running the optimization study. (C) The final alignment of the knee after the optimization was performed. AxisRot of the right knee was optimized to 1.38 degrees and 0.39 degrees for the left knee in both cases (varus or valgus perturbation).

2.6.2 Dynamic sub-model

The dynamic model (**Fig. 20**) was designed to utilize the optimized segment lengths and knee alignment to produce an optimized motion and save the joint angles in files that would subsequently be employed in the inverse dynamic model. The dynamic model is located in "...\MyModels\ MoCapModelGC5\ Input\ Subjects\ PS_PreOp\Overground Gait Trials\PS_ngait_og_ss1" folder. The optimized parameters obtained from the static model were directly imported into this model. In "Kinematics.any" file, a class operation reads "optimized parameters" file from the static model folder and updates the same parameters within the dynamic model directly. Dynamic C3D files from the activities conducted in the lab along with the optimized parameters served as the input to this sub-model. The dynamic trial C3D files were added to the model's folder and defined in "TrialSpecificData.any" file that belongs to the dynamic model. The joint angle files produced from this model were generated automatically in the model's folder after running "Motion&ParameterOptimizationModel" study of the dynamic model.

Moreover, the saved Marker Local Coordinates (MLCs) of the thigh and shank marker clusters, from the static model, were imported to create marker drivers (highlighted in red) on the skeleton, replicating the activities performed in the lab. To accomplish this, a specialized marker driver class was developed. It can be found in "ModelSetup.any under ../Input/MarkersMSATest.any subscript". In this subscript, the class can be located under the name "CreateMarkerDriverEx". This class reads the computed local coordinates of the respective marker from MLCs file generated from the static model and assigns that location to the markers in the clusters on the skeleton automatically. This approach streamlines the placement of marker drivers, eliminating the need for manual adjustments typically required in AMS MoCap models especially for markers placed on soft tissues like thigh and shank cluster markers. The positioning of other markers was conducted manually as they were placed on distinct bony prominences.

The segments with no markers, such as the head, trunk, and back, were controlled and driven using soft drivers to synchronize with the movement rhythm. These soft drivers controlled the degrees of freedom (DOFs) of these segments, ensuring their alignment with the motion dynamics. The configuration of the soft drivers can be found in "ExtraDrivers.any". The user can always call a joint of interest (e.g., neck joint) and set a soft driver for it. The position and velocity drivers for the joint were set to zero. After that, reaction forces were turned off, so it does not influence the dynamic equilibrium of the model. This was achieved by setting Reaction.Type to Off. Finally, the constraint type (CType) was defined as soft. This allows some flexibility, meaning the joint can deviate slight from the specific position and velocity (i.e., zero) if necessary, during the movement. The user can switch these

drivers on or off in "TrialSpecificData.any" depending on the availability of the markers on the body segments. For this protocol, segments with no markers (head, and trunk) were assigned zero which implies the absence of markers on these segments and activates their soft drivers. On the other hand, three markers were attached to foot; thus, the soft drivers on the foot were not activated (assigned 1 to the foot segment definition).

To configure the force plates, the type of the force plate should be carefully considered. The type of the force plate depends on the motion capture lab settings. This being said, there are three types of force plates configured in the model: type 2, type 3, and type 4. More information about force plate types can be found in (80). A class template for each force plate type was created. The classes are defined in "PreMainIncludes.any" under "classes.any" subscript. With this, the user can easily switch between force plate types. In this study, force plates type 2 were installed in the lab. This can be seen in the model tree directory "Main. Modelsetup.C3dfiledata.Groups. Force_Platform.Type.Data". Therefore, in "ForcePlates.any", the class "ForcePlateType2" was defined. However, if the user has a force plate of type 3 or 4, he/ she has to change the class template name to ForcePlateType3, or ForcePlateType4, respectively. With this, the system will refer to the class template directly. After that, the foot-forceplate contact is defined. Mokka software can be used to inspect force plate(s) and the foot that comes in contact with it. For instance, the left foot in the walking trial came in contact with force plate 1 in the lab. Therefore, the left foot segment was linked to force plate 1. The definition of the foot of contact can be found in "TrialSepcificData.any". Similarly, force plate 2 was linked to the right foot but was excluded and not displayed as the focus was on the left leg. A detailed explanation of the configuration of the C3D files can be found in Anybody available guidelines (81). Lastly, forces and moments in X, Y, and Z directions of the force plate were defined. It is quite important to define them based on their respective names/ labels in the C3D file. The labels can be found within the following directory "C3DFileData.Analog.DataFiltered" in the model tree.

Finally, to drive the model, MotionAndParamterOptimizationSequence operation was run. As the name of the operation suggests, the model underwent the following sequence of operations (check "Kinematics.any" file). First, the optimized parameters obtained from the static model were loaded from "OptimizedParameters" file produced from the static model (refer to static sub-model section above). Secondly, the model looked for the parameters that were optimized in the static model and updated their values in the dynamic model. Lastly, the model was driven using AnyBodyStudy study-class to obtain hip, knee, ankle, and subtalar joint angles. These angles were saved in files within the dynamic model folder to be used later in the inverse dynamic model. The model utilized AnyOperationMacro operation-class to perform each step consecutively.

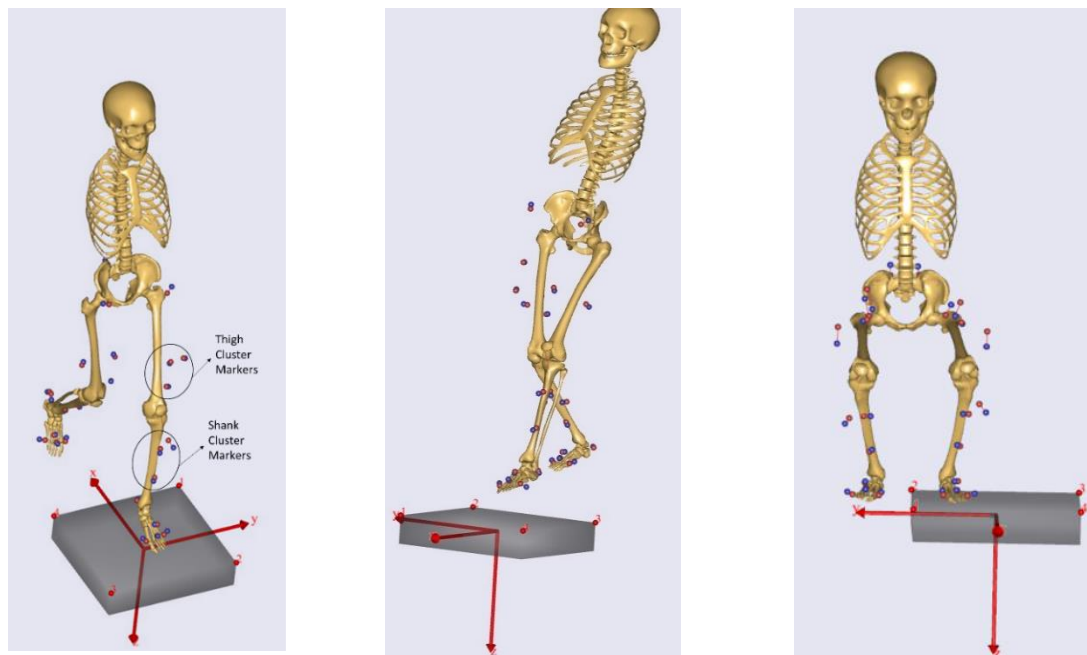


Figure 20 Dynamic trials of the activities recorded in the gait lab that were used to drive the model. (Left) walking at selected pace. (Middle) stepping off from a 15cm-heigh block. (Right) squatting to a preferred depth. Note that this sub-model contains markers on the thigh and shank and the configuration of the force plate of the left leg.

2.7 Inverse Dynamic Model

2.7.1 Contact Model

Within the workflow of the personalized model, contact model was defined to calculate the knee contact forces at the lateral and medial tibiofemoral (TF) and patellofemoral (PF) compartments. Three files were used to define the contact model: ContactSurfacesPreOp.any, ContactForcesPreOp.any, and ReactionForces.any.

In ContactSurfacesPreOp.any file, surfaces of contact models were defined. It was applicable to use bones STL files for the contact surfaces with an offset that represent the thickness of the cartilage (**Fig. 21.A**). These offsets were created in the direction of the anticipated cartilage. For instance, the femur bone was scaled with an offset representing the femoral cartilage thickness: in the positive X direction (anteriorly) for patellofemoral (PF) contact, and in the negative Y direction (inferiorly) for medial and lateral tibiofemoral (TF) contacts. Similarly, the lateral and medial tibial bone offsets were created in the positive Y direction (superiorly) to represent the medial and lateral tibial cartilages for TF contacts. Finally, the patella offset was applied in the negative X direction (posteriorly) to represent the patellar cartilage for PF contact. However, using bone offsets was not a straightforward process. It required a sequence of transformations to the bone prior to registering it as contact surfaces. First, the bone contact surface was transformed to the coordinate system center described in 2.5.2 of the respective segments. This step was necessary to align the contact surface (e.g., femur surfaces) with the global coordinate system by removing any initial positional and rotational offsets. Secondly, the offset (scaled bone) was created around this origin with the cartilage thicknesses. Currently, the offsets were defined as 2.14mm for the femur, 3.08mm for the patella based on (82), 3.13mm for the lateral tibia, and 2.56mm for the medial tibia according to (83). However, these values can be substituted with the participant's segmented cartilage thicknesses once being estimated. Lastly, the scaled bone was moved from the coordinate system origin to its spatial location in the model space. Nevertheless, a more representable and direct approach would be the utilization of the segmented cartilages to create the contact surfaces. The cartilages can be registered directly (using the morphing function) at the knee joint (**Fig. 21.B**) and used as contact surfaces to compute the contact forces.

In ContactForcesPreOp.any, three contact models were defined. The femur contact surface was defined with the medial tibial contact surface to create the contact model in the medially, with the lateral tibial surface to create the contact model in the laterally, and with the patella contact surface to create the patellofemoral contact model. For each force-surface-contact model, properties such as pressure module can be based on literature; the common value used is 9.3 GN/m³ because it offered a favorable balance between the degree of penetration achieved and the computational issues encountered in resolving contact between surfaces with relatively high rigidity (32); or it can be defined by the thickness of cartilages as follows:

$$\text{Pressure Module} = P = \frac{(1 - ni)}{(1 + ni)(1 + 2 \cdot ni)} * E/h \quad (5)$$

where E, ni are young modulus and Poisson's ratio (E = 5e6, and ni =0.42), h is the thicknesses of the articulating surfaces (e.g., femur cartilage thickness and patella thickness for PF contact model).

$$\text{Contact force} = F_i = P \cdot V_i \quad (6)$$

where, V_i represents the linear volume estimated by the depth of penetration (d_i) of a vertex from one mesh's triangle into the nearest triangle area (A_i) of the opposing STL's mesh.

$$\text{Penetration volume} = V_i = A_i \cdot d_i \quad (7)$$

Finally, ReactionForcePreOp.any measures the total forces and the moments at each of the contact models defined in ContactForcesPreOp.any. The contact model defined in ContactForcesPreOp was used as the ForceBase class and AnyForceMomentMeasure2 class was used to measure the forces and moments. Within this file, forces and moments in all direction were also computed.

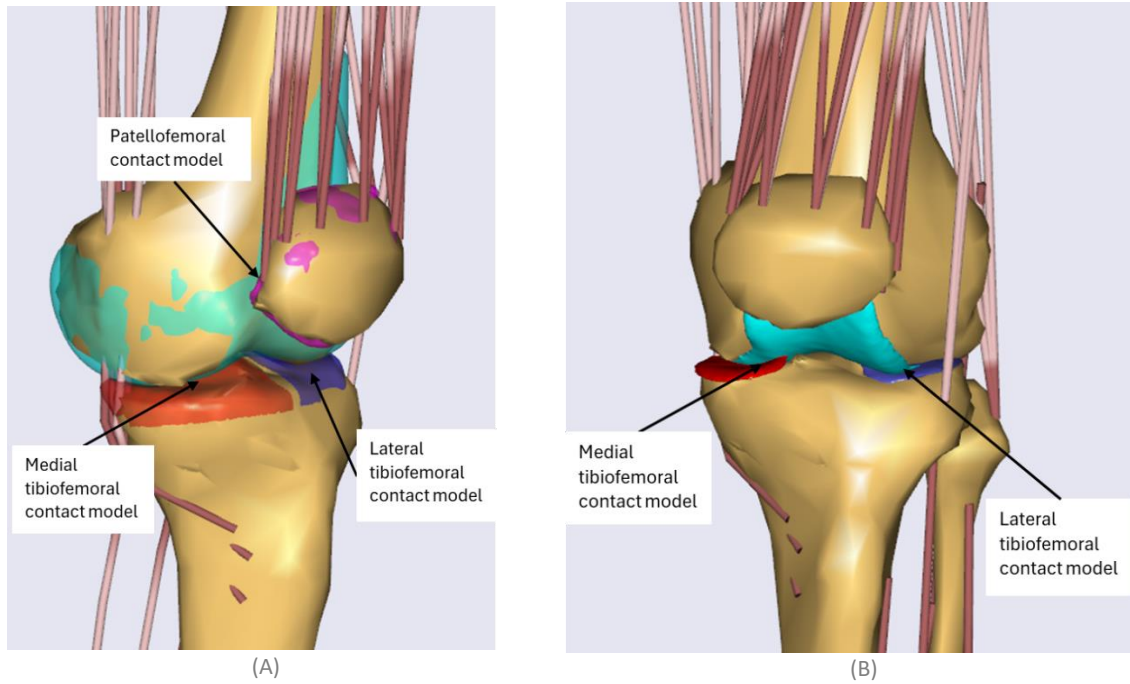


Figure 21 Contact surfaces configuration on the left knee. (A) Contact surfaces were defined as bone offsets. Bone surfaces for each contact model were defined (colored surfaces). Then, an offset that represented the cartilage thickness was used to scale these bones, so they signify cartilages. (B) Contact surfaces were defined based on the segmented cartilages. Note that the patella cartilage was not used because the patella bone used within this workflow belongs to another subject (as described in 2.3) whose cartilage was not segmented. However, it was used for the purpose of building the workflow.

2.7.2 Ligament Model

The workflow lacks the development of the ligament model. For future perspectives, the model should be investigated and incorporated in the current workflow because it is required as it provides stability to the unconstrained joints in the FDK (Force-dependent kinematic) model. There are four files within the model that are used to build such a model. They can be found in Inverse "Dynamic.any" file under the following subscripts "Knee LigamentGeometry.any", "LineLigamentMeasure.any", "LigamentParameters.any", and "Ligament Model.any".

3. Discussion

This study aimed to critically describe workflow steps that would enable simulating an image-based, motion-capture-driven personalized MS model based on partial femur and tibia MRI bone scans which to our knowledge no other studies have adopted it. To achieve this, partial MRI scans of the tibia and femur were taken, and motion capture data was collected using markers attached exclusively to the lower extremities. Morphing accuracy was evaluated with the maximum morphing error between the morphed source landmark to the corresponding target landmark at 4.25mm for the femur, 6.40mm for the tibia, and 5.13mm for the patella. Additionally, an error of 3 degrees of flexion (about z axis) was found between the tibia coordinate systems defined with the malleoli markers and the generic model ankle center. The optimization of the model parameters appeared to be quite sensitive to the marker's placement in the gait lab. Contact surfaces can be configured with bone offsets that represent cartilage thickness, or using segmented cartilages directly. The implementation of the current workflow reveals that using partial bones introduces several limitations, increased complexity, and uncertainty in the modeling framework due to the lack of data on the proximal femur and distal tibia.

Morphing discrepancy (less overlapping between source and target bones) was clear at the region highlighted within the yellow rectangle in **Fig. 22**. This outcome was anticipated due to the absence of selected landmarks in that region, as there are no distinct landmarks available for selection. At this region, three muscle attachments (Sartorius, Gracilis, and Semitendinosus) exist which subsequently were not morphed. It is known that morphing has influence on muscles architecture (84). In fact, the level of morphing changes the muscle behavior by altering the moment arm and line of action. Marra et al., for instance, mentioned that for accurate MS personalization, better morphing is required to modify muscle attachment sites, as the forces generated by muscles are significantly affected by their moment arm and line of action during movement (32). While this might be true, it might not be applied to all muscles. A study showed that the muscle attachments with long distances showed low sensitivity to attachment site variations and deviations (71). It is also worth mentioning that, in this protocol, morphing was regionally limited. The attachment sites of the model were maintained (not morphed) at the proximal femur and distal tibia due to incomplete scans. Moreover, biceps femoris muscle attachment sites, highlighted within the red rectangle, at the fibula head were not morphed because the fibula bone was not segmented from the MRI scans; thus, not included in the morphing. The effect of these limitations remains unknown, and no study has investigated that since partial bone morphing has not been adopted before. Therefore, to realize the effect, validation of the model is required. The methods used to validate such models are highlighted below (last paragraphs).

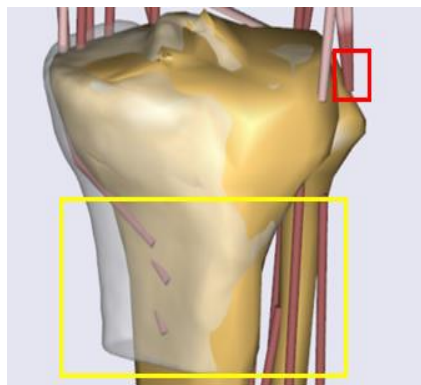


Figure 22 Discrepancy (less overlapping) between generic morphed bone (Gold) and the target bone (transparent white) in tibia bone morphing. Yellow rectangle shows the region where discrepancy was the highest mainly because no landmarks were selected for the morphing process. As a result, the three muscle attachments were not morphed. The red rectangle locates the insertion points of the biceps femoris muscles on the fibula head. This region was not morphed as well because fibula bone was not segmented from the MRI scan.

Since the landmarks were manually selected and representing bony prominences, it remains challenging to identify them accurately due to the lack of a guiding protocol for landmark selection on the bone (85). That said, the discrepancy is attributed to the low number of landmarks (e.g., 11 landmarks) used for the morphing algorithm on the proximal tibia. Additionally, the selection of landmarks was subjective and thus susceptible to human error. For example, the corresponding landmarks chosen for morphing might not precisely match on both bones, and the user may select a point that does not accurately represent a distinct bony landmark. In this workflow, the maximum morphing error of the tibia, femur, and patella were 6.40mm, and 4.25mm, and 5.13mm respectively. This range of error, however, remains reasonable because according to (30), the maximal acceptable morphing

error should be smaller than 10mm. Moreover, these errors appeared in regions with more curvatures, aligning with the findings in (71). Additionally, the morphing algorithm seemed sensitive to the number of the landmarks. This was found when adding an additional landmark at the anterior edge of the lateral region of the tibia (**Fig. 23**). The added landmark reduced the morphing error of landmark J from 6.40mm to 5.59mm. However, it was noticed that the new maximum morphing error appeared at a different landmark (landmark H) at 5.72mm. Observably, the new maximum morphing error was lower than the previous one (6.40mm). This was expected because it was reported that increasing the number of landmarks affects the accuracy of morphing (84).

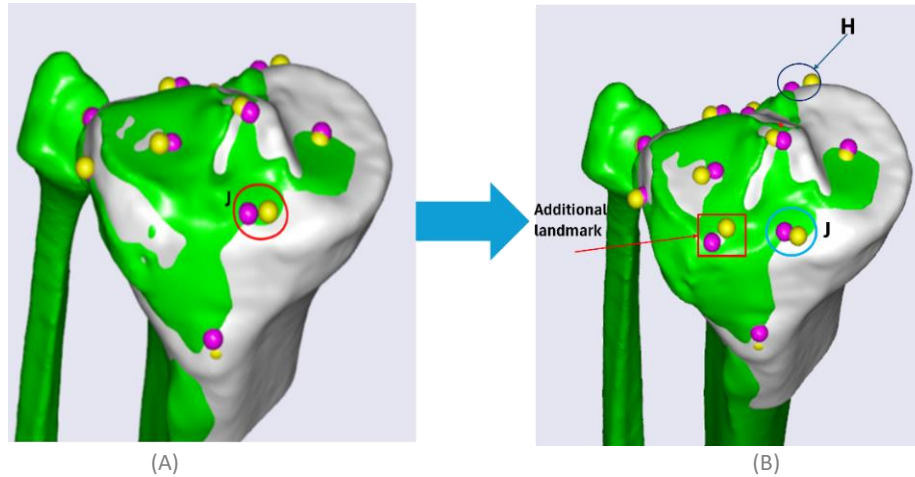


Figure 23 Improving the morphing accuracy with additional landmark. (A) The maximum morphing error was recorded at landmark J at 6.40mm. (B) Adding one landmark (highlighted within the red square) improved the accuracy of morphing. The maximum morphing error (6.40mm) which was observed at landmark J dropped to 5.59mm after adding the landmark. The new maximum error was recorded at 5.72mm but was located at another landmark (landmark H).

Since the ultimate goal of building this workflow is to feed Finite Element (FE) model with contact forces at the knee for personalized cartilage testing, it was observed that the accuracy of morphing may have an impact on the contact model configuration and eventually the contact force. Initially, the contact surfaces did not appear to be consistent across the tibial plateau (**Fig. 24.A**). This might be due to the fact that partial morphing in this workflow relied on a low number of landmarks for the morphing process. However, after adding the landmark (described above), the contact surfaces appeared to be consistent over the tibia plateau possibly because this landmark improved the morphing accuracy as mentioned above (**Fig. 24.B**). A study investigated the contact forces at the knee joint reported that different morphing and scaling techniques utilized for the MS models led to discrepancy in contact forces at the medial tibia compartment (41). Muscle forces give support during daily activities which in turn, defines the forces at the joint. Any discrepancy in the contact forces should be investigated within the architecture of the model (e.g., moment arms, muscle strength, and joint axes (32). It is also known that that the contact force depends on the penetration depth (32), which may be influenced by the configuration of contact surfaces. Therefore, improved morphing would lead to more consistent and reliable contact surface configuration which would ensure accurate estimation of contact forces. This underscores the need to explore approaches to enhance morphing (i.e., Glue&Cut Method described below) to prepare the model for use in the TopTreat project.

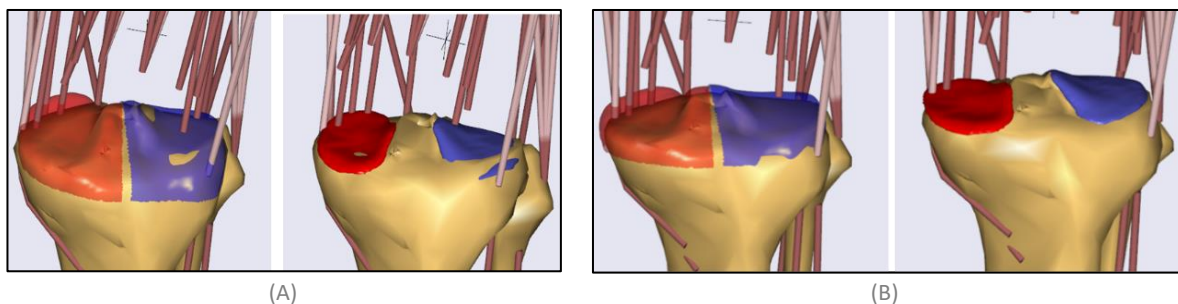


Figure 24 Contact surfaces configuration over the tibia plateau. (A) Contact surfaces (bone offsets/ cartilages) inconsistency over the lateral tibial plateau due to the limited number of landmarks (11 landmarks). (B) Contact surfaces consistency after adding a marker at the anterior edge of the lateral tibia region. This landmark improved morphing accuracy; thus, may result in better contact surfaces consistency.

It remains difficult to find a better method to enhance the morphing level with partial bones. Although some studies suggested methods to partially morph the bone, all of them still rely on the entire bone scan (e.g., for training their model). A study, for instance, applied statistical shape method to morph the proximal femur structure using statistical shape model (86,87). However, this method adds more complexity to the current workflow because it requires a trained dataset that requires the whole bone for surface morphing training. Additionally, the morphing is still constrained by a set of landmarks that are manually selected. Then, Principal Component Analysis (PCA) is performed to extract some bone features but none of these features includes landmarks which AnyBody software utilizes for morphing. Therefore, this method is not feasible to be integrated into the workflow. However, since the main solution is to utilize as many corresponding landmarks as possible in the morphing algorithm, a Glue&Cut approach might be applicable. The idea is to initially glue the target bone (i.e., proximal tibia) to the proximal end of the source tibia bone (**Fig. 25.A**). Secondly, cut the source bone by using the edge of the target bone mesh. This would result in two bones (proximal source and proximal target) with the same topology at the proximal region of the tibia (**Fig. 25.B**). With this, preprocessing of the bones meshes is required. Using MeshLab, the meshes can be adjusted so that both bones have the same number of vertices and faces. There is no specific number to adhere to. However, the more vertices the mesh has the more landmarks can be extracted for morphing. The reason of doing this is to allow STL_Vertices function predefined in AnyBody software to be able to pick up as many corresponding landmarks as possible for the morphing algorithm. A piece of code detailing the extraction of the corresponding landmarks has been included in **Appendix H**. The advantage of this method is that it provides a semi-automated approach, eliminates human error with landmarks selection, and uses more landmarks for morphing.

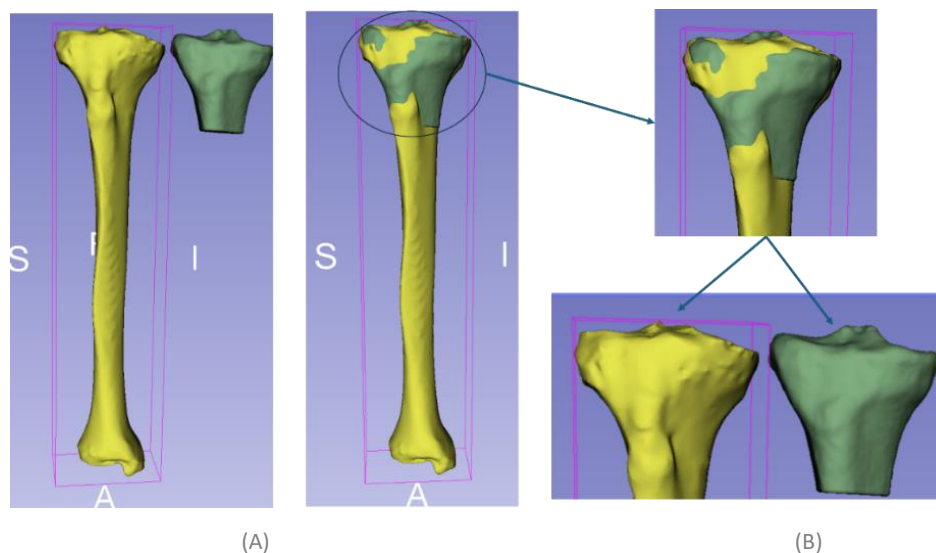


Figure 25 Glue&Cut method to improve partial morphing. (A) Target bone (green) is glued to the source bone (yellow). In a software like 3D slicer, both bones can be loaded. The target bone is then transformed to the proximal end of the source tibia bone. Once both bones are aligned properly (Glue), the user can identify where to cut the source bone. (B) After gluing the target bone, the user can cut the source bone with the help of the target bone edges. The result of this method is two bones having the same topology. Then the user can use STL_Vertices in AnyBody modelling system to extract the corresponding landmarks.

Coordinate systems to measure knee kinematics, in this workflow, were defined with the generic bone hip and ankle centers. This, of course, introduced some uncertainty about the neutral position of the knee, which is depicted with the vertical axes on the thigh and shank being aligned, because the scaled hip and ankle centers do not represent the subject's bony landmarks. Although it was possible to define the tibial coordinate system with the makers locations of the malleoli, the femoral coordinate system was not possible to be obtained through the markers attached to the pelvis, or thigh. This is because it is quite challenging to locate the hip center with such markers especially due to the absence of the great trochanter marker. A study managed to estimate the hip center using markers on the lateral and medial femoral condyles, pelvis, thigh segment plates and greater trochanters (88). The study highlighted that the hip joint center was calculated based on regression equation made by (89). Since the greater trochanter markers were not used within the current workflow, considering this method is not applicable. This introduces the need to an alternative method to calculate the origin of the femur head (hip center) of the femoral coordinate system. Analytical surface fitting technique to clinical images has been utilized in the literature. For example, (17,32) utilized this technique to accurately obtain joint centers and axes for the femoral head, PF and TF joints. The center of the hip joint can be determined through a spherical fit to the femoral head.

This method eliminates the human error of selecting the relevant bony landmarks to define tracking frames based on ISB protocol (90). In fact, obtaining joint positions from patient-specific images has been demonstrated to be a reliable approach within the context of MS simulations (91). Therefore, it is better to apply this method to obtain the coordinate system for the femur and optionally for the tibial coordinate system because it was achievable with the malleoli markers and patella was fully scanned. However, this still requires the information at the proximal femur which can be obtained through MRI scanning. For future perspectives, at least, scanning the femur head should be considered. Interestingly, it is practical to scan regions of interest of the lower leg while skipping the remaining regions (**Fig. 26**). For instance, it is possible to scan the proximal femur region to extract the femur head. Subsequently, the femur shaft can be skipped in the scan to reduce the scanning time and scan the proximal tibia and distal femur directly while maintaining the same scanning setup to preserve the anthropometric distance consistency. Lastly, the tibia shaft can also be skipped and scan the distal tibial region only. The femur head can be fitted with a sphere (92) to obtain the origin of the femur head (hip center). Then, the femur coordinate system can be defined based on femoral medial and lateral epicondyles as outlined in section 2.5.2, with the center of the femur head replacing the generic model hip center.

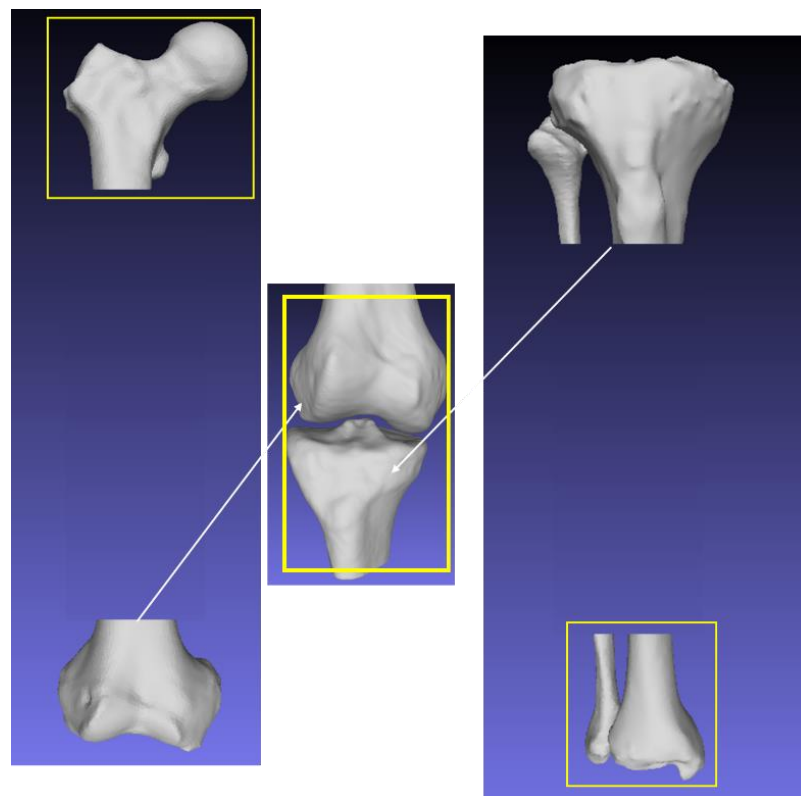


Figure 26 Scanning the regions of interest of the lower leg. A localizer sequence can be used to select the field of view (the lower leg). Then, femur head can be scanned first, the femur shaft can be skipped, and the knee joint can be scanned. Note that it is important to maintain the same scanning setup and field of view; otherwise, scans will be distorted. The anthropometric distance can be maintained between, for instance, the femur head and the distal femur bone with the same setup and localizer sequence. Finally, the tibial shaft can be skipped, and the distal tibia can be scanned similar to the femur head. Eventually, the regions within the yellow rectangles will be output of the MRI scan which captures the missing data needed in this study's protocol.

Given the abovementioned limitations, one critical element of the model is how to validate it. Evaluating if the model's predictions correspond with experimental measurements from real-life scenarios is crucial. Joint reaction and muscle forces are the common output variables from a model (93). So, an ideal validation process would aim to conform these variables against experimental measurements (94); this is known as direct validation. But direct validation of muscle forces is impractical since there is not a direct method to measure the forces of the muscle in vivo. However, another method involves using EMG, that monitors the electrical signals from muscles and offers a technique to validate the models indirectly. In this protocol, 16 EMG electrodes were used to measure the muscle activation of 16 muscles in the lower extremity (as described in section 2.4). It is possible to utilize the measured EMGs to eventually validate the model prior using it for TopTreat project because the current model was designed to predict EMG signals. The prediction of EMG signals was incorporated into the inverse dynamic study routine defined in AnyBody (95). The routine includes a criterion for muscle activation that can be customized based on

the user's specific application. For instance, two relevant studies (17,32) utilized a polynomial cost function of power three (96) for their muscle recruitment problem which was also considered in this workflow.

A direct method for validating musculoskeletal (MS) models is by evaluating joint kinematics (9). Technology such as bi-planar fluoroscopy, including EOS imaging (97), has been developed to estimate knee joint motion in vivo under different loading conditions. The method records bi-planar scans and reconstructs 3D bone trajectory in real-time. It has been exploited to explore the rotations and translations of the PF and TF joints while performing some dynamic movements (98) because it is impractical to obtain accurate measurements of the knee joint translations and rotations using the traditional motion capture method (9). For this reason, this technology has been considered by researchers to obtain knee secondary kinematics (99–101). A recent study utilized this method to capture right kinematics knee in vivo during a quasi-static lunge at 90, 60, 45, and 20 degrees of tibiofemoral flexion for the purpose of validating its model (17). Unfortunately, this method was not considered in the current workflow. However, it might be beneficial to account for it in the future.

4. Conclusion

In summary, the current workflow possesses several limitations mainly due to the lack of information at the proximal femur and distal tibia (incomplete MRI scans). Initially, to establish a robust and consistent contact model, it became evident that enhancements in morphing were necessary. This can be achieved with the Glue&Cut method proposed in the discussion section. Additionally, hip and ankle centers of the generic model were not feasibly applicable to be used to define the femoral and tibial tracking reference frames as they introduced uncertainty in the knee neutral position. While malleoli marker locations can be used to define tibia coordinate system, scanning the femur head is required to be able to obtain the femur head/ hip center and subsequently defining its coordinate system origin and axes. Finally, MoCap markers should be carefully placed during the gait lab experiment as they impact the optimization process. Specifically, the marker on the 2nd metatarsal should be placed on the tip of the 2nd toe to avoid misplacement and uncertainty on the marker location. The ligament model should be added and incorporated in the model. An ideal situation for building a subject specific MS model is through the utilization of full leg bones. Eventually, it is essential to validate the model generated by this workflow because of the modifications it introduces to bone and muscle architecture before utilizing it for the TopTreat project.

References

1. Chu CR, Millis MB, Olson SA. Osteoarthritis: From Palliation to Prevention. *Journal of Bone and Joint Surgery*. 2014 Aug 6;96(15):e130.
2. Lespasio MJ, Piuzzi NS, Husni ME, Muschler GF, Guarino A, Mont MA. Knee Osteoarthritis: A Primer. *Perm J*. 2017 Dec;21(4).
3. Amiri P, Davis EM, Outerleys J, Miller RH, Brandon S, Astephen Wilson JL. High tibiofemoral contact and muscle forces during gait are associated with radiographic knee OA progression over 3 years. *Knee*. 2023 Mar;41:245–56.
4. Fitzgerald GK, Piva SR, Irrgang JJ. Reports of Joint Instability in Knee Osteoarthritis: Its Prevalence and Relationship to Physical Function. 2004 [cited 2024 Jan 12]; Available from: <https://onlinelibrary.wiley.com/doi/10.1002/art.20825>
5. Lawrence RC, Felson DT, Helmick CG, Arnold LM, Choi H, Deyo RA, et al. Estimates of the prevalence of arthritis and other rheumatic conditions in the United States: Part II. *Arthritis Rheum*. 2008 Jan 28;58(1):26–35.
6. Roos EM, Arden NK. Strategies for the prevention of knee osteoarthritis. *Nat Rev Rheumatol*. 2016 Feb 6;12(2):92–101.
7. Kiadaliri AA, Lohmander S, Moradi-Lakeh M, Petersson IF, Englund M. High and rising burden of hip and knee osteoarthritis in the Nordic region, 1990-2015 Findings from the Global Burden of Disease Study 2015. *Acta Orthop [Internet]*. 2018 [cited 2024 Feb 23];89(2):177–83. Available from: <http://www.thelancet>.
8. Peitola JPJ, Esralian A, Eskelinen ASA, Andersen MS, Korhonen RK. Comparison of knee cartilage biomechanics in finite element analysis using inputs from AnyBody and OpenSim. 2023 Oct 23 [cited 2024 Mar 8]; Available from: <https://www.researchsquare.com>
9. Dzialo CM. Personalized musculoskeletal modeling: Bone morphing, knee joint modeling, and applications. 2018 [cited 2024 Feb 9]; Available from: <https://vbn.aau.dk/da/publications/personalized-musculoskeletal-modeling-bone-morphing-knee-joint-mo>
10. Mahir L, Belhaj K, Zahi S, Azanmasso H, Lmidmani F, El Fatimi A. Impact of knee osteoarthritis on the quality of life. *Ann Phys Rehabil Med [Internet]*. 2016;59:e159. Available from: <https://www.sciencedirect.com/science/article/pii/S1877065716304365>
11. Dell'Isola A, Allan R, Smith SL, Marreiros SSP, Steultjens M. Identification of clinical phenotypes in knee osteoarthritis: a systematic review of the literature. *BMC Musculoskelet Disord*. 2016 Dec 12;17(1):425.
12. Scanzello CR, Goldring SR. The role of synovitis in osteoarthritis pathogenesis. *Bone*. 2012 Aug;51(2):249–57.
13. Orłowsky EW, Kraus VB. The Role of Innate Immunity in Osteoarthritis: When Our First Line of Defense Goes On the Offensive. *J Rheumatol*. 2015 Mar;42(3):363–71.

14. Malfait AM. Osteoarthritis year in review 2015: biology. *Osteoarthritis Cartilage*. 2016 Jan;24(1):21–6.
15. Li G, Yin J, Gao J, Cheng TS, Pavlos NJ, Zhang C, et al. Subchondral bone in osteoarthritis: insight into risk factors and microstructural changes. *Arthritis Res Ther* [Internet]. 2013 Dec 9 [cited 2024 May 31];15(6):223. Available from: [/pmc/articles/PMC4061721/](https://pubmed.ncbi.nlm.nih.gov/22118977/)
16. Zeighami A, Dumas R, Kanhonou M, Hagemester N, Lavoie F, de Guise JA, et al. Tibio-femoral joint contact in healthy and osteoarthritic knees during quasi-static squat: A bi-planar X-ray analysis. *J Biomech* [Internet]. 2017 Feb 28 [cited 2024 Feb 9];53:178–84. Available from: <https://pubmed.ncbi.nlm.nih.gov/28118977/>
17. Dejtjar DL, Dzialo CM, Pedersen PH, Jensen KK, Fleron MK, Andersen MS. Development and evaluation of a subject-specific lower limb model with an eleven-degrees-of-freedom natural knee model using magnetic resonance and biplanar x-ray imaging during a quasi-static lunge. *J Biomech Eng*. 2020;142:061001.
18. Manal K, Buchanan TS. An electromyogram-driven musculoskeletal model of the knee to predict in vivo joint contact forces during normal and novel gait patterns. *J Biomech Eng* [Internet]. 2013 [cited 2024 Feb 9];135(2). Available from: <https://pubmed.ncbi.nlm.nih.gov/23445059/>
19. Lund ME, Andersen MS, de Zee M, Rasmussen J. Scaling of musculoskeletal models from static and dynamic trials. *Int Biomech*. 2015;2(1):1–11.
20. Hast MW, Piazza SJ. Dual-joint modeling for estimation of total knee replacement contact forces during locomotion. *J Biomech Eng* [Internet]. 2013 Feb 1 [cited 2024 Feb 12];135(2). Available from: <https://dx.doi.org/10.1115/1.4023320>
21. Rasmussen J, Damsgaard M, Voigt M. Muscle recruitment by the min/max criterion - A comparative numerical study. *J Biomech* [Internet]. 2001 [cited 2024 Feb 9];34(3):409–15. Available from: <https://pubmed.ncbi.nlm.nih.gov/11182135/>
22. Pellikaan P, Krogt M van der, Carbone V, Verdonshot N, Koopman B. Are muscle volumes linearly scalable in musculoskeletal models? *J Biomech* [Internet]. 2012 Jul 1 [cited 2024 Feb 12];45(Suppl. 1):S498. Available from: <https://research.utwente.nl/en/publications/are-muscle-volumes-linearly-scalable-in-musculoskeletal-models>
23. Handsfield GG, Meyer CH, Hart JM, Abel MF, Blemker SS. Relationships of 35 lower limb muscles to height and body mass quantified using MRI. *J Biomech*. 2014 Feb;47(3):631–8.
24. Fregly BJ, Besier TF, Lloyd DG, Delp SL, Banks SA, Pandy MG, et al. Grand challenge competition to predict in vivo knee loads. *J Orthop Res* [Internet]. 2012 Apr [cited 2024 Feb 12];30(4):503–13. Available from: <https://pubmed.ncbi.nlm.nih.gov/22161745/>
25. Carbone V, Fluit R, Pellikaan P, van der Krogt MM, Janssen D, Damsgaard M, et al. TLEM 2.0 - a comprehensive musculoskeletal geometry dataset for subject-specific modeling of lower extremity. *J Biomech* [Internet]. 2015 Mar 18 [cited 2024 Feb 9];48(5):734–41. Available from: <https://pubmed.ncbi.nlm.nih.gov/25627871/>

26. Carbone V, Krogt M van der, Koopman HFJM, Verdonschot NJJ. Functional scaling of subject-specific musculo-tendon parameters in the lower extremity. *J Biomech* [Internet]. 2012 Jul 1 [cited 2024 Feb 12];45(Suppl. 1):S492–S492. Available from: <https://research.utwente.nl/en/publications/functional-scaling-of-subject-specific-musculo-tendon-parameters->
27. Pellikaan P, van der Krogt MM, Carbone V, Fluit R, Vigneron LM, Van Deun J, et al. Evaluation of a morphing based method to estimate muscle attachment sites of the lower extremity. *J Biomech* [Internet]. 2014 Mar 21 [cited 2024 Feb 9];47(5):1144–50. Available from: <https://pubmed.ncbi.nlm.nih.gov/24418197/>
28. Thelen DG, Choi KW, Schmitz AM. Co-simulation of neuromuscular dynamics and knee mechanics during human walking. *J Biomech Eng* [Internet]. 2014 Feb 1 [cited 2024 Feb 12];136(2). Available from: <https://dx.doi.org/10.1115/1.4026358>
29. Roemer FW, Eckstein F, Hayashi D, Guermazi A. The role of imaging in osteoarthritis. *Best Pract Res Clin Rheumatol*. 2014 Feb;28(1):31–60.
30. Carbone V, van der Krogt MM, Koopman HFJM, Verdonschot N. Sensitivity of subject-specific models to errors in musculo-skeletal geometry. *J Biomech*. 2012 Sep;45(14):2476–80.
31. Guess TM, Stylianou AP, Kia M. Concurrent prediction of muscle and tibiofemoral contact forces during treadmill gait. *J Biomech Eng* [Internet]. 2014 Feb 1 [cited 2024 Feb 12];136(2). Available from: <https://dx.doi.org/10.1115/1.4026359>
32. Marra MA, Vanheule V, Fluit R, Koopman BHFJM, Rasmussen J, Verdonschot N, et al. A subject-specific musculoskeletal modeling framework to predict in vivo mechanics of total knee arthroplasty. *J Biomech Eng*. 2015;137:020904.
33. Andersen MS, Damsgaard M, MacWilliams B, Rasmussen J. A computationally efficient optimisation-based method for parameter identification of kinematically determinate and over-determinate biomechanical systems. *Comput Methods Biomech Biomed Engin* [Internet]. 2010 [cited 2024 Feb 9];13(2):171–83. Available from: <https://www.tandfonline.com/doi/abs/10.1080/10255840903067080>
34. Robertson DGE, Caldwell GE, Hamil J, Kamen G, Whittlesey SN. Research Methods in Biomechanics. *J Sports Sci Med* [Internet]. 2014 [cited 2024 Feb 9];13(1):i. Available from: [/pmc/articles/PMC3918575/](https://pubmed.ncbi.nlm.nih.gov/24418197/)
35. Fregly BJ, Boninger ML, Reinkensmeyer DJ. Personalized neuromusculoskeletal modeling to improve treatment of mobility impairments: A perspective from European research sites. *J Neuroeng Rehabil* [Internet]. 2012 Mar 30 [cited 2024 May 29];9(1):1–11. Available from: <https://jneuroengrehab.biomedcentral.com/articles/10.1186/1743-0003-9-18>
36. Fregly BJ, D’Lima DD, Colwell CW. Effective gait patterns for offloading the medial compartment of the knee. *J Orthop Res* [Internet]. 2009 Aug [cited 2024 Feb 9];27(8):1016–21. Available from: <https://pubmed.ncbi.nlm.nih.gov/19148939/>
37. Ardestani MM, Moazen M, Jin Z. Gait modification and optimization using neural network-genetic algorithm approach: Application to knee rehabilitation. *Expert Syst Appl*. 2014 Nov 15;41(16):7466–77.

38. Uhlich SD, Silder A, Beaupre GS, Shull PB, Delp SL. Subject-specific toe-in or toe-out gait modifications reduce the larger knee adduction moment peak more than a non-personalized approach. *J Biomech*. 2018 Jan 3;66:103–10.
39. Caldwell LK, Laubach LL, Barrios JA. Effect of specific gait modifications on medial knee loading, metabolic cost and perception of task difficulty. *Clinical Biomechanics*. 2013 Jul 1;28(6):649–54.
40. Miller RH, Esterson AY, Shim JK. Joint contact forces when minimizing the external knee adduction moment by gait modification: A computer simulation study. *Knee*. 2015 Dec 1;22(6):481–9.
41. Dzialo CM, Mannisi M, Halonen KS, de Zee M, Woodburn J, Andersen MS. Gait alteration strategies for knee osteoarthritis: a comparison of joint loading via generic and patient-specific musculoskeletal model scaling techniques. *Int Biomech [Internet]*. 2019 Jan 1 [cited 2024 Feb 9];6(1):54. Available from: /pmc/articles/PMC7857308/
42. Halonen KS, Dzialo CM, Mannisi M, Venäläinen MS, De Zee M, Andersen MS. Workflow assessing the effect of gait alterations on stresses in the medial tibial cartilage - combined musculoskeletal modelling and finite element analysis. *Scientific Reports* 2017 7:1 [Internet]. 2017 Dec 12 [cited 2024 Feb 9];7(1):1–14. Available from: <https://www.nature.com/articles/s41598-017-17228-x>
43. Petersen ET, Rytter S, Koppens D, Dalsgaard J, Hansen TB, Larsen NE, et al. Patients with knee osteoarthritis can be divided into subgroups based on tibiofemoral joint kinematics of gait - an exploratory and dynamic radiostereometric study. *Osteoarthritis Cartilage [Internet]*. 2022 Feb 1 [cited 2024 May 29];30(2):249–59. Available from: <https://pubmed.ncbi.nlm.nih.gov/34757027/>
44. Fregly BJ, Boninger ML, Reinkensmeyer DJ. Personalized neuromusculoskeletal modeling to improve treatment of mobility impairments: A perspective from European research sites. *J Neuroeng Rehabil [Internet]*. 2012 Mar 30 [cited 2024 May 29];9(1):1–11. Available from: <https://jneuroengrehab.biomedcentral.com/articles/10.1186/1743-0003-9-18>
45. de Campos GC, Tieppo AM, de Almeida CS, Hamdan PC, Alves WM, de Rezende MU. Target-based approach for osteoarthritis treatment. *World J Orthop [Internet]*. 2020 Jun 6 [cited 2024 May 29];11(6):278. Available from: /pmc/articles/PMC7298451/
46. Semelka RC, Armao DM, Elias J, Huda W. Imaging strategies to reduce the risk of radiation in CT studies, including selective substitution with MRI. *Journal of Magnetic Resonance Imaging [Internet]*. 2007 May 1 [cited 2024 Jun 4];25(5):900–9. Available from: <https://onlinelibrary.wiley.com/doi/full/10.1002/jmri.20895>
47. Halonen KS, Dzialo CM, Mannisi M, Venäläinen MS, De Zee M, Andersen MS. Workflow assessing the effect of gait alterations on stresses in the medial tibial cartilage - combined musculoskeletal modelling and finite element analysis. *Scientific Reports* 2017 7:1 [Internet]. 2017 Dec 12 [cited 2024 Mar 8];7(1):1–14. Available from: <https://www.nature.com/articles/s41598-017-17228-x>
48. Andersen MS, De Zee M, Damsgaard M, Nolte D, Rasmussen J. Introduction to force-dependent kinematics: Theory and application to mandible modeling. *J Biomech Eng*

[Internet]. 2017 Sep 1 [cited 2024 Mar 8];139(9). Available from:
<https://dx.doi.org/10.1115/1.4037100>

49. Mononen ME, Tanska P, Isaksson H, Korhonen RK. A Novel Method to Simulate the Progression of Collagen Degeneration of Cartilage in the Knee: Data from the Osteoarthritis Initiative. *Scientific Reports* 2016 6:1 [Internet]. 2016 Feb 24 [cited 2024 Mar 8];6(1):1–14. Available from: <https://www.nature.com/articles/srep21415>
50. Astephen JL, Deluzio KJ, Caldwell GE, Dunbar MJ, Hubley-Kozey CL. Gait and neuromuscular pattern changes are associated with differences in knee osteoarthritis severity levels. *J Biomech*. 2008 Jan 1;41(4):868–76.
51. Fernandez J, Zhang J, Heidlauf T, Sartori M, Besier T, Röhrle O, et al. Multiscale musculoskeletal modelling, data–model fusion and electromyography-informed modelling. *Interface Focus* [Internet]. 2016 Apr 6 [cited 2024 Mar 8];6(2). Available from: <https://royalsocietypublishing.org/doi/10.1098/rsfs.2015.0084>
52. Navacchia A, Hume DR, Rullkoetter PJ, Shelburne KB. A computationally efficient strategy to estimate muscle forces in a finite element musculoskeletal model of the lower limb. *J Biomech*. 2019 Feb 14;84:94–102.
53. Marouane H, Shirazi-Adl A, Adouni M. Alterations in knee contact forces and centers in stance phase of gait: A detailed lower extremity musculoskeletal model. *J Biomech*. 2016 Jan 25;49(2):185–92.
54. Esrafilian A, Stenroth L, Mononen ME, Tanska P, Avela J, Korhonen RK. EMG-Assisted Muscle Force Driven Finite Element Model of the Knee Joint with Fibril-Reinforced Poroelastic Cartilages and Menisci. *Scientific Reports* 2020 10:1 [Internet]. 2020 Feb 20 [cited 2024 Mar 8];10(1):1–16. Available from: <https://www.nature.com/articles/s41598-020-59602-2>
55. Esrafilian A, Stenroth L, Mononen ME, Tanska P, Van Rossom S, Lloyd DG, et al. 12 Degrees of Freedom Muscle Force Driven Fibril-Reinforced Poroelastoc Finite Element Model of the Knee Joint. *IEEE Trans Neural Syst Rehabil Eng* [Internet]. 2021 [cited 2024 Mar 8];29:123–33. Available from: <https://pubmed.ncbi.nlm.nih.gov/33175682/>
56. Esrafilian A, Stenroth L, Mononen ME, Vartiainen P, Tanska P, Karjalainen PA, et al. An EMG-Assisted Muscle-Force Driven Finite Element Analysis Pipeline to Investigate Joint- and Tissue-Level Mechanical Responses in Functional Activities: Towards a Rapid Assessment Toolbox. *IEEE Trans Biomed Eng*. 2022 Sep 1;69(9):2860–71.
57. Tanska P, Mononen ME, Korhonen RK. A multi-scale finite element model for investigation of chondrocyte mechanics in normal and medial meniscectomy human knee joint during walking. *J Biomech*. 2015 Jun 1;48(8):1397–406.
58. Baliunas AJ, Hurwitz DE, Ryals AB, Karrar A, Case JP, Block JA, et al. Increased knee joint loads during walking are present in subjects with knee osteoarthritis. *Osteoarthritis Cartilage* [Internet]. 2002 [cited 2024 Mar 8];10(7):573–9. Available from: <https://pubmed.ncbi.nlm.nih.gov/12127838/>
59. Richards RE, Andersen MS, Harlaar J, van den Noort JC. Relationship between knee joint contact forces and external knee joint moments in patients with medial knee

- osteoarthritis: effects of gait modifications. *Osteoarthritis Cartilage* [Internet]. 2018 Sep 1 [cited 2024 Mar 8];26(9):1203–14. Available from: <https://pubmed.ncbi.nlm.nih.gov/29715509/>
60. Wilson W, van Burken C, van Donkelaar CC, Buma P, van Rietbergen B, Huiskes R. Causes of mechanically induced collagen damage in articular cartilage. *Journal of Orthopaedic Research* [Internet]. 2006 Feb 1 [cited 2024 Mar 8];24(2):220–8. Available from: <https://onlinelibrary.wiley.com/doi/full/10.1002/jor.20027>
 61. Eskelinen ASA, Tanska P, Florea C, Orozco GA, Julkunen P, Grodzinsky AJ, et al. Mechanobiological model for simulation of injured cartilage degradation via pro-inflammatory cytokines and mechanical stimulus. *PLoS Comput Biol* [Internet]. 2020 Jun 1 [cited 2024 Mar 8];16(6):e1007998. Available from: <https://journals.plos.org/ploscompbiol/article?id=10.1371/journal.pcbi.1007998>
 62. Orozco GA, Tanska P, Florea C, Grodzinsky AJ, Korhonen RK. A novel mechanobiological model can predict how physiologically relevant dynamic loading causes proteoglycan loss in mechanically injured articular cartilage. *Scientific Reports* 2018 8:1 [Internet]. 2018 Oct 22 [cited 2024 Mar 8];8(1):1–16. Available from: <https://www.nature.com/articles/s41598-018-33759-3>
 63. Eskelinen ASA, Mononen ME, Venäläinen MS, Korhonen RK, Tanska P. Maximum shear strain-based algorithm can predict proteoglycan loss in damaged articular cartilage. *Biomech Model Mechanobiol* [Internet]. 2019 Jun 15 [cited 2024 Mar 8];18(3):753–78. Available from: <https://link.springer.com/article/10.1007/s10237-018-01113-1>
 64. Esrafilian A, Stenroth L, Mononen ME, Vartiainen P, Tanska P, Karjalainen PA, et al. Toward Tailored Rehabilitation by Implementation of a Novel Musculoskeletal Finite Element Analysis Pipeline. *IEEE Trans Neural Syst Rehabil Eng* [Internet]. 2022 [cited 2024 Mar 8];30:789–802. Available from: <https://pubmed.ncbi.nlm.nih.gov/35286263/>
 65. GitHub - MIC-DKFZ/nnUNet [Internet]. [cited 2024 Jun 20]. Available from: <https://github.com/MIC-DKFZ/nnUNet>
 66. Ambellan F, Tack A, Ehlke M, Zachow S. Automated segmentation of knee bone and cartilage combining statistical shape knowledge and convolutional neural networks: Data from the Osteoarthritis Initiative. *Med Image Anal*. 2019 Feb 1;52:109–18.
 67. Recommendations for sensor locations in lower leg or foot muscles [Internet]. [cited 2024 Jul 3]. Available from: http://seniam.org/lowerleg_location.htm
 68. Vicon Nexus User Guide - Nexus 2.16 documentation - Vicon Help [Internet]. [cited 2024 Jun 18]. Available from: <https://help.vicon.com/space/Nexus216/11605325/Vicon+Nexus+User+Guide>
 69. Damsgaard M, Rasmussen J, Christensen ST, Surma E, de Zee M. Analysis of musculoskeletal systems in the AnyBody Modeling System. *Simul Model Pract Theory*. 2006 Nov 1;14(8):1100–11.
 70. Lesson 1: Personalizing individual segments based on geometric data from medical images — AnyBody Tutorials v8.0.3 [Internet]. [cited 2024 Jun 19]. Available from: <https://anyscript.org/tutorials/Scaling/lesson1.html>

71. Pellikaan P, van der Krogt MM, Carbone V, Fluit R, Vigneron LM, Van Deun J, et al. Evaluation of a morphing based method to estimate muscle attachment sites of the lower extremity. *J Biomech* [Internet]. 2014 Mar 21 [cited 2024 Jun 25];47(5):1144–50. Available from: <https://pubmed.ncbi.nlm.nih.gov/24418197/>
72. Grood ES, Suntay WJ. A joint coordinate system for the clinical description of three-dimensional motions: application to the knee. *J Biomech Eng* [Internet]. 1983 [cited 2024 May 14];105(2):136–44. Available from: <https://pubmed.ncbi.nlm.nih.gov/6865355/>
73. Chocron O. Handout No 2. 2000 [cited 2024 Jul 8]; Available from: <https://web.mit.edu/2.05/www/Handout/HO2.PDF>
74. lower body c3d file into GaitLowerExtremity - Main Forum - AnyScript forum [Internet]. [cited 2024 Jul 4]. Available from: <https://forum.anyscript.org/t/lower-body-c3d-file-into-gaitlowerextremity/1289>
75. Winter DA. Biomechanics and Motor Control of Human Movement: Fourth Edition. *Biomechanics and Motor Control of Human Movement: Fourth Edition* [Internet]. 2009 Sep 17 [cited 2024 May 7];1–370. Available from: <https://onlinelibrary.wiley.com/doi/book/10.1002/9780470549148>
76. Bogin B, Varela-Silva MI. Leg Length, Body Proportion, and Health: A Review with a Note on Beauty. *International Journal of Environmental Research and Public Health* 2010, Vol 7, Pages 1047-1075 [Internet]. 2010 Mar 11 [cited 2024 Jul 1];7(3):1047–75. Available from: <https://www.mdpi.com/1660-4601/7/3/1047/htm>
77. Segments length optimization - Main Forum - AnyScript forum [Internet]. [cited 2024 Jun 26]. Available from: <https://forum.anyscript.org/t/segments-length-optimization/7691/5>
78. Effect of partial morphing - Main Forum - AnyScript forum [Internet]. [cited 2024 Jul 1]. Available from: <https://forum.anyscript.org/t/effect-of-partial-morphing/7705>
79. Qin S, Li M, Jia Y, Gao W, Xu J, Zhang B, et al. How Do the Morphological Abnormalities of Femoral Head and Neck, Femoral Shaft and Femoral Condyle Affect the Occurrence and Development of Medial Knee Osteoarthritis. *Orthop Surg* [Internet]. 2023 Dec 1 [cited 2024 Jul 1];15(12):3174–81. Available from: <https://onlinelibrary.wiley.com/doi/full/10.1111/os.13910>
80. C3D.ORG - The biomechanics standard file format [Internet]. [cited 2024 Jun 24]. Available from: <https://www.c3d.org/>
81. Home · AnyBody/support Wiki · GitHub [Internet]. [cited 2024 Jun 8]. Available from: <https://github.com/anybody/support/wiki>
82. Cohen ZA, McCarthy DM, Kwak SD, Legrand P, Fogarasi F, Ciaccio EJ, et al. Knee cartilage topography, thickness, and contact areas from MRI: in-vitro calibration and in-vivo measurements. *Osteoarthritis Cartilage*. 1999 Jan 1;7(1):95–109.
83. Burgkart R, Glaser C, Hyhlik-Dürr A, Englmeier KH, Reiser M, Eckstein F. Magnetic Resonance Imaging-Based Assessment of Cartilage Loss in Severe Osteoarthritis Accuracy, Precision, and Diagnostic Value. *Arthritis Rheum* [Internet]. 2001 [cited 2024

Jul 4];44(9):2072–7. Available from:
<https://onlinelibrary.wiley.com/doi/10.1002/1529-0131>

84. Appendix: Morphing based on landmarks — AnyBody Tutorials v8.0.3-1 [Internet]. [cited 2024 Jun 25]. Available from:
https://anyscript.org/tutorials/Scaling/lesson1_appendix.html
85. Suggestion landmarks for morphing - Main Forum - AnyScript forum [Internet]. [cited 2024 Jun 25]. Available from: <https://forum.anyscript.org/t/suggestion-landmarks-for-morphing/2536>
86. Rajamani KT, Hug J, Nolte LP, Styner M, Müller ME. Bone morphing with statistical shape models for enhanced visualization. <https://doi.org/10.1117/12535000> [Internet]. 2004 May 5 [cited 2024 Jun 25];5367:122–30. Available from:
<https://www.spiedigitallibrary.org/conference-proceedings-of-spie/5367/0000/Bone-morphing-with-statistical-shape-models-for-enhanced-visualization/10.1117/12.535000.full>
87. Hraiech N, Boichon C, Rochette M, Marchal T, Horner M. Statistical shape modeling of femurs using morphing and principal component analysis. *Journal of Medical Devices, Transactions of the ASME* [Internet]. 2010 [cited 2024 Jul 2];4(2):1–1. Available from:
https://www.researchgate.net/publication/239403907_Statistical_Shape_Modeling_of_Femurs_Using_Morphing_and_Principal_Component_Analysis
88. Lopez S, Johnson C, Frankston N, Ruh E, McClincy M, Anderst W. Accuracy of conventional motion capture in measuring hip joint center location and hip rotations during gait, squat, and step-up activities. *J Biomech*. 2024 Apr 1;167:112079.
89. Bell AL, Brand RA, Pedersen DR. Prediction of hip joint centre location from external landmarks. *Hum Mov Sci*. 1989 Feb 1;8(1):3–16.
90. Wu G, Siegler S, Allard P, Kirtley C, Leardini A, Rosenbaum D, et al. ISB recommendation on definitions of joint coordinate system of various joints for the reporting of human joint motion—part I: ankle, hip, and spine. *J Biomech*. 2002 Apr 1;35(4):543–8.
91. Martelli S, Valente G, Viceconti M, Taddei F. Sensitivity of a subject-specific musculoskeletal model to the uncertainties on the joint axes location. *Comput Methods Biomech Biomed Engin* [Internet]. 2015 Oct 26 [cited 2024 Jun 26];18(14):1555–63. Available from:
<https://www.tandfonline.com/doi/abs/10.1080/10255842.2014.930134>
92. Sphere Fit (least squared) - File Exchange - MATLAB Central [Internet]. [cited 2024 Jul 3]. Available from: <https://nl.mathworks.com/matlabcentral/fileexchange/34129-sphere-fit-least-squared>
93. Marra MA. Personalized musculoskeletal modeling of the knee joint.
94. Lund ME, de Zee M, Andersen MS, Rasmussen J. On validation of multibody musculoskeletal models. *Proc Inst Mech Eng H*. 2012 Feb 25;226(2):82–94.

95. Inverse Dynamics of Muscle Systems — AnyBody Tutorials v8.0.3-1 [Internet]. [cited 2024 Jun 27]. Available from:
<https://anyscript.org/tutorials/MuscleRecruitment/index.html>
96. Lesson 4: Polynomial Muscle Recruitment — AnyBody Tutorials v8.0.3-1 [Internet]. [cited 2024 Jun 27]. Available from:
<https://anyscript.org/tutorials/MuscleRecruitment/lesson4.html>
97. Azmy C, Guérard S, Bonnet X, Gabrielli F, Skalli W. EOS® orthopaedic imaging system to study patellofemoral kinematics: Assessment of uncertainty. *Orthopaedics & Traumatology: Surgery & Research*. 2010 Feb 1;96(1):28–36.
98. Myers CA, Torry MR, Shelburne KB, Giphart JE, Laprade RF, Woo SLY, et al. In vivo tibiofemoral kinematics during 4 functional tasks of increasing demand using biplane fluoroscopy. *American Journal of Sports Medicine* [Internet]. 2012 Jan 13 [cited 2024 Jun 27];40(1):170–8. Available from:
<https://journals.sagepub.com/doi/10.1177/0363546511423746>
99. Kozanek M, Hosseini A, Liu F, Van de Velde SK, Gill TJ, Rubash HE, et al. TIBIOFEMORAL KINEMATICS AND CONDYLAR MOTION DURING THE STANCE PHASE OF GAIT. *J Biomech* [Internet]. 2009 Aug 8 [cited 2024 Jun 27];42(12):1877. Available from:
[/pmc/articles/PMC2725209/](https://pubmed.ncbi.nlm.nih.gov/1925209/)
100. Myers CA, Torry MR, Shelburne KB, Giphart JE, Laprade RF, Woo SLY, et al. In vivo tibiofemoral kinematics during 4 functional tasks of increasing demand using biplane fluoroscopy. *American Journal of Sports Medicine* [Internet]. 2012 Jan 13 [cited 2024 Jun 27];40(1):170–8. Available from:
<https://journals.sagepub.com/doi/10.1177/0363546511423746>
101. Clément J, Dumas R, Hagemester N, de Guise JA. Soft tissue artifact compensation in knee kinematics by multi-body optimization: Performance of subject-specific knee joint models. *J Biomech*. 2015 Nov 5;48(14):3796–802.

Appendices

Appendix A: C3D Files and Respective Activities

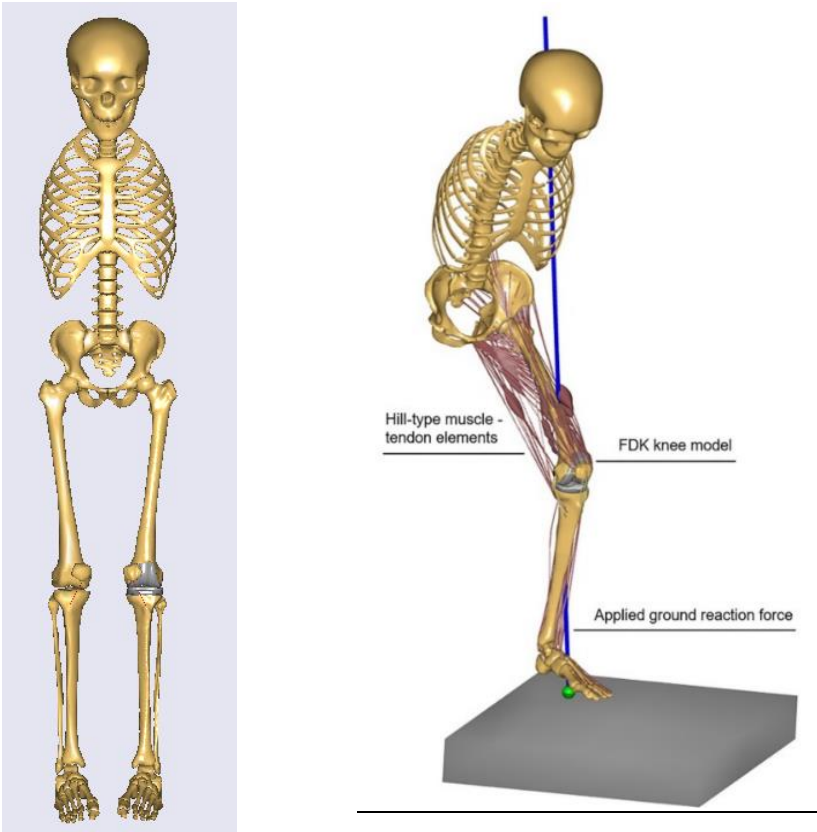
Trial name	Activity
2024032701.C3D and 2024032702.C3D	Static trials - subject standing quiet
2024032703.C3D until 2024032716.C3D	Walking trials
The following files contain proper foot contacts on the force plates for both feet: 2024032706.C3D, 2024032707.C3D, 2024032709.C3D, 2024032711.C3D, 2024032712.C3D, 2024032714.C3D, 2024032715.C3D and 2024032716.C3D	
2024032717.C3D, 2024032718.C3D and 2024032719.C3D contain data for stepping down with the left foot on the force plate.	Stepping off
2024032720.C3D, 2024032721.C3D and 2024032722.C3D contain data for stepping down with the right foot on the force plate.	
2024032727.C3D, 2024032728.C3D and 2024032729.C3D	Squatting

Appendix B: MoCap Markers' label renaming

Table 5 Marker location and the respective name it should be assigned with for AnyBody software integration.

Marker location (Figure 5)	The assigned name
Right anterior superior iliac spine	RAsis
Left anterior superior iliac spine	LAsis
Right posterior superior iliac spine	RPsis
Left posterior superior iliac spine	RPsis
Right Thigh superior	RThighSuperior
Right Thigh lateral	RThighLateral
Right Thigh inferior	RThighInferior
Right Medial knee	RKneeMedial
Right Lateral knee	RKneeLateral
Right Shank superior	RShankSuperior
Right Shank lateral	RShankLateral
Right Shank inferior	RShankInferior
Right Medial malleolus	RAnkleMedial
Right Lateral malleolus	RAnkleLateral
Right Distal 1 st metatarsal	RToeMedial
Right Distal 2 nd metatarsal	RToe
Right Distal 5 th metatarsal	RToeLateral
Right 2 nd metatarsal	RMidfootSuperior
Right heel	RHeel
Left Thigh superior	LThighSuperior
Left Thigh lateral	LThighLateral
Left Thigh inferior	LThighInferior
Left Medial knee	LKneeMedial
Left Lateral knee	LKneeLateral
Left Shank superior	LShankSuperior
Left Shank lateral	LShankLateral
Left Shank inferior	LShankInferior
Left Medial malleolus	LAnkleMedial
Left Lateral malleolus	LAnkleLateral
Left Distal 1 st metatarsal	LToeMedial
Left Distal 2 nd metatarsal	LToe
Left Distal 5 th metatarsal	LToeLateral
Left 2 nd metatarsal	LMidfootSuperior
Left heel	LHeel

Appendix C: Template Model



Marco Marra model from GC 2014 (32)

Appendix D: Femur Landmarks

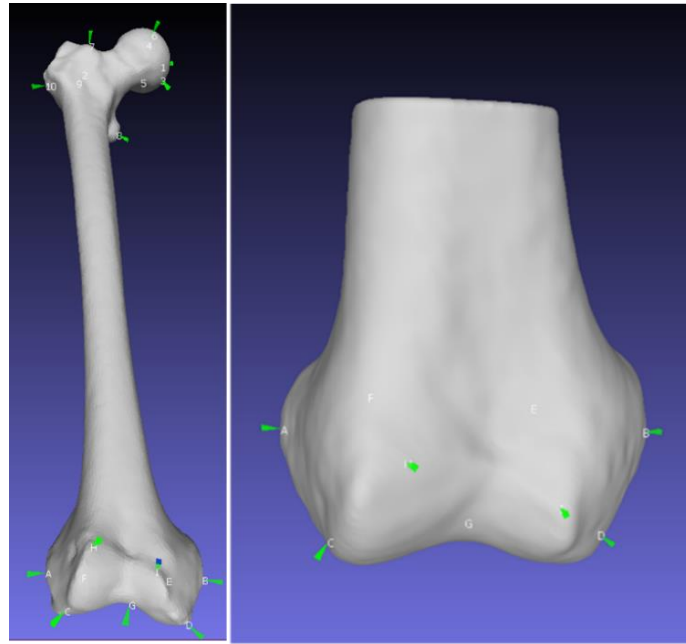




Table 6 List of landmarks used for partial femur morphing based on Figure 9

Proximal landmark	Number	Distal landmarks	Letter	MeshLab file
Fovea capitis	1	Lateral epicondyle	A	Source landmarks:  Femur_source_picked _points.pp
Greater Trochanter	2	Medial epicondyle	B	
Femur Head Inferior	3	Distal lateral resection	C	Target landmarks:  Linda_femur_picked_p oints.pp
Femur Head Superior	4	Distal medial resection	D	
Femur Head Posterior	5	Posterior medial resection	E	
Femur Head Anterior	6	Posterior lateral resection	F	
Anterior Trochanter	7	Trochanter center	G	
Posterior Trochanter	8	Lateral peak	H	
Femur Head Fossa	9	Medial peak	I	
Lateral Trochanter	10			

Appendix E: Tibia and Patella Landmarks

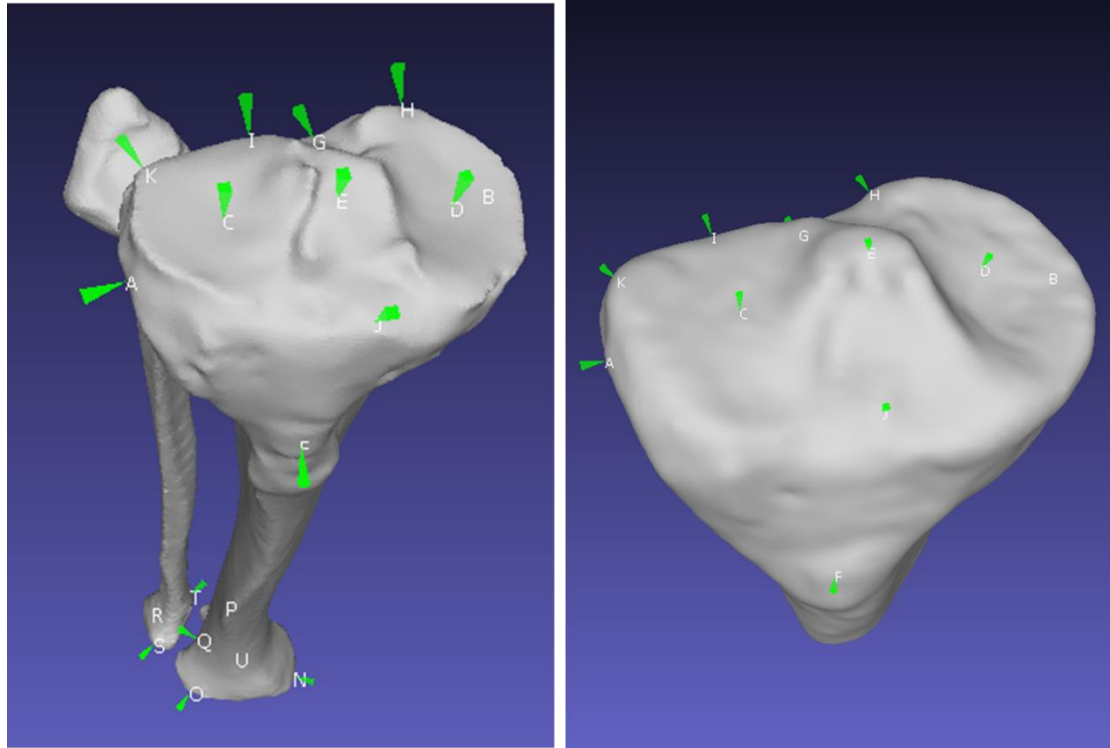




Figure 27 Tibia landmarks used for partial tibia morphing. Left: Landmarks selected on the source bone, right: landmarks selected on the target bone

Table 7 List of landmarks used for partial tibia morphing.

Proximal landmark	Letter	Distal landmarks	Letter	MeshLab picked-points file
Lateral condyle	A	Medial malleolus	N	Source landmarks
Medial condyle	B	Anterior malleolus	O	 Tibiafibula_source_picked_points.pp
Lateral tibial resection	C	Posterior malleolus	P	
Medial tibial resection	D	Malleolus fossa	Q	Target landmarks:  Linda_Tibia_picked_points.pp
Tibial knee center	E	Bottom fibula	R	
Anterior tibial rotational	F	Anterior bottom fibula	S	
Posterior tibial rotational	G	Posterior bottom fibula	T	
Posterior medial tibial rotational	H	Bottom tibia	U	
Posterior lateral tibial rotational	I			
Anterior tibia	J			
Posterior lateral tibia	K			

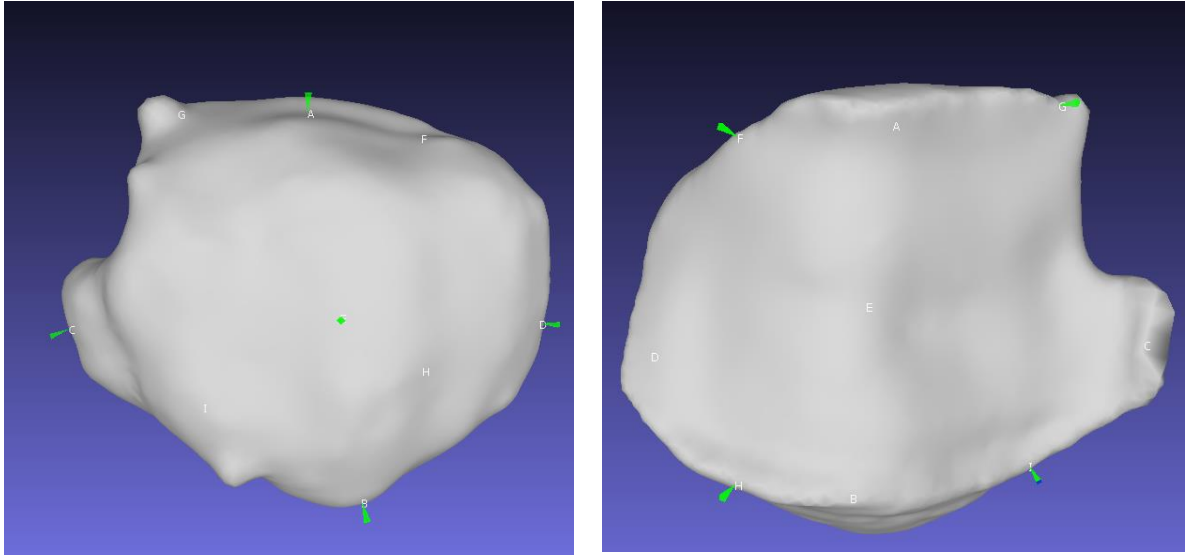




Figure 28 Patella landmarks for patella morphing; left (anterior view), right (posterior view)

Table 8 List of landmarks used for patella morphing.

Landmark	Letter	MeshLab picked-points file
Patella base	A	Source landmarks:  Patella_source_picked_points.pp
Patella apex	B	
Lateral border	C	
Medial border	D	
Patella belly	E	
Superior-medial border	F	Target landmarks:  Patella_target_picked_points.pp
Superior-lateral border	G	
Inferior-medial border	H	
Inferior-lateral border	I	

Appendix F.1: Right Knee Morphing

```

AnyFolder SubjectSpecificScaling =
{
  AnyFolder Source = {
    #include "SourceSTLs.any"
  };
  AnyFolder Target = {
    #include "TargetSTLs.any"
  };

  AnyFolder Right =
  {
    AnyFolder Shank =
    {

#if InverseDynamicModel== 0 | INV_DYN_EXCLUDE_RIGHT_LEG == 0
  // TSeg2ScaleFrame transforms source entities to the scaling frame (Pre-defined in the model)
  AnyFunTransform3D &TSeg2ScaleFrame = ..BodyModel.Right.Leg.Seg.Shank.Scale.T0;
  // Anthropometric scaling (in this case Uniform scaling law) to control the length of the bone:
  AnyFunTransform3D &AnthropometricScaling =
Main.Studies.HumanModel.Scaling.Scaling.GeometricalScaling.Right.Shank.ScaleFunction; //To scale the length of the
shank to the subject's shank length

  // Landmarks to be used for partial scaling: proximal and distal source landmarks and proximal target
landmarks
  // Proximal landmarks for morphing the proximal part of the shank (region of interest):
  AnyMatrix proximal_tibial_landmarks_source =
  {
    {-3.73991, 325.037, 38.1545}*0.001, //A
    {1.53631, 320.754, -38.6415}*0.001, //B
    {-0.78102088, 331.89825, 19.865219}*0.001, //C
    {3.2023861, 328.15952, -23.625978}*0.001, //D
    {-2.62091, 336.765, -2.6878}*0.001, //E
    {32.696163, 300.36832, 10.931908}*0.001, //F
    {-23.028795, 319.39224, -5.6062117}*0.001, //G
    {-22.6758, 325.479, -22.7989}*0.001, //H
    {-20.8676, 326.536, 9.02121}*0.001, //I
    {26.1913, 334.097, -0.0629725}*0.001, //J
    {-21.5649, 320.47, 29.081}*0.001, //K
    {17.7141, 333.82, 18.9313}*0.001 //newpoint1 (additional landmark)
  };

  //Fake landmarks to control the distla part of the shank (obtained from the distal part of the source shank):
  AnyMatrix distal_tibial_landmarks_source =
  {
    {20.925146, 6.5778065, -26.710907}*0.001, //MedMalleolus
    {18.156538, 15.352763, 17.543905}*0.001, //AntMalleolus
    {-13.426257, 12.377143, -6.296061}*0.001, //PostrMalleolus
    {-1.012019, 19.532932, 9.9422092}*0.001, //Malleolus fossa
    {-24.919279, -14.116476, 22.652632}*0.001, //BottomFibula
    {-7.0291848, 5.1006417, 26.307983}*0.001, //AntBottomFibula
    {-23.858505, 4.5135241, 6.7474461}*0.001, //PostrBottomFibula
    {8.339242, 9.1078835, -4.8120413}*0.001 //Bottom Tibia
  };

  // Proximal landmarks for morphing the proximal part of the shank
  AnyMatrix proximal_tibial_landmarks_target =
  {
    {-87.709061, 23.179075, -10.374002 }*0.001, //A
    {-17.481573, 36.884048, -14.64732 }*0.001, //B
    {-68.371178, 24.572445, -4.3031507 }*0.001, //C
    {-31.35747, 31.967342, -6.8477278 }*0.001, //D
    {-49.815659, 28.02079, 1.7582881 }*0.001, //E
    {-57.746017, -1.10416, -35.023369 }*0.001, //F
    {-56.765385, 48.046593, -11.288908 }*0.001, //G
    {-44.755947, 51.979549, -7.3099227 }*0.001, //H
    {-64.4467, 44.0938, -5.56098 }*0.001, //I
    {-51.05154, 7.2466393, -8.2094469 }*0.001, //J
    {-85.520149, 40.196625, -10.986394 }*0.001, //K
    {-70.9997, 5.34935, -8.54293 }*0.001 //newpoint1 (additional landmark)
  };

  // A rigid body transformation to align proximal target bone with the expected anthropometrically scaled
generic bone:
  AnyFunTransform3DLin2 RegProximallandmarks = {
    Points0 = .proximal_tibial_landmarks_target;
    Points1 = .AnthropometricScaling(.proximal_tibial_landmarks_source);
    //Mode = VTK_LANDMARK_RIGIDBODY; //By default it is RIGIDBODY transformation
  };

  AnyMatrix P0 = arccat (
    distal_tibial_landmarks_source,
    proximal_tibial_landmarks_source

```

```

);

AnyMatrix P1 = arccat (
    AnthropometricScaling(distal_tibial_landmarks_source),
    RegProximalLandmarks(proximal_tibial_landmarks_target)
);

AnyFunTransform3Dlin2 reg = {
    PreTransforms = {&.AnthropometricScaling}; //To control the length of the bone
    Points0 = .TSeg2ScaleFrame(.P0); // TSeg2ScaleFrame esures that scaling is applied properly (You can find
info about it in AnyBody Forum)
    Points1 = .P1;
    Mode = VTK_LANDMARK_AFFINE;
};

AnyFunTransform3DRBF rbf = {
    PreTransforms = {&.reg};
    RBFDef.Type = RBF_Triharmonic;
    PolynomDegree = 1;
    Points0 = .reg.Points0; //Using the same source points in the affine transformation
    Points1 = .reg.Points1; //Using the same target points in the affine transformation
    BoundingBoxOnOff = On;
    BoundingBox.Type = BB_Cartesian;
    BoundingBox.ScaleXYZ = {2,2,2}*2;
    BoundingBox.DivisionFactorXYZ = {1,1,1}*3;
};

// To bring all entities to the model reference frame:
AnyFunTransform3Dlin2 inv = {
    Points0=.reg.Points1;
    Points1=.reg.Points0;
    Mode = VTK_LANDMARK_RIGIDBODY;
};

//To register any STL, nodes etc.. Only proximal landmarks are used because these points belong to each STL
seperately (Using P0 and P1 does not work):
AnyFunTransform3Dlin2 RegistrationTransform = {
    Points0 = Main.Studies.HumanModel.SubjectSpecificScaling.Right.Shank.proximal_tibial_landmarks_target;
//Try points without the fake points (same for points1)
    Points1 =
Main.Studies.HumanModel.BodyModel.Right.Leg.Seg.Shank.Scale(Main.Studies.HumanModel.SubjectSpecificScaling.Right.Sh
ank.proximal_tibial_landmarks_source);
    Mode = VTK_LANDMARK_RIGIDBODY;
};

// Applying RBF and inverse transformations to the model bone for morphing:
AnyFunTransform3Didentity ScaleFunction = {
//     ScaleMat = {{1,0,0},{0,1,0},{0,0,1}};
//     Offset = {0,0,0};
//     PreTransforms = {&.AnthropometricScaling, &.rbf, &.inv};
    PreTransforms = {&.rbf, &.inv};
};

#endif
};

// The process described for the shank is similar for the thigh except for the change (proximal --> distal)
because distal part is the region of interest:
AnyFolder Thigh =
{
#if InverseDynamicModel== 0 | INV_DYN_EXCLUDE_RIGHT_LEG == 0
    AnyFunTransform3D &TSeg2ScaleFrame = ...BodyModel.Right.Leg.Seg.Thigh.Scale.T0;
    AnyFunTransform3D &AnthropometricScaling =
Main.Studies.HumanModel.Scaling.Scaling.GeometricalScaling.Right.Thigh.ScaleFunction;

// Landmarks to be used for partial morphing
AnyMatrix distal_femur_landmarks_source =
{
    {1.4667782, -7.5853477, 40.188442}*0.001,
    {-1.3872523, -7.2713323, -42.379215}*0.001,
    {10.828313, -25.093184, 28.204765}*0.001,
    {-1.2590836, -28.866749, -33.724697}*0.001,
    {-32.232922, -6.8122239, -26.237719}*0.001,
    {-24.200073, -7.6667924, 21.916771}*0.001,
    {8.2392998, -20.800543, -3.7793131}*0.001,
    {37.3533, 2.90245, 16.3532}*0.001,
    {30.2449, -6.11178, -14.9986}*0.001
};

AnyMatrix proximal_femur_landmarks_source =
{
    {-10.852421, 364.76874, -16.379839}*0.001, // Fovea capitis
    {-19.912188, 362.50815, 45.109447}*0.001, // GTroch
    {-5.6486459, 345.51443, -16.411469}*0.001, // FHInferior
    {-7.7841983, 383.60883, -4.7216892}*0.001, // FHSuperior

```

```

    {-26.837152, 364.57211, -1.9582478}*0.001, // FHPosterior
    {16.8262, 364.84927, -7.9468064}*0.001, // FHAnterior
    {19.468042, 347.74265, 37.701233}*0.001, // AnteriorTroch
    {-23.268379, 307.04941, 15.143285}*0.001, // PosteriorTroch
    {-10.340069, 342.99069, 47.364712}*0.001, // FHFossa
    {1.5367945, 326.92096, 69.202797}*0.001 // LateralTroch
};

AnyMatrix distal_femur_landmarks_target =
{
    {-84.080986, 16.148844, 23.621426 }*0.001,
    {-6.3988762, 21.174944, 22.413633 }*0.001,
    {-72.88195, 6.6869726, 3.1665409 }*0.001,
    {-15.23773, 17.9653, -0.32281268 }*0.001,
    {-28.150251, 48.55592, 17.956514 }*0.001,
    {-68.966331, 41.242916, 22.455288 }*0.001,
    {-44.91415, 10.987182, 5.6923642 }*0.001,
    {-55.113194, -18.12281, 31.525492 }*0.001,
    {-28.581356, -10.463104, 20.333908 }*0.001
};

AnyFunTransform3Dlin2 RegProximalLandmarks =
{
    Points0 = .distal_femur_landmarks_target;
    Points1 = .AnthropometricScaling(.distal_femur_landmarks_source);
    //Mode = VTK_LANDMARK_RIGIDBODY; //Pavel did not use this line
};

AnyMatrix P0 = arccat (
    proximal_femur_landmarks_source,
    distal_femur_landmarks_source
);
AnyMatrix P1 = arccat (
    AnthropometricScaling(proximal_femur_landmarks_source),
    RegProximalLandmarks(distal_femur_landmarks_target)
);

AnyFunTransform3Dlin2 reg = { //Affine transformation
    PreTransforms = {&.AnthropometricScaling};
    Points0 = .TSeg2ScaleFrame(.P0);
    Points1 = .P1;
    Mode = VTK_LANDMARK_AFFINE;
};

AnyFunTransform3DRBF rbf = {
    PreTransforms = {&.reg};
    RBFDef.Type = RBF_Triharmonic;
    PolynomDegree = 1;
    Points0 = .reg.Points0;
    Points1 = .reg.Points1;
    BoundingBoxOnOff = On;
    BoundingBox.Type = BB_Cartesian;
    BoundingBox.ScaleXYZ = {1,1,1}*2;
    BoundingBox.DivisionFactorXYZ = {1,1,1}*5;
};

AnyFunTransform3Dlin2 inv = {
    Points0=.reg.Points1;
    Points1=.reg.Points0;
    Mode = VTK_LANDMARK_RIGIDBODY;
};

AnyFunTransform3Dlin2 RegistrationTransform = {
    Points0 = Main.Studies.HumanModel.SubjectSpecificScaling.Right.Thigh.distal_femur_landmarks_target; //Try
    points without the fake points (same for points1)
    Points1 =
    Main.Studies.HumanModel.BodyModel.Right.Leg.Seg.Thigh.Scale(Main.Studies.HumanModel.SubjectSpecificScaling.Right.Thigh.distal_femur_landmarks_source);
    Mode = VTK_LANDMARK_RIGIDBODY;
};

AnyFunTransform3DIdentity ScaleFunction = {
//    ScaleMat = {{1,0,0},{0,1,0},{0,0,1}};
//    Offset = {0,0,0};
    PreTransforms = {&.rbf, &.inv};
};

#endif
};
// Using direct morphing as in the tutorials:
AnyFolder Patella = {
#if InverseDynamicModel== 0 | INV_DYN_EXCLUDE_RIGHT_LEG == 0

#if STL_VERTICES_BASED_AFFINE_TRANSFORM == 0
    AnyFunTransform3Dlin2 AffineTransform =

```

```

{
  Points0 =
  {
    { -1.6161, 15.6771, 2.1432}*0.001 ,
    { 2.7866, -20.7290, 0.5057}*0.001,
    { 1.2818, 1.8216, 22.4619}*0.001,
    { 5.4503, 2.2603, -19.4518}*0.001,
    { 9.3115, -0.1980, 0.3074}*0.001,
    { -8.9995, 16.7536, -8.1021}*0.001,
    { -7.0651, 16.4740, 11.3233}*0.001,
    { -7.5038, -11.8735, -11.0086}*0.001,
    { -3.0860, -12.6480, 11.8364}*0.001
  };

  Points1 =
  {
    { 0.4197, -14.7245, -11.2685}*0.001,
    { 6.2192, 13.5610, 14.8240}*0.001,
    { -4.7543, 16.9626, -17.5548}*0.001,
    { 5.9572, -11.4507, 19.9053}*0.001,
    { 12.2253, 0.0409, 0.0052}*0.001,
    { -5.4724, -22.0833, 1.3320}*0.001,
    { -8.6438, -8.0622, -21.5758}*0.001,
    { -8.7171, -0.9614, 19.4212}*0.001,
    { -7.1259, 16.8070, -0.6811}*0.001
  };
  Mode = VTK_LANDMARK_AFFINE;
};

// The following method can be used if the source and target patella have the same topology (same NO.of
// vertices, and faces).
// However, it is not used here. Instead Landmarks were utilized above.
#else
AnyFunTransform3DLin2 AffineTransform = {
  AnyFileVar SourceSTL = FilePathCompleteOf(...Source.Right.FilenamePatella) + ".stl";
  AnyFileVar TargetSTL = FilePathCompleteOf(...Target.Right.FilenamePatella) + ".stl";
  Points0 = STL_Vertices(SourceSTL, iarr(0, floor(NumPoints0/NumPoints), NumPoints0 - 1), 1)*0.001;
  Points1 = STL_Vertices(TargetSTL, iarr(0, floor(NumPoints1/NumPoints), NumPoints1 - 1), 1)*0.001;
  AnyInt NumPoints0 = STL_Size(SourceSTL, 1)[0];
  AnyInt NumPoints1 = STL_Size(TargetSTL, 1)[0];
  AnyVar NumPoints = ...NumPointsAffine;
  Mode = VTK_LANDMARK_AFFINE;
};
#endif

AnyFunTransform3DLin2 ReverseTransform = {
  Points0 = .AffineTransform.Points1;
  Points1 = .AffineTransform.Points0;
  Mode = VTK_LANDMARK_RIGIDBODY;
};

AnyFunTransform3DLin2 RegistrationTransform = {
  Points0 = .AffineTransform.Points1;
  Points1 = Main.Studies.HumanModel.BodyModel.Right.Leg.Seg.Patella.Scale(.AffineTransform.Points0);
  Mode = VTK_LANDMARK_RIGIDBODY;
};

AnyFunTransform3DRBF RBF=
{
  PreTransforms = {&.AffineTransform};
  RBFDef.Type = RBF_Triharmonic;
  PolynomDegree = 1;
  Points0 = .AffineTransform.Points0;
  Points1 = .AffineTransform.Points1;
  BoundingBoxOnOff = On;
  BoundingBox.Type = BB_Cartesian;
  BoundingBox.ScaleXYZ = {2,2,2}*2;
  BoundingBox.DivisionFactorXYZ = {1,1,1}*3;
};

AnyFunTransform3DIdentity ScaleFunction = {
  // ScaleMat = {{1,0,0},{0,1,0},{0,0,1}};
  // Offset = {0,0,0};
  PreTransforms = {&.RBF , &.ReverseTransform};
};
#endif
}; // Right

```

Appendix F.2: Left Knee Morphing (Mirrored)

```
AnyFolder Left =
{
  AnyFolder Shank =
  {
    AnyFunTransform3D &TSeg2ScaleFrame = ...BodyModel.Left.Leg.Seg.S Shank.Scale.T0;
    AnyFunTransform3D &AnthropometricScaling =
Main.Studies.HumanModel.Scaling.Scaling.GeometricalScaling.Left.S Shank.ScaleFunction;

    AnyMatrix AMirroring = {
      {1,0,0},
      {0,1,0},
      {0,0,-1}
    };

    AnyMatrix proximal_tibial_landmarks_source =
    {
      {2.4553533, 322.60641, 38.435726}*0.001, //A
      {-4.6470823, 317.59225, -35.667347}*0.001, //B
      {-0.78102088, 331.89825, 19.865219}*0.001, //C
      {3.2023861, 328.15952, -23.625978}*0.001, //D
      {1.9201577, 336.08969, -0.26364601}*0.001, //E
      {32.696163, 300.36832, 10.931908}*0.001, //F
      {-23.028795, 319.39224, -5.6062117}*0.001, //G
      {-22.6758, 325.479, -22.7989}*0.001, //H
      {-20.8676, 326.536, 9.02121}*0.001, //I
      {26.1913, 334.097, -0.0629725}*0.001, //J
      {-21.5649, 320.47, 29.081}*0.001 //K
    }*Main.Studies.HumanModel.SubjectSpecificScaling.Left.S Shank.AMirroring;

    AnyMatrix distal_tibial_landmarks_source =
    {
      {20.925146, 6.5778065, -26.710907}*0.001, //MedMalleolus
      {18.156538, 15.352763, 17.543905}*0.001, //AntMalleolus
      {-13.426257, 12.377143, -6.296061}*0.001, //PostrMalleolus
      {-1.012019, 19.532932, 9.9422092}*0.001, //Malleolus fossa
      {-24.919279, -14.116476, 22.652632}*0.001, //BottomFibula
      {-7.0291848, 5.1006417, 26.307983}*0.001, //AntBottomFibula
      {-23.858505, 4.5135241, 6.7474461}*0.001, //PostrBottomFibula
      {8.339242, 9.1078835, -4.8120413}*0.001 //Bottom Tibia
    }*Main.Studies.HumanModel.SubjectSpecificScaling.Left.S Shank.AMirroring;

    AnyMatrix proximal_tibial_landmarks_target =
    {
      { -87.709061, 23.179075, -10.374002 }*0.001,
      { -17.481573, 36.884048, -14.64732 }*0.001,
      { -68.371178, 24.572445, -4.3031507 }*0.001,
      { -31.35747, 31.967342, -6.8477278 }*0.001,
      { -49.815659, 28.02079, 1.7582881 }*0.001,
      { -57.746017, -1.10416, -35.023369 }*0.001,
      { -56.765385, 48.046593, -11.288908 }*0.001,
      { -44.755947, 51.979549, -7.3099227 }*0.001,
      { -70.79277, 42.849827, -6.0324082 }*0.001,
      { -51.05154, 7.2466393, -8.2094469 }*0.001,
      { -85.520149, 40.196625, -10.986394 }*0.001
    }*Main.Studies.HumanModel.SubjectSpecificScaling.Left.S Shank.AMirroring;

    AnyFunTransform3D Lin2 RegProximalLandmarks = { // To align proximal target bone with the expected
    anthropometrically scaled generic bone
      Points0 = .proximal_tibial_landmarks_target;
      Points1 = .AnthropometricScaling(.proximal_tibial_landmarks_source);
      //Mode = VTK_LANDMARK_RIGIDBODY; //Pavel did not use this line
    };

    AnyMatrix P0 = arccat (
      distal_tibial_landmarks_source,
      proximal_tibial_landmarks_source
    );

    AnyMatrix P1 = arccat (
      AnthropometricScaling(distal_tibial_landmarks_source),
      RegProximalLandmarks(proximal_tibial_landmarks_target)
    );

    AnyFunTransform3D Lin2 reg = {
      PreTransforms = {&.AnthropometricScaling};
      Points0 = .TSeg2ScaleFrame(.P0);
      Points1 = .P1;
      Mode = VTK_LANDMARK_AFFINE;
    };

    AnyFunTransform3D RBF rbf = {
```

```

PreTransforms = {&.reg};
RBFDef.Type = RBF_Triharmonic;
PolynomDegree = 1;
Points0 = .reg.Points0;
Points1 = .reg.Points1;
BoundingBoxOnOff = On;
BoundingBox.Type = BB_Cartesian;
BoundingBox.ScaleXYZ = {2,2,2}*2;
BoundingBox.DivisionFactorXYZ = {1,1,1}*3;
};

AnyFunTransform3Dlin2 inv = {
  Points0=.reg.Points1;
  Points1=.reg.Points0;
  Mode = VTK_LANDMARK_RIGIDBODY;
};

AnyFunTransform3Dlin2 RegistrationTransform = {
  Points0 = Main.Studies.HumanModel.SubjectSpecificScaling.Left.Shank.proximal_tibial_landmarks_target; //Try
  points without the fake points (same for points1)
  Points1 =
Main.Studies.HumanModel.BodyModel.Left.Leg.Seg.Shank.Scale(Main.Studies.HumanModel.SubjectSpecificScaling.Left.Shan
k.proximal_tibial_landmarks_source);
  Mode = VTK_LANDMARK_RIGIDBODY;
};

AnyFunTransform3DIdentity ScaleFunction = {
//   ScaleMat = {{1,0,0},{0,1,0},{0,0,1}};
//   Offset = {0,0,0};
  PreTransforms = {&.rbf, &.inv};
};

};

AnyFolder Thigh =
{
  AnyFunTransform3D &TSeg2ScaleFrame = ...BodyModel.Left.Leg.Seg.Thigh.Scale.T0;
  AnyFunTransform3D &AnthropometricScaling =
Main.Studies.HumanModel.Scaling.Scaling.GeometricalScaling.Left.Thigh.ScaleFunction;

  AnyMatrix AMirroring = {
    {1,0,0},
    {0,1,0},
    {0,0,-1}
  };

  AnyMatrix distal_femur_landmarks_source =
  {
    {1.4667782, -7.5853477, 40.188442}*0.001,
    {-1.3872523, -7.2713323, -42.379215}*0.001,
    {10.828313, -25.093184, 28.204765}*0.001,
    {-1.2590836, -28.866749, -33.724697}*0.001,
    {-32.232922, -6.8122239, -26.237719}*0.001,
    {-24.200073, -7.6667924, 21.916771}*0.001,
    {8.2392998, -20.800543, -3.7793131}*0.001,
    {37.3533, 2.90245, 16.3532}*0.001,
    {30.2449, -6.11178, -14.9986}*0.001
  }*Main.Studies.HumanModel.SubjectSpecificScaling.Left.Thigh.AMirroring;

  AnyMatrix proximal_femur_landmarks_source =
  {
    {-10.852421, 364.76874, -16.379839}*0.001, // Fovea capitis
    {-19.912188, 362.50815, 45.109447}*0.001, // GTroch
    {-5.6486459, 345.51443, -16.411469}*0.001, // FHInferior
    {-7.7841983, 383.60883, -4.7216892}*0.001, // FHSuperior
    {-26.837152, 364.57211, -1.9582478}*0.001, // FHPosterior
    {16.8262, 364.84927, -7.9468064}*0.001, // FHAnterior
    {19.468042, 347.74265, 37.701233}*0.001, // AnteriorTroch
    {-23.268379, 307.04941, 15.143285}*0.001, // PosteriorTroch
    {-10.340069, 342.99069, 47.364712}*0.001, // FHFossa
    {1.5367945, 326.92096, 69.202797}*0.001 // LateralTroch
  }*Main.Studies.HumanModel.SubjectSpecificScaling.Left.Thigh.AMirroring;

  AnyMatrix distal_femur_landmarks_target =
  {
    {-84.080986, 16.148844, 23.621426 }*0.001,
    {-6.3988762, 21.174944, 22.413633 }*0.001,
    {-72.88195, 6.6869726, 3.1665409 }*0.001,
    {-15.23773, 17.9653, -0.32281268 }*0.001,
    {-28.150251, 48.55592, 17.956514 }*0.001,
    {-68.966331, 41.242916, 22.455288 }*0.001,
    {-44.91415, 10.987182, 5.6923642 }*0.001,
    {-55.113194, -18.12281, 31.525492 }*0.001,
    {-28.581356, -10.463104, 20.333908 }*0.001
  }*Main.Studies.HumanModel.SubjectSpecificScaling.Left.Thigh.AMirroring;
};

```

```

AnyFunTransform3DLin2 RegProximallLandmarks =
{
    Points0 = .distal_femur_landmarks_target;
    Points1 = .AnthropometricScaling(.distal_femur_landmarks_source);
    //Mode = VTK_LANDMARK_RIGIDBODY; //Pavel did not use this line
};

AnyMatrix P0 = arccat (
    proximal_femur_landmarks_source,
    distal_femur_landmarks_source
);
AnyMatrix P1 = arccat (
    AnthropometricScaling(proximal_femur_landmarks_source),
    RegProximallLandmarks(distal_femur_landmarks_target)
);

AnyFunTransform3DLin2 reg = {
    PreTransforms = {&.AnthropometricScaling};
    Points0 = .TSeg2ScaleFrame(.P0);
    Points1 = .P1;
    Mode = VTK_LANDMARK_AFFINE;
};

AnyFunTransform3DRBF rbf = {
    PreTransforms = {&.reg};
    RBFDef.Type = RBF_Triharmonic;
    PolynomDegree = 1;
    Points0 = .reg.Points0;
    Points1 = .reg.Points1;
    BoundingBoxOnOff = On;
    BoundingBox.Type = BB_Cartesian;
    BoundingBox.ScaleXYZ = {1,1,1}*2;
    BoundingBox.DivisionFactorXYZ = {1,1,1}*5;
};

AnyFunTransform3DLin2 inv = {
    Points0=.reg.Points1;
    Points1=.reg.Points0;
    Mode = VTK_LANDMARK_RIGIDBODY;
};

AnyFunTransform3DLin2 RegistrationTransform = {
    Points0 = Main.Studies.HumanModel.SubjectSpecificScaling.Left.Thigh.distal_femur_landmarks_target; //
without the fake points (same for points1)
    Points1 =
Main.Studies.HumanModel.BodyModel.Left.Leg.Seg.Thigh.Scale(Main.Studies.HumanModel.SubjectSpecificScaling.Left.Thigh.distal_femur_landmarks_source);
    Mode = VTK_LANDMARK_RIGIDBODY;
};

AnyFunTransform3DIdentity ScaleFunction = {
    PreTransforms = {&.rbf, &.inv};
};

AnyFolder Patella = {
    AnyMatrix AMirroring = {
        {1,0,0},
        {0,1,0},
        {0,0,-1}
    };
};

#if STL_VERTICES_BASED_AFFINE_TRANSFORM == 0
AnyFunTransform3DLin2 AffineTransform =
{
    Points0 =
    {
        { -1.6161, 15.6771, 2.1432}*0.001*.AMirroring ,
        {2.7866, -20.7290, 0.5057}*0.001*.AMirroring,
        { 1.2818, 1.8216, 22.4619}*0.001*.AMirroring,
        { 5.4503,2.2603, -19.4518}*0.001*.AMirroring,
        { 9.3115, -0.1980, 0.3074}*0.001*.AMirroring,
        { -8.9995, 16.7536, -8.1021}*0.001*.AMirroring,
        {-7.0651,16.4740,11.3233}*0.001*.AMirroring,
        {-7.5038, -11.8735, -11.0086}*0.001*.AMirroring,
        {-3.0860, -12.6480, 11.8364}*0.001*.AMirroring
    };

    Points1 =
    {
        { 0.4197,-14.7245, -11.2685}*0.001*.AMirroring,
        {6.2192, 13.5610, 14.8240}*0.001*.AMirroring,
        {-4.7543, 16.9626, -17.5548}*0.001*.AMirroring,
        {5.9572, -11.4507, 19.9053}*0.001*.AMirroring,
    };
};
#endif

```



```

        {12.2253, 0.0409,0.0052}*0.001*.AMirroring,
        { -5.4724,-22.0833, 1.3320}*0.001*.AMirroring,
        {-8.6438,-8.0622,-21.5758}*0.001*.AMirroring,
        { -8.7171, -0.9614, 19.4212}*0.001*.AMirroring,
        { -7.1259, 16.8070, -0.6811}*0.001*.AMirroring
    };
    Mode = VTK_LANDMARK_AFFINE;
};
#else
AnyFunTransform3DLin2 AffineTransform = {
    AnyFileVar SourceSTL = FilePathCompleteOf(...Source.Right.FileNamePatella) + ".stl";
    AnyFileVar TargetSTL = FilePathCompleteOf(...Target.Right.FileNamePatella) + ".stl";
    Points0 = STL_Vertices(SourceSTL, iarr(0, floor(NumPoints0/NumPoints), NumPoints0 - 1),
1)*0.001*.AMirroring;
    Points1 = STL_Vertices(TargetSTL, iarr(0, floor(NumPoints1/NumPoints), NumPoints1 - 1),
1)*0.001*.AMirroring;
    AnyInt NumPoints0 = STL_Size(SourceSTL, 1)[0];
    AnyInt NumPoints1 = STL_Size(TargetSTL, 1)[0];
    AnyVar NumPoints = ...NumPointsAffine;
    Mode = VTK_LANDMARK_AFFINE;
};
#endif

AnyFunTransform3DLin2 ReverseTransform = {
    Points0 = .AffineTransform.Points1;
    Points1 = .AffineTransform.Points0;
    Mode = VTK_LANDMARK_RIGIDBODY;
};
AnyFunTransform3DLin2 RegistrationTransform = {
    Points0 = .AffineTransform.Points1;
    Points1 = Main.Studies.HumanModel.BodyModel.Left.Leg.Seg.Patella.Scale(.AffineTransform.Points0);
    Mode = VTK_LANDMARK_RIGIDBODY;
};

AnyFunTransform3DRBF RBF=
{
    PreTransforms = {&.AffineTransform};
    RBFDef.Type = RBF_Triharmonic;
    PolynomDegree = 1;
    Points0 = .AffineTransform.Points0;
    Points1 = .AffineTransform.Points1;
    BoundingBoxOnOff = On;
    BoundingBox.Type = BB_Cartesian;
    BoundingBox.ScaleXYZ = {2,2,2}*2;
    BoundingBox.DivisionFactorXYZ = {1,1,1}*3;
};

AnyFunTransform3DLin ScaleFunction = {
    ScaleMat = {{1,0,0},{0,1,0},{0,0,1}};
    Offset = {0,0,0};
    PreTransforms = {&.RBF, &.ReverseTransform};
};
}; // Left
}; // SubjectSpecificScaling

```

Appendix G: Rotational Error (MATLAB)

```
% Define rotation matrix A (Malleoli location)
A = [0.9945709, 0.03602191, 0.09762719;
     -0.03219507, 0.9986609, -0.04049478;
     -0.09895516, 0.03713181, 0.9943989];

% Define rotation matrix B (Generic bone ankle center)
B = [0.9951051, -0.01531953, 0.09762719;
     0.01935221, 0.9989923, -0.04049478;
     -0.09690845, 0.04218586, 0.9943989];

% Compute the transpose of A
A_T = A';

% Compute the relative rotation matrix R
R = A_T * B;

% Convert rotation matrix R to Euler angles (z-y-x convention)
% Extract the elements of the rotation matrix R
r11 = R(1,1);
r12 = R(1,2);
r13 = R(1,3);
r21 = R(2,1);
r22 = R(2,2);
r23 = R(2,3);
r31 = R(3,1);
r32 = R(3,2);
r33 = R(3,3);
root11_21 = sqrt (r11^2+r21^2);

% Calculate the Euler angles (in radians)
theta_x = atan2(r32, r33); % roll
%theta_y = atan2(-r31, root11_21); % pitch
theta_y = asin(-r31); % pitch
theta_z = atan2(r21, r11); % yaw

% Convert the Euler angles to degrees
theta_x_deg = rad2deg(theta_x);
theta_y_deg = rad2deg(theta_y);
theta_z_deg = rad2deg(theta_z);

% Display the results
fprintf('Roll (about x-axis): %e degrees\n', theta_x_deg);
fprintf('Pitch (about y-axis): %e degrees\n', theta_y_deg);
fprintf('Yaw (about z-axis): %.2f degrees\n', theta_z_deg);
```

Appendix H: Extracting Landmarks

```
// There are two folders at the top of SubjectSpecificScaling named Source and Target. Defined the STL
files (Target proximal tibia and the source proximal tibia bone produced from Glue&Cut method).

//Add the following in Shank folder:
AnyFileVar SourceSTL = FilePathCompleteOf (...Source.Right.FileNamePatella) + ".stl";
AnyFileVar TargetSTL = FilePathCompleteOf (...Target.Right.FileNamePatella) + ".stl";

// The function STL_Vertices reads each STL and returns the coordinates of a set of landmarks:
// NumPoints0 is the number of vertices in the STL file, and NumPoints is the number of the landmarks
// intended to be extracted.
// Floor () indicates how many steps is taken between one landmark and the next one. For instance, if
// NumPoints0=15,000, and NumPoints=100, the function will return 100 landmarks starting from the first
// landmark with 150 steps to the next one.
// STL vertices coordinates are expressed in mm. It is important to convert them to m by multiplying.

AnyInt NumPoints0 = STL_Size (SourceSTL, 1)[0];
AnyInt NumPoints1 = STL_Size (TargetSTL, 1)[0];
AnyVar NumPoints = ; // number of landmarks to be extracted for morphing.

AnyMatrix proximal_tibial_landmarks_source = STL_Vertices (SourceSTL, iarr (0,
floor(NumPoints0/NumPoints), NumPoints0 - 1), 1)*0.001;

AnyMatrix proximal_tibial_landmarks_target = STL_Vertices (TargetSTL, iarr (0, floor
(NumPoints1/NumPoints), NumPoints1 - 1), 1)*0.001;

// Instead of the 11 landmarks used in appendix E, use the proximal_tibial_landmarks_source and
proximal_tibial_landmarks_target landmarks defined above for the RegProximalLandmarks transformation.
// For distal landmarks (Fake landmarks), use the same landmarks defined in appendix E.
```

Appendix I: Morphing Errors

• Femur morphing errors:

Target landmarks	Source landmarks after morphing	Point	Error (mm)
{{-0.000614093, -0.006329669, 0.03766277}},	{{0.0006271375, -0.007742251, 0.03906446}},	A	2.3454
{{-0.0003392534, -0.004062971, -0.04015765}},	{{-0.0003368361, -0.007074811, -0.04086341}},	B	3.0934
{{0.009402613, -0.02638633, 0.02622846}},	{{0.009984407, -0.02526258, 0.02692393}},	C	1.4439
{{0.002052086, -0.02720303, -0.03214564}},	{{-0.0004063226, -0.02870663, -0.03247213}},	D	2.9002
{{-0.02918003, -0.009138243, -0.02053221}},	{{-0.03066836, -0.006481111, -0.0234931}},	E	4.2476
{{-0.02462806, -0.006525827, 0.02084563}},	{{-0.02391713, -0.007583118, 0.02276809}},	F	2.3063
{{0.007043841, -0.02258241, -0.001825702}},	{{0.00817012, -0.02082332, -0.003955914}},	G	2.9834
{{0.03562485, 0.002422237, 0.0114655}},	{{0.03602853, 0.002609708, 0.01394949}},	H	2.5236
{{0.0296913, -0.007499257, -0.01599753}},	{{0.02980547, -0.006231449, -0.01606351}},	I	1.2746
{{-0.01085242, 0.3647687, -0.01637984}},	{{-0.01003041, 0.3649293, -0.0151876}},	1	1.4570
{{-0.01991219, 0.3625082, 0.04510945}},	{{-0.02018344, 0.362478, 0.04495769}},	2	0.3123
{{-0.005648646, 0.3455144, -0.01641147}},	{{-0.004976236, 0.345641, -0.0155039}},	3	1.1366
{{-0.007784198, 0.3836088, -0.004721689}},	{{-0.007300224, 0.3837026, -0.004053736}},	4	0.8302
{{-0.02683715, 0.3645721, -0.001958248}},	{{-0.02588154, 0.3647779, -0.0003111503}},	5	1.9153
{{0.0168262, 0.3648493, -0.007946806}},	{{0.01668467, 0.3647961, -0.008546}},	6	0.6180
{{0.01946804, 0.3477427, 0.03770123}},	{{0.01824822, 0.3474868, 0.0355866}},	7	2.4546
{{-0.02326838, 0.3070494, 0.01514329}},	{{-0.02279962, 0.3071614, 0.0160887}},	8	1.0612
{{-0.01034007, 0.3429907, 0.04736471}},	{{-0.01093401, 0.3428889, 0.04661687}},	9	0.9604
{{0.001536795, 0.326921, 0.0692028}}	{{0.000126818, 0.3266532, 0.06714169}}	10	2.5116

• Tibia morphing errors

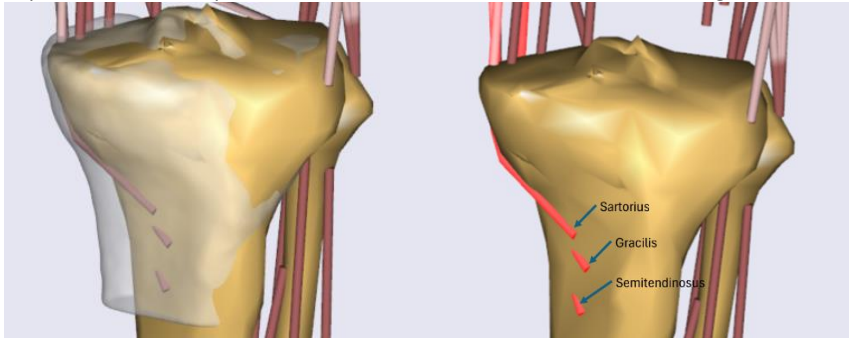
Target landmarks	Source landmarks after morphing	Point	Error (mm)	With the additional landmark
-0.004264361, 0.3237958, 0.03382476;	-0.004171063, 0.3247786, 0.03518994;	A	1.6847	2.1896
0.001740127, 0.3210873, -0.0375517;	0.001737326, 0.3209349, -0.03554154;	B	2.0159	1.9556
-0.001415167, 0.3305509, 0.01487744;	-0.001194122, 0.331737, 0.0183038;	C	3.6325	4.2712
0.001629192, 0.3288103, -0.02279053;	0.003070916, 0.3282452, -0.02176942;	D	1.8548	2.1828
-0.0007293544, 0.3369703, -0.003864493;	-0.002588582, 0.3367386, -0.002414152;	E	2.3693	2.62064
0.03040835, 0.3042913, 0.01118781;	0.02983255, 0.30019, 0.0095155;	F	4.4664	5.38977
-0.01971486, 0.3209199, -0.002641026;	-0.02138285, 0.3194403, -0.004703829;	G	3.0375	3.20912
-0.02090125, 0.3248915, -0.0152246;	-0.02082588, 0.3256246, -0.0205327;	H	5.3590	5.72367
-0.01881147, 0.3267624, 0.005872849;	-0.01958696, 0.32649, 0.008702585;	I	2.9466	3.07985
0.02023068, 0.329965, 0.002772628;	0.02397073, 0.3339854, -0.0005223991;	J	6.4038	5.58561
-0.01982467, 0.3209116, 0.02716733;	-0.02050048, 0.3203105, 0.02717501;	K	0.9044	1.28175
0.02092515, 0.006577807, -0.02671091;	0.01953057, 0.006769716, -0.02452013;	N	2.6040	5.61386
0.01815654, 0.01535276, 0.0175439;	0.01637557, 0.01528823, 0.0162269;	O	2.2159	2.61218
-0.01342626, 0.01237714, -0.006296061;	-0.01245339, 0.01253143, -0.005121753;	P	1.5327	1.80205
-0.001012019, 0.01953293, 0.009942209;	-0.00121549, 0.01955846, 0.009579166;	Q	0.4169	1.21276
-0.02491928, -0.01411648, 0.02265263;	-0.02344789, -0.0140929, 0.02175031;	R	1.7261	0.33057
-0.007029185, 0.005100642, 0.02630798;	-0.006987898, 0.005050869, 0.02476148;	S	1.5478	1.81254
-0.02385851, 0.004513524, 0.006747446;	-0.02225734, 0.004620177, 0.00707681;	T	1.6381	1.38094
0.008339242, 0.009107884, -0.004812041	0.007617184, 0.009201241, -0.004149933;	U	0.9841	1.51262

• Patella morphing errors:

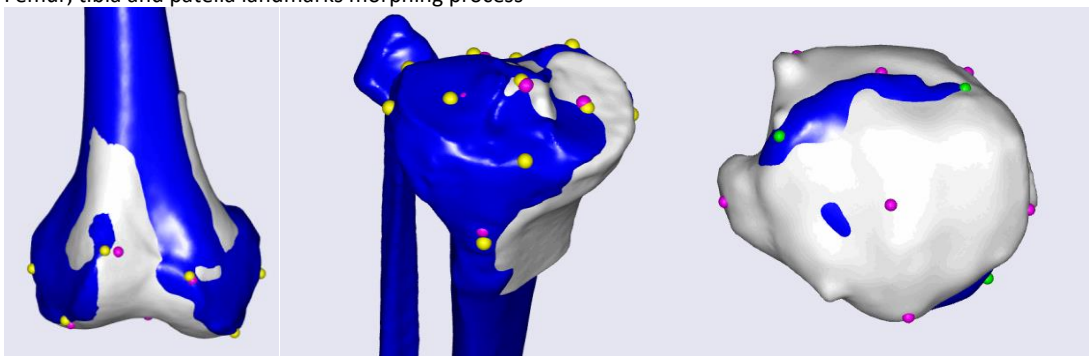
Target landmarks	Source landmarks after morphing	Point	Error (mm)
0.0004197, -0.0147245, -0.0112685;	-0.001134802, -0.01195903, -0.01010716;	A	3.3783
0.0062192, 0.013561, 0.014824;	0.002151404, 0.01611746, 0.01496489;	B	4.8064
-0.0047543, 0.0169626, -0.0175548;	-0.001956111, 0.01364987, -0.02029656;	C	5.1304
0.0059572, -0.0114507, 0.0199053;	0.009560287, -0.01475836, 0.01871565;	D	5.0337
0.0122253, 4.09e-05, 5.2e-06;	0.01048652, 0.001950356, 0.001617062;	E	3.0442
-0.0054724, -0.0220833, 0.001332;	-0.007602132, -0.02193262, -0.0009551517;	F	3.1288
-0.0086438, -0.0080622, -0.0215758;	-0.008649243, -0.007657013, -0.01909939;	G	2.5093
-0.0087171, -0.0009614, 0.0194212;	-0.006936845, -0.001517652, 0.02033976;	H	2.0791
-0.0071259, 0.016807, -0.0006811	-0.005811182, 0.01619639, -0.000771599	I	1.4524

Appendix J: Other

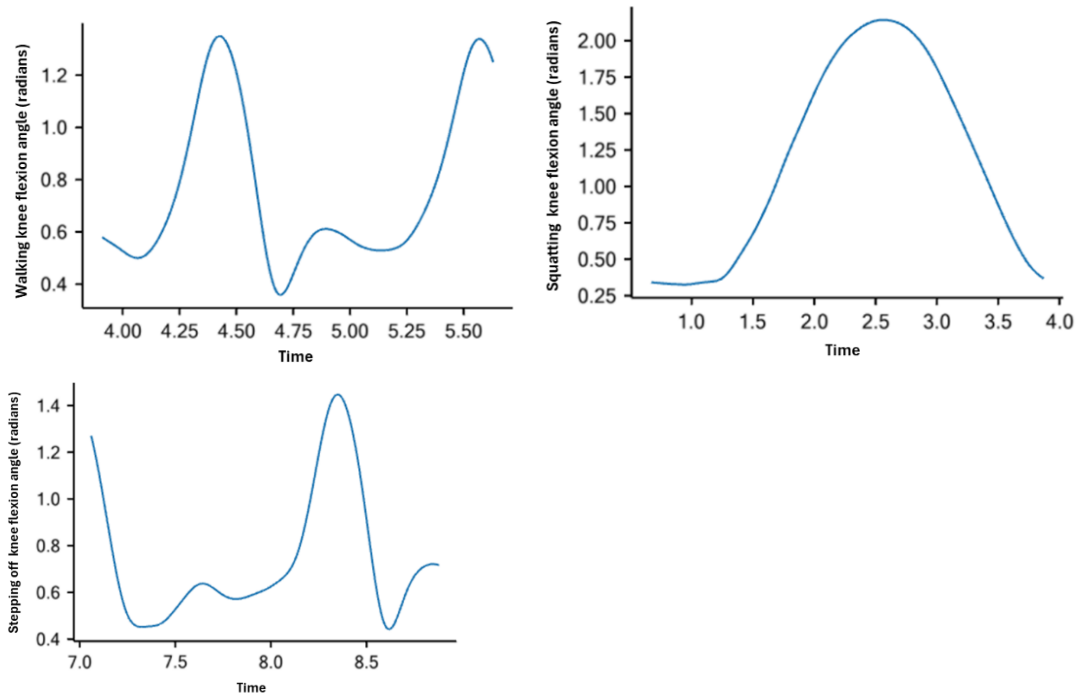
Muscles attachments at the proximal tibia region where morphing discrepancy was shown. In this region, the bone was impractical to be morphed due to the lack of distinct landmarks at this region.



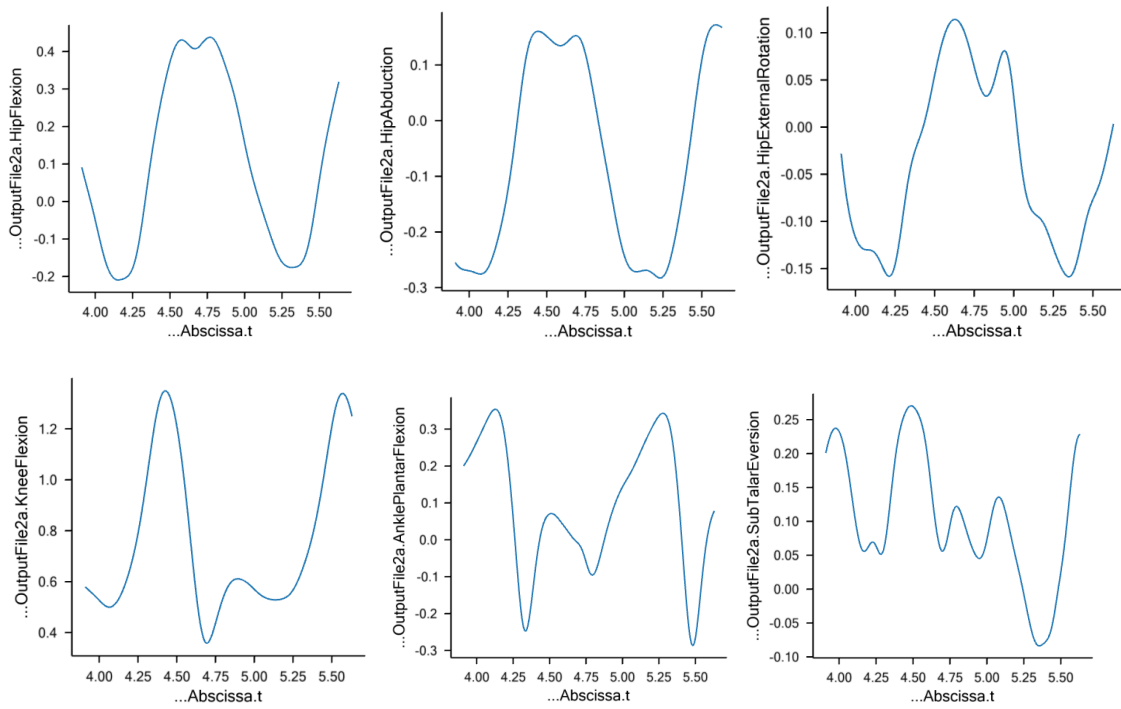
Femur, tibia and patella landmarks morphing process



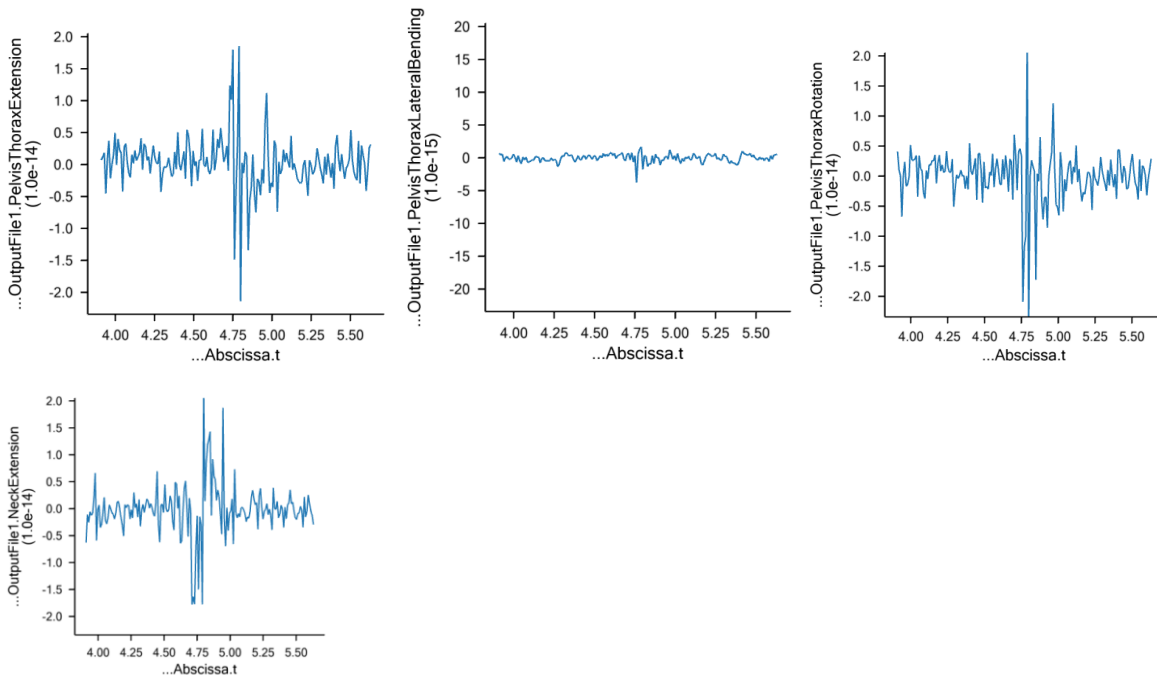
Knee flexion angle of the three activities



Joints (Hip, knee and ankle) angles for walking:



Other joints (PelvisThorax, and neck) angles during walking:





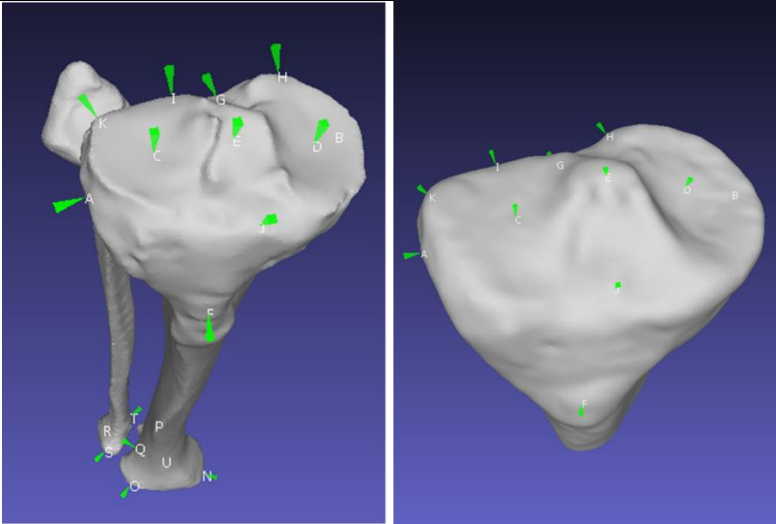
Appendix K: Workflow Tracing

1. Bone morphing:

- Changes to do/ consider before applying the morphing algorithm to display the model's morphed bones and hide the participant bones. Without doing these, you won't be able to visualize the effects of the morphing algorithm and you would run into errors.

Changes	.any file	Description
Showing the model morphed bones	PostOpSTLs.any	At the bottom of the script, I defined SHOW_ANYBODY_SURF to show the model's surfaces based on the if statement
Hiding PostOp surfaces	PostOpSTLs.any	Just to ensure the post op surfaces are not shown, HIDE_POSTOP_SURF was defined
Hiding the talus	PostOpSTLs.any	Comment the surface drawing definition
Hiding tibia and fibula	PostOpSTLs.any	Comment the surface drawing definition
Hiding DistalFemurSTL_smooth	PostOpSTLs.any	Comment the surface drawing definition
Hiding patella and femur	PostOpSTLs.any	Comment the surface drawing definition
Excluding talus morphing	HumanModel.any	Comment CUSTOM_SCALING_Right_Talus
	HumanModel.any	Comment CUSTOM_SCALING_Left_Talus
	HumanModel.any	Comment Scaling.GeometricalScaling.Left.Talus = {}
	HumanModel.any	Comment Scaling.GeometricalScaling.Right.Talus = {}
Excluding Talus joint CS redefinition	SubjectSpecificJoints.any	Making the definition of PATIENT_SPECIFIC_ANKLE_JOINTAXIS == 0 instead of 1 in libdef.any
Excluding Subtalar joint CS redefinition	SubjectSpecificJoints.any	Making the definition of PATIENT_SPECIFIC_SUBTALAR_JOINTAXIS == 0 instead of 1 in libdef.any
Defining the segments length as a function of the height	SubjectSpecificData.any	<pre> AnyVar PelvisWidth = 0.176*BodyHeight/1.75; //distance between hip joints AnyVar HeadHeight = 0.14*BodyHeight/1.75; //height in neutral position from C1HatNode to top of head AnyVar TrunkHeight = 0.620233*BodyHeight/1.75; //height in neautral position from C1HatNode to L5SacrumJnt AnyVar UpperArmLength = 0.340079*BodyHeight/1.75; AnyVar LowerArmLength = 0.2690167*BodyHeight/1.75; AnyVar HandLength = 0.182*BodyHeight/1.75; AnyVar HandBreadth = 0.085*BodyHeight/1.75; AnyFolder Right = { //righth and left side is mirrored in AnyMan.any script AnyVar ThighLength = 0.4098364*.BodyHeight/1.75; AnyVar ShankLength = 0.4210448*.BodyHeight/1.75; AnyVar FootLength = 0.2571425*.BodyHeight/1.75; //Lindas foot length =22cm }; </pre>

- **Morphing algorithm:** Please refer to the table below for detailed description of how to apply it. Note that the template SubjectSpecificScaling.any script was fully changed in order to apply partial morphing. The file where these changes were made is SubjectSpecificScaling.any.
 - Tibia partial morphing:

Steps	Explanation																																						
<p>Select bony landmarks to be used for the morphing process. Please note that there is no specific protocol for selecting these landmarks. Some of these landmarks were used by Iris (another student did her thesis within the research group) and some of them were selected by me. After all, these landmarks represent a bony landmark that exists in both bones. These landmarks were selected/ defined with MeshLab PickPoints feature.</p> <p>From the source bone, select the landmarks at the proximal tibia and distal tibia as well.</p> <p>Load this file in MeshLab to display the picked points.</p>  <p>Tibiafibula_source_picked_points.pp</p> <p>From the subject's bone, select the same landmarks at the proximal region that were selected in the proximal tibia source bone.</p>  <p>Linda_Tibia_picked_points.pp</p>																																							
<table border="1"> <thead> <tr> <th>Proximal landmark</th> <th>Letter</th> </tr> </thead> <tbody> <tr><td>Lateral condyle</td><td>A</td></tr> <tr><td>Medial condyle</td><td>B</td></tr> <tr><td>Lateral tibial resection</td><td>C</td></tr> <tr><td>Medial tibial resection</td><td>D</td></tr> <tr><td>Tibial knee center</td><td>E</td></tr> <tr><td>Anterior tibial rotational</td><td>F</td></tr> <tr><td>Posterior tibial rotational</td><td>G</td></tr> <tr><td>Posterior medial tibial rotational</td><td>H</td></tr> </tbody> </table>		Proximal landmark	Letter	Lateral condyle	A	Medial condyle	B	Lateral tibial resection	C	Medial tibial resection	D	Tibial knee center	E	Anterior tibial rotational	F	Posterior tibial rotational	G	Posterior medial tibial rotational	H	<table border="1"> <thead> <tr> <th>Distal landmarks</th> <th>Letter</th> </tr> </thead> <tbody> <tr><td>Medial malleolus</td><td>N</td></tr> <tr><td>Anterior malleolus</td><td>O</td></tr> <tr><td>Posterior malleolus</td><td>P</td></tr> <tr><td>Malleolus fossa</td><td>Q</td></tr> <tr><td>Bottom fibula</td><td>R</td></tr> <tr><td>Anterior bottom fibula</td><td>S</td></tr> <tr><td>Posterior bottom fibula</td><td>T</td></tr> <tr><td>Bottom tibia</td><td>U</td></tr> </tbody> </table>		Distal landmarks	Letter	Medial malleolus	N	Anterior malleolus	O	Posterior malleolus	P	Malleolus fossa	Q	Bottom fibula	R	Anterior bottom fibula	S	Posterior bottom fibula	T	Bottom tibia	U
Proximal landmark	Letter																																						
Lateral condyle	A																																						
Medial condyle	B																																						
Lateral tibial resection	C																																						
Medial tibial resection	D																																						
Tibial knee center	E																																						
Anterior tibial rotational	F																																						
Posterior tibial rotational	G																																						
Posterior medial tibial rotational	H																																						
Distal landmarks	Letter																																						
Medial malleolus	N																																						
Anterior malleolus	O																																						
Posterior malleolus	P																																						
Malleolus fossa	Q																																						
Bottom fibula	R																																						
Anterior bottom fibula	S																																						
Posterior bottom fibula	T																																						
Bottom tibia	U																																						

Change the block of code within **AnyFolder Shank** to the following code. You can find description within this code to understand the purpose of each step.

```

AnyFolder Shank =
{
  #if InverseDynamicModel== 0 | INV_DYN_EXCLUDE_RIGHT_LEG == 0

  // TSeg2ScaleFrame transforms source entities to the scaling frame (Pre-defined in the model)
  AnyFunTransform3D &TSeg2ScaleFrame = ...BodyModel.Right.Leg.Seg.Shank.Scale.T0;

  // Anthropometric scaling (in this case Uniform scaling law) to control the length of the bone:
  AnyFunTransform3D &AnthropometricScaling =
  Main.Studies.HumanModel.Scaling.Scaling.GeometricalScaling.Right.Shank.ScaleFunction; //To scale the length of the shank to the subject's shank length

  // Landmarks to be used for partial scaling: proximal and distal source landmarks and proximal target landmarks
  // Proximal landmarks for morphing the proximal part of the shank (region of interest):
  AnyMatrix proximal_tibial_landmarks_source =
  {
    {2.4553533, 322.60641, 38.435726}*0.001, //A
    {-4.6470823, 317.59225, -35.667347}*0.001, //B
    {-0.78102088, 331.89825, 19.865219}*0.001, //C
    {3.2023861, 328.15952, -23.625978}*0.001, //D
    {1.9201577, 336.08969, -0.26364601}*0.001, //E
    {32.696163, 300.36832, 10.931908}*0.001, //F
    {-23.028795, 319.39224, -5.6062117}*0.001, //G
    {-22.6758, 325.479, -22.7989}*0.001, //H
    {-20.8676, 326.536, 9.02121}*0.001, //I
    {26.1913, 334.097, -0.0629725}*0.001, //J
    {-21.5649, 320.47, 29.081}*0.001 //k
  };

  //Fake landmarks to control the distla part of the shank (obtained from the distal part of the source shank):
  AnyMatrix distal_tibial_landmarks_source =
  {
    {20.925146, 6.5778065, -26.710907}*0.001, //MedMalleolus
    {18.156538, 15.352763, 17.543905}*0.001, //AntMalleolus
    {-13.426257, 12.377143, -6.296061}*0.001, //PostrMalleolus
    {-1.012019, 19.532932, 9.9422092}*0.001, //Malleolus fossa
    {-24.919279, -14.116476, 22.652632}*0.001, //BottomFibula
    {-7.0291848, 5.1006417, 26.307983}*0.001, //AntBottomFibula
    {-23.858505, 4.5135241, 6.7474461}*0.001, //PostrBottomFibula
    {8.339242, 9.1078835, -4.8120413}*0.001 //Bottom Tibia
  };

  // Proximal landmarks for morphing the proximal part of the shank
  AnyMatrix proximal_tibial_landmarks_target =
  {
    {-87.709061, 23.179075, -10.374002 }*0.001,
    {-17.481573, 36.884048, -14.64732 }*0.001,
    {-68.371178, 24.572445, -4.3031507 }*0.001,
    {-31.35747, 31.967342, -6.8477278 }*0.001,
    {-49.815659, 28.02079, 1.7582881 }*0.001,
    {-57.746017, -1.10416, -35.023369 }*0.001,
    {-56.765385, 48.046593, -11.288908 }*0.001,
    {-44.755947, 51.979549, -7.3099227 }*0.001,
    {-70.79277, 42.849827, -6.0324082 }*0.001,
    {-51.05154, 7.2466393, -8.2094469 }*0.001,
  }
}

```

```

    { -85.520149, 40.196625, -10.986394 }*0.001
    };

// A rigid body transformation to align proximal target bone with the expected anthropometrically scaled generic bone:
AnyFunTransform3DLin2 RegProximallandmarks = {
    Points0 = .proximal_tibial_landmarks_target;
    Points1 = .AnthropometricScaling(.proximal_tibial_landmarks_source);
    //Mode = VTK_LANDMARK_RIGIDBODY; //By default it is RIGIDBODY transformation
};

// Augmenting distal tibia source landmarks:
AnyMatrix P0 = arccat (
    distal_tibial_landmarks_source,
    proximal_tibial_landmarks_source
);

AnyMatrix P1 = arccat (
    AnthropometricScaling(distal_tibial_landmarks_source),
    RegProximallandmarks(proximal_tibial_landmarks_target)
);

// Affine transformation:
AnyFunTransform3DLin2 reg = {
    PreTransforms = {&.AnthropometricScaling}; //Applying uniform scaling as pre-transform to control the length of the bone
    Points0 = .TSeg2ScaleFrame(.P0); // TSeg2ScaleFrame ensures that scaling is applied properly (You can find info about it in AnyBody Forum)
    Points1 = .P1;
    Mode = VTK_LANDMARK_AFFINE;
};

// RBF transformation:
AnyFunTransform3DRBF rbf = {
    PreTransforms = {&.reg};
    RBFDef.Type = RBF_Triharmonic;
    PolynomDegree = 1;
    Points0 = .reg.Points0; //Using the same source points in the affine transformation
    Points1 = .reg.Points1; //Using the same target points in the affine transformation
    BoundingBoxOnOff = On;
    BoundingBox.Type = BB_Cartesian;
    BoundingBox.ScaleXYZ = {2,2,2}*2;
    BoundingBox.DivisionFactorXYZ = {1,1,1}*3;
};

// To bring all entities to the model reference frame:
AnyFunTransform3DLin2 inv = {
    Points0=.reg.Points1;
    Points1=.reg.Points0;
    Mode = VTK_LANDMARK_RIGIDBODY;
};

//To register any STL, nodes etc.
AnyFunTransform3DLin2 RegistrationTransform = {
    Points0 =
Main.Studies.HumanModel.SubjectSpecificScaling.Right.Shank.proximal_tibial_landmarks_target;

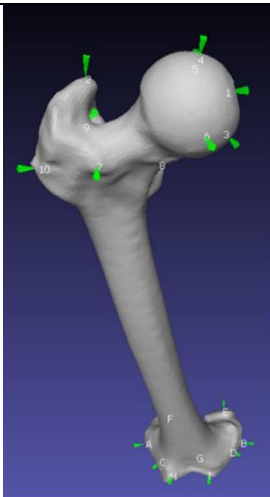
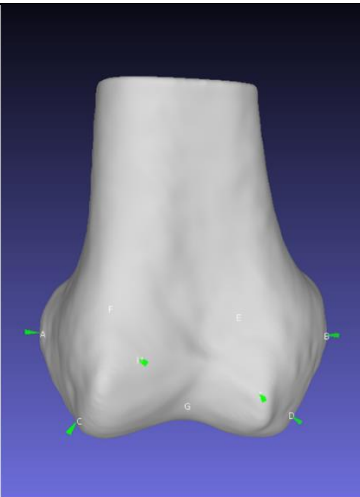
```

```
Points1 =
Main.Studies.HumanModel.BodyModel.Right.Leg.Seg.Shank.Scale(Main.Studies.HumanModel.SubjectSpecificScaling.Right.Shank.proximal_tibial_landmarks_source);
Mode = VTK_LANDMARK_RIGIDBODY;
};

// Applying RBF and inverse transformations to the model bone for morphing:
AnyFunTransform3DIdentity ScaleFunction = {
PreTransforms = {&.rbf, &.inv};
};

#endif
};
```

- Femur partial morphing:

Steps	Explanation																																															
<p>Select bony landmarks to be used for the morphing process. Please note that there is no specific protocol for selecting these landmarks. Some of these landmarks were based on AnyBody Scaling tutorial, some of them were selected by me, and some of them were used by Iris (the student mentioned above). After all, these landmarks represent a bony landmark that exists in both bones.</p> <p>From the source bone, select landmarks at the proximal femur and distal femur as well.</p>  <p>Femur_source_picked_points.pp</p> <p>From the subject's bone, select the same landmarks at the distal region that were selected in the distal femur source bone.</p>  <p>Linda_femur_picked_points.pp</p> <p>These landmarks were selected/ defined with MeshLab PickPoints feature.</p>	<table border="1"> <thead> <tr> <th data-bbox="728 798 1025 833">Proximal landmark</th> <th data-bbox="1025 798 1368 833">Number</th> <th data-bbox="1368 798 1727 833">Distal landmarks</th> <th data-bbox="1727 798 2154 833">Letter</th> </tr> </thead> <tbody> <tr> <td data-bbox="728 833 1025 868">Fovea capitis</td> <td data-bbox="1025 833 1368 868">1</td> <td data-bbox="1368 833 1727 868">Lateral epicondyle</td> <td data-bbox="1727 833 2154 868">A</td> </tr> <tr> <td data-bbox="728 868 1025 903">Greater Trochanter</td> <td data-bbox="1025 868 1368 903">2</td> <td data-bbox="1368 868 1727 903">Medial epicondyle</td> <td data-bbox="1727 868 2154 903">B</td> </tr> <tr> <td data-bbox="728 903 1025 938">Femur Head Inferior</td> <td data-bbox="1025 903 1368 938">3</td> <td data-bbox="1368 903 1727 938">Distal lateral resection</td> <td data-bbox="1727 903 2154 938">C</td> </tr> <tr> <td data-bbox="728 938 1025 973">Femur Head Superior</td> <td data-bbox="1025 938 1368 973">4</td> <td data-bbox="1368 938 1727 973">Distal medial resection</td> <td data-bbox="1727 938 2154 973">D</td> </tr> <tr> <td data-bbox="728 973 1025 1008">Femur Head Posterior</td> <td data-bbox="1025 973 1368 1008">5</td> <td data-bbox="1368 973 1727 1008">Posterior medial resection</td> <td data-bbox="1727 973 2154 1008">E</td> </tr> <tr> <td data-bbox="728 1008 1025 1043">Femur Head Anterior</td> <td data-bbox="1025 1008 1368 1043">6</td> <td data-bbox="1368 1008 1727 1043">Posterior lateral resection</td> <td data-bbox="1727 1008 2154 1043">F</td> </tr> <tr> <td data-bbox="728 1043 1025 1078">Anterior Trochanter</td> <td data-bbox="1025 1043 1368 1078">7</td> <td data-bbox="1368 1043 1727 1078">Trochanter center</td> <td data-bbox="1727 1043 2154 1078">G</td> </tr> <tr> <td data-bbox="728 1078 1025 1114">Posterior Trochanter</td> <td data-bbox="1025 1078 1368 1114">8</td> <td data-bbox="1368 1078 1727 1114">Lateral peak</td> <td data-bbox="1727 1078 2154 1114">H</td> </tr> <tr> <td data-bbox="728 1114 1025 1149">Femur Head Fossa</td> <td data-bbox="1025 1114 1368 1149">9</td> <td data-bbox="1368 1114 1727 1149">Medial peak</td> <td data-bbox="1727 1114 2154 1149">I</td> </tr> <tr> <td data-bbox="728 1149 1025 1168">Lateral Trochanter</td> <td data-bbox="1025 1149 1368 1168">10</td> <td></td> <td></td> </tr> </tbody> </table>				Proximal landmark	Number	Distal landmarks	Letter	Fovea capitis	1	Lateral epicondyle	A	Greater Trochanter	2	Medial epicondyle	B	Femur Head Inferior	3	Distal lateral resection	C	Femur Head Superior	4	Distal medial resection	D	Femur Head Posterior	5	Posterior medial resection	E	Femur Head Anterior	6	Posterior lateral resection	F	Anterior Trochanter	7	Trochanter center	G	Posterior Trochanter	8	Lateral peak	H	Femur Head Fossa	9	Medial peak	I	Lateral Trochanter	10		
Proximal landmark	Number	Distal landmarks	Letter																																													
Fovea capitis	1	Lateral epicondyle	A																																													
Greater Trochanter	2	Medial epicondyle	B																																													
Femur Head Inferior	3	Distal lateral resection	C																																													
Femur Head Superior	4	Distal medial resection	D																																													
Femur Head Posterior	5	Posterior medial resection	E																																													
Femur Head Anterior	6	Posterior lateral resection	F																																													
Anterior Trochanter	7	Trochanter center	G																																													
Posterior Trochanter	8	Lateral peak	H																																													
Femur Head Fossa	9	Medial peak	I																																													
Lateral Trochanter	10																																															

Change the block of code within **AnyFolder Thigh** to the following code. You can find description within this code to understand the purpose of each step.

```
AnyFolder Thigh =
{
  #if InverseDynamicModel== 0 | INV_DYN_EXCLUDE_RIGHT_LEG == 0
    AnyFunTransform3D &Tseg2ScaleFrame = ...BodyModel.Right.Leg.Seg.Thigh.Scale.T0;
    AnyFunTransform3D &AnthropometricScaling =
Main.Studies.HumanModel.Scaling.Scaling.GeometricalScaling.Right.Thigh.ScaleFunction;

    // Landmarks to be used for partial morphing
    AnyMatrix distal_femur_landmarks_source =
    {
      {1.4667782, -7.5853477, 40.188442}*0.001,
      {-1.3872523, -7.2713323, -42.379215}*0.001,
      {10.828313, -25.093184, 28.204765}*0.001,
      {-1.2590836, -28.866749, -33.724697}*0.001,
      {-32.232922, -6.8122239, -26.237719}*0.001,
      {-24.200073, -7.6667924, 21.916771}*0.001,
      {8.2392998, -20.800543, -3.7793131}*0.001,
      {37.3533, 2.90245, 16.3532}*0.001,
      {30.2449, -6.11178, -14.9986}*0.001
    };

    AnyMatrix proximal_femur_landmarks_source =
    {
      {-10.852421, 364.76874, -16.379839}*0.001, // Fovea capitis
      {-19.912188, 362.50815, 45.109447}*0.001, // GTroch
      {-5.6486459, 345.51443, -16.411469}*0.001, // FHInferior
      {-7.7841983, 383.60883, -4.7216892}*0.001, // FHSuperior
      {-26.837152, 364.57211, -1.9582478}*0.001, // FHPosterior
      {16.8262, 364.84927, -7.9468064}*0.001, // FHAnterior
      {19.468042, 347.74265, 37.701233}*0.001, // AnteriorTroch
      {-23.268379, 307.04941, 15.143285}*0.001, // PosteriorTroch
      {-10.340069, 342.99069, 47.364712}*0.001, // FHFossa
      {1.5367945, 326.92096, 69.202797}*0.001 // LateralTroch
    };

    AnyMatrix distal_femur_landmarks_target =
    {
      { -84.080986, 16.148844, 23.621426 }*0.001,
```

```

    { -6.3988762, 21.174944, 22.413633 }*0.001,
    { -72.88195, 6.6869726, 3.1665409 }*0.001,
    { -15.23773, 17.9653, -0.32281268 }*0.001,
    { -28.150251, 48.55592, 17.956514 }*0.001,
    { -68.966331, 41.242916, 22.455288 }*0.001,
    { -44.91415, 10.987182, 5.6923642 }*0.001,
    { -55.113194, -18.12281, 31.525492 }*0.001,
    { -28.581356, -10.463104, 20.333908 }*0.001
};

AnyFunTransform3DLin2 RegProximalLandmarks =
{
    Points0 = .distal_femur_landmarks_target;
    Points1 = .AnthropometricScaling(.distal_femur_landmarks_source);
    //Mode = VTK_LANDMARK_RIGIDBODY; // default is RIGIDBODY
};

AnyMatrix P0 = arccat (
    proximal_femur_landmarks_source,
    distal_femur_landmarks_source
);
AnyMatrix P1 = arccat (
    AnthropometricScaling(proximal_femur_landmarks_source),
    RegProximalLandmarks(distal_femur_landmarks_target)
);

AnyFunTransform3DLin2 reg = {
    PreTransforms = {&.AnthropometricScaling};
    Points0 = .TSeg2ScaleFrame(.P0);
    Points1 = .P1;
    Mode = VTK_LANDMARK_AFFINE;
};

AnyFunTransform3DRBF rbf = {
    PreTransforms = {&.reg};
    RBFDef.Type = RBF_Triharmonic;
    PolynomDegree = 1;
    Points0 = .reg.Points0;
};

```

```

Points1 = .reg.Points1;
BoundingBoxOnOff = On;
BoundingBox.Type = BB_Cartesian;
BoundingBox.ScaleXYZ = {1,1,1}*2;
BoundingBox.DivisionFactorXYZ = {1,1,1}*5;
};

AnyFunTransform3DLin2 inv = {
Points0=.reg.Points1;
Points1=.reg.Points0;
Mode = VTK_LANDMARK_RIGIDBODY;
};



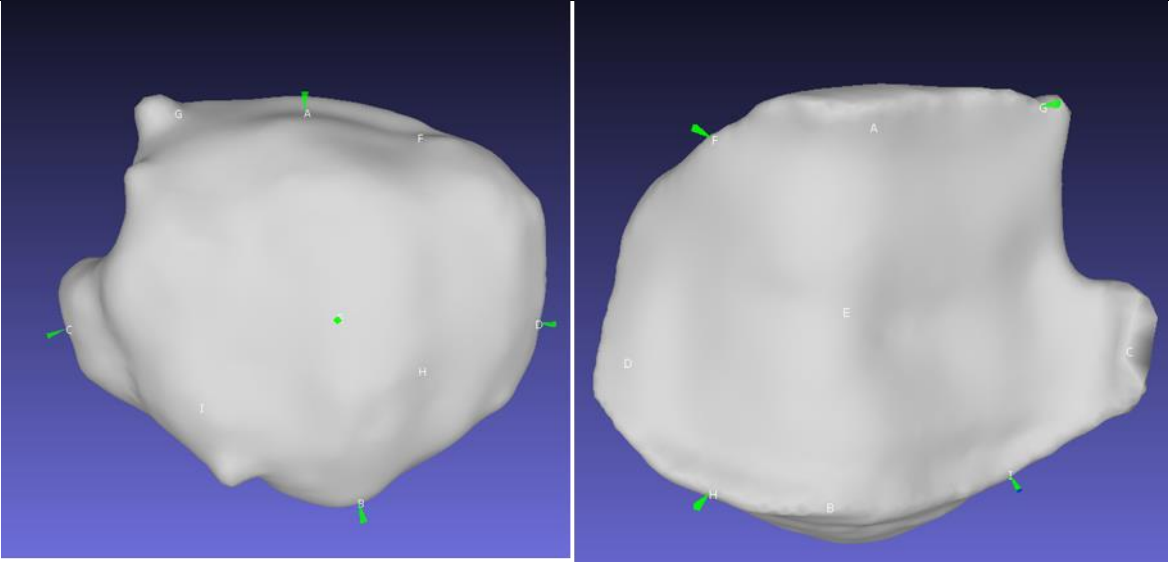
AnyFunTransform3DLin2 RegistrationTransform = {
Points0 =
Main.Studies.HumanModel.SubjectSpecificScaling.Right.Thigh.distal_femur_landmarks_target; //Try
Points1 =
Main.Studies.HumanModel.BodyModel.Right.Leg.Seg.Thigh.Scale(Main.Studies.HumanModel.SubjectSpecificScaling.Right.Thigh.distal_femur_landmarks_source);
Mode = VTK_LANDMARK_RIGIDBODY;
};

AnyFunTransform3DIdentity ScaleFunction = {
PreTransforms = {&.rbf, &.inv};
};

#endif
};

```

○ Patella morphing:

Steps	Explanation																				
<p>Select bony landmarks to be used for the morphing process. Please note that there is no specific protocol for selecting these landmarks. These landmarks were seen in the template model and considered for the morphing process. After all, these landmarks represent a bony landmark that exists in both bones.</p> <p>From the source bone, select landmarks at anterior side of the patella and the posterior side as well.</p>  <p>Patella_source_picked_points.pp</p> <p>From the subject's bone, select the same landmarks that were selected in the distal femur source bone.</p>  <p>Patella_target_picked_points.pp</p> <p>These landmarks were selected/ defined with MeshLab PickPoints feature.</p>	 <table border="1" data-bbox="730 866 1935 1195"> <thead> <tr> <th>Landmark</th> <th>Letter</th> </tr> </thead> <tbody> <tr> <td>Patella base</td> <td>A</td> </tr> <tr> <td>Patella apex</td> <td>B</td> </tr> <tr> <td>Lateral border</td> <td>C</td> </tr> <tr> <td>Medial border</td> <td>D</td> </tr> <tr> <td>Patella belly</td> <td>E</td> </tr> <tr> <td>Superior-medial border</td> <td>F</td> </tr> <tr> <td>Superior-lateral border</td> <td>G</td> </tr> <tr> <td>Inferior-medial border</td> <td>H</td> </tr> <tr> <td>Inferior-lateral border</td> <td>I</td> </tr> </tbody> </table>	Landmark	Letter	Patella base	A	Patella apex	B	Lateral border	C	Medial border	D	Patella belly	E	Superior-medial border	F	Superior-lateral border	G	Inferior-medial border	H	Inferior-lateral border	I
Landmark	Letter																				
Patella base	A																				
Patella apex	B																				
Lateral border	C																				
Medial border	D																				
Patella belly	E																				
Superior-medial border	F																				
Superior-lateral border	G																				
Inferior-medial border	H																				
Inferior-lateral border	I																				

Change the block of code within **AnyFolder Patella** with the following code.

```
AnyFolder Patella = {
#if InverseDynamicModel== 0 | INV_DYN_EXCLUDE_RIGHT_LEG == 0

// set the following to 0 to be able to use the landmarks:
#if STL_VERTICES_BASED_AFFINE_TRANSFORM == 0
AnyFunTransform3DLin2 AffineTransform =
{
Points0 =
{
{ -1.6161, 15.6771, 2.1432}*0.001 ,
{ 2.7866, -20.7290, 0.5057}*0.001,
{ 1.2818, 1.8216, 22.4619}*0.001,
{ 5.4503,2.2603, -19.4518}*0.001,
{ 9.3115, -0.1980, 0.3074}*0.001,
{ -8.9995, 16.7536, -8.1021}*0.001,
{-7.0651,16.4740,11.3233}*0.001,
{-7.5038, -11.8735, -11.0086}*0.001,
{-3.0860, -12.6480, 11.8364}*0.001
};

Points1 =
{
{ 0.4197, -14.7245, -11.2685}*0.001,
{6.2192, 13.5610, 14.8240}*0.001,
{-4.7543, 16.9626, -17.5548}*0.001,
{5.9572, -11.4507, 19.9053}*0.001,
{12.2253, 0.0409,0.0052}*0.001,
{ -5.4724, -22.0833, 1.3320}*0.001,
{-8.6438, -8.0622, -21.5758}*0.001,
{ -8.7171, -0.9614, 19.4212}*0.001,
{ -7.1259, 16.8070, -0.6811}*0.001
};
Mode = VTK_LANDMARK_AFFINE;
};

// The following method can be used if the source and target patella have the same topology (same NO.of vertices, and
faces).
// However, it is not used here. Instead Landmarks were utilized above.
#else
AnyFunTransform3DLin2 AffineTransform = {
AnyFileVar SourceSTL = FilePathCompleteOf(...Source.Right.FileNamePatella) + ".stl";
AnyFileVar TargetSTL = FilePathCompleteOf(...Target.Right.FileNamePatella) + ".stl";
Points0 = STL_Vertices(SourceSTL, iarr(0, floor(NumPoints0/NumPoints), NumPoints0 - 1), 1)*0.001;
Points1 = STL_Vertices(TargetSTL, iarr(0, floor(NumPoints1/NumPoints), NumPoints1 - 1), 1)*0.001;
AnyInt NumPoints0 = STL_Size(SourceSTL, 1)[0];
AnyInt NumPoints1 = STL_Size(TargetSTL, 1)[0];
AnyVar NumPoints = ...NumPointsAffine;
Mode = VTK_LANDMARK_AFFINE;
};
#endif
};
};
```

```

    };
#endif

    AnyFunTransform3DLin2 ReverseTransform = {
        Points0 = .AffineTransform.Points1;
        Points1 = .AffineTransform.Points0;
        Mode = VTK_LANDMARK_RIGIDBODY;
    };

    AnyFunTransform3DLin2 RegistrationTransform = {
        Points0 = .AffineTransform.Points1;
        Points1 = Main.Studies.HumanModel.BodyModel.Right.Leg.Seg.Patella.Scale(.AffineTransform.Points0);
        Mode = VTK_LANDMARK_RIGIDBODY;
    };

    AnyFunTransform3DRBF RBF=
    {
        PreTransforms = {&.AffineTransform};
        RBFDef.Type = RBF_Triharmonic;
        PolynomDegree = 1;
        Points0 = .AffineTransform.Points0;
        Points1 = .AffineTransform.Points1;
        BoundingBoxOnOff = On;
        BoundingBox.Type = BB_Cartesian;
        BoundingBox.ScaleXYZ = {2,2,2}*2;
        BoundingBox.DivisionFactorXYZ = {1,1,1}*3;
    };

    AnyFunTransform3DIdentity ScaleFunction = {
//        ScaleMat = {{1,0,0},{0,1,0},{0,0,1}};
//        Offset = {0,0,0};
        PreTransforms = {&.RBF , &.ReverseTransform};
    };

#endif
};

```

- Morphing the left knee: Please note that since the scans were of the right knee only, morphing the left knee was done by mirroring the right knee morphing algorithm. Mainly speaking, the landmarks were mirrored about z axis by a mirroring matrix.

Step	Explanation
Replace AnyFolder Left with the following block of code	<pre> AnyFolder Left = { AnyFolder Shank = { AnyFunTransform3D &TSeg2ScaleFrame = ...BodyModel.Left.Leg.Seg.Shank.Scale.T0; AnyFunTransform3D &AnthropometricScaling = Main.Studies.HumanModel.Scaling.Scaling.GeometricalScaling.Left.Shank.ScaleFunction; // Mirroring matrix: AnyMatrix AMirroring = { {1,0,0}, {0,1,0}, {0,0,-1} }; AnyMatrix proximal_tibial_landmarks_source = { {2.4553533, 322.60641, 38.435726}*0.001, //A {-4.6470823, 317.59225, -35.667347}*0.001, //B {-0.78102088, 331.89825, 19.865219}*0.001, //C {3.2023861, 328.15952, -23.625978}*0.001, //D {1.9201577, 336.08969, -0.26364601}*0.001, //E {32.696163, 300.36832, 10.931908}*0.001, //F {-23.028795, 319.39224, -5.6062117}*0.001, //G {-22.6758, 325.479, -22.7989}*0.001, //H {-20.8676, 326.536, 9.02121}*0.001, //I {26.1913, 334.097, -0.0629725}*0.001, //J {-21.5649, 320.47, 29.081}*0.001 //k }*Main.Studies.HumanModel.SubjectSpecificScaling.Left.Shank.AMirroring; AnyMatrix distal_tibial_landmarks_source = { {20.925146, 6.5778065, -26.710907}*0.001, //MedMalleolus {18.156538, 15.352763, 17.543905}*0.001, //AntMalleolus {-13.426257, 12.377143, -6.296061}*0.001, //PostrMalleolus {-1.012019, 19.532932, 9.9422092}*0.001, //Malleolus fossa {-24.919279, -14.116476, 22.652632}*0.001, //BottomFibula {-7.0291848, 5.1006417, 26.307983}*0.001, //AntBottomFibula {-23.858505, 4.5135241, 6.7474461}*0.001, //PostrBottomFibula {8.339242, 9.1078835, -4.8120413}*0.001 //Bottom Tibia }*Main.Studies.HumanModel.SubjectSpecificScaling.Left.Shank.AMirroring; </pre>

```

AnyMatrix proximal_tibial_landmarks_target =
{
  { -87.709061, 23.179075, -10.374002 }*0.001,
  { -17.481573, 36.884048, -14.64732 }*0.001,
  { -68.371178, 24.572445, -4.3031507 }*0.001,
  { -31.35747, 31.967342, -6.8477278 }*0.001,
  { -49.815659, 28.02079, 1.7582881 }*0.001,
  { -57.746017, -1.10416, -35.023369 }*0.001,
  { -56.765385, 48.046593, -11.288908 }*0.001,
  { -44.755947, 51.979549, -7.3099227 }*0.001,
  { -70.79277, 42.849827, -6.0324082 }*0.001,
  { -51.05154, 7.2466393, -8.2094469 }*0.001,
  { -85.520149, 40.196625, -10.986394 }*0.001
}*Main.Studies.HumanModel.SubjectSpecificScaling.Left.Shank.AMirroring;

AnyFunTransform3DLin2 RegProximalLandmarks = { // To align proximal target bone with the expected
anthropometrically scaled generic bone
  Points0 = .proximal_tibial_landmarks_target;
  Points1 = .AnthropometricScaling(.proximal_tibial_landmarks_source);
  //Mode = VTK_LANDMARK_RIGIDBODY; //Pavel did not use this line
};

AnyMatrix P0 = arccat (
  distal_tibial_landmarks_source,
  proximal_tibial_landmarks_source
);

AnyMatrix P1 = arccat (
  AnthropometricScaling(distal_tibial_landmarks_source),
  RegProximalLandmarks(proximal_tibial_landmarks_target)
);

AnyFunTransform3DLin2 reg ={
  PreTransforms = {&.AnthropometricScaling};
  Points0 = .TSeg2ScaleFrame(.P0);
  Points1 = .P1;
  Mode = VTK_LANDMARK_AFFINE;
};

AnyFunTransform3DRBF rbf = {
  PreTransforms = {&.reg};
  RBFDef.Type = RBF_Triharmonic;
  PolynomDegree = 1;
  Points0 = .reg.Points0;
  Points1 = .reg.Points1;
  BoundingBoxOnOff = On;
  BoundingBox.Type = BB_Cartesian;
  BoundingBox.ScaleXYZ ={2,2,2}*2;
};

```

```

BoundingBox.DivisionFactorXYZ = {1,1,1}*3;
};

AnyFunTransform3DLin2 inv = {
  Points0=.reg.Points1;
  Points1=.reg.Points0;
  Mode = VTK_LANDMARK_RIGIDBODY;
};

AnyFunTransform3DLin2 RegistrationTransform = {
  Points0 = Main.Studies.HumanModel.SubjectSpecificScaling.Left.Shank.proximal_tibial_landmarks_target;
  Points1 =
Main.Studies.HumanModel.BodyModel.Left.Leg.Seg.Shank.Scale(Main.Studies.HumanModel.SubjectSpecificScaling.Left.Shank.pr
oximal_tibial_landmarks_source);
  Mode = VTK_LANDMARK_RIGIDBODY;
};

AnyFunTransform3DIdentity ScaleFunction = {
//   ScaleMat = {{1,0,0},{0,1,0},{0,0,1}};
//   Offset = {0,0,0};
  PreTransforms = {&.rbf, &.inv};
};

};

AnyFolder Thigh =
{
  AnyFunTransform3D &TSeg2ScaleFrame = ...BodyModel.Left.Leg.Seg.Thigh.Scale.T0;
  AnyFunTransform3D &AnthropometricScaling =
Main.Studies.HumanModel.Scaling.Scaling.GeometricalScaling.Left.Thigh.ScaleFunction;

  AnyMatrix AMirroring = {
    {1,0,0},
    {0,1,0},
    {0,0,-1}
  };

  AnyMatrix distal_femur_landmarks_source =
  {
    {1.4667782, -7.5853477, 40.188442}*0.001,
    {-1.3872523, -7.2713323, -42.379215}*0.001,
    {10.828313, -25.093184, 28.204765}*0.001,
    {-1.2590836, -28.866749, -33.724697}*0.001,
    {-32.232922, -6.8122239, -26.237719}*0.001,
    {-24.200073, -7.6667924, 21.916771}*0.001,
    {8.2392998, -20.800543, -3.7793131}*0.001,
    {37.3533, 2.90245, 16.3532}*0.001,
    {30.2449, -6.11178, -14.9986}*0.001
  }
};

```

```

}*Main.Studies.HumanModel.SubjectSpecificScaling.Left.Thigh.AMirroring;

AnyMatrix proximal_femur_landmarks_source =
{
{-10.852421, 364.76874, -16.379839}*0.001, // Fovea capitis
{-19.912188, 362.50815, 45.109447}*0.001, // GTroch
{-5.6486459, 345.51443, -16.411469}*0.001, // FHInferior
{-7.7841983, 383.60883, -4.7216892}*0.001, // FHSuperior
{-26.837152, 364.57211, -1.9582478}*0.001, // FHPosterior
{16.8262, 364.84927, -7.9468064}*0.001, // FHAnterior
{19.468042, 347.74265, 37.701233}*0.001, // AnteriorTroch
{-23.268379, 307.04941, 15.143285}*0.001, // PosteriorTroch
{-10.340069, 342.99069, 47.364712}*0.001, // FHFossa
{1.5367945, 326.92096, 69.202797}*0.001 // LateralTroch
}*Main.Studies.HumanModel.SubjectSpecificScaling.Left.Thigh.AMirroring;

AnyMatrix distal_femur_landmarks_target =
{
{-84.080986, 16.148844, 23.621426 }*0.001,
{-6.3988762, 21.174944, 22.413633 }*0.001,
{-72.88195, 6.6869726, 3.1665409 }*0.001,
{-15.23773, 17.9653, -0.32281268 }*0.001,
{-28.150251, 48.55592, 17.956514 }*0.001,
{-68.966331, 41.242916, 22.455288 }*0.001,
{-44.91415, 10.987182, 5.6923642 }*0.001,
{-55.113194, -18.12281, 31.525492 }*0.001,
{-28.581356, -10.463104, 20.333908 }*0.001
}*Main.Studies.HumanModel.SubjectSpecificScaling.Left.Thigh.AMirroring;

AnyFunTransform3DLin2 RegProximalLandmarks =
{
Points0 = .distal_femur_landmarks_target;
Points1 = .AnthropometricScaling(.distal_femur_landmarks_source);
//Mode = VTK_LANDMARK_RIGIDBODY; //Pavel did not use this line
};

AnyMatrix P0 = arccat (
proximal_femur_landmarks_source,
distal_femur_landmarks_source
);
AnyMatrix P1 = arccat (
AnthropometricScaling(proximal_femur_landmarks_source),
RegProximalLandmarks(distal_femur_landmarks_target)
);

AnyFunTransform3DLin2 reg ={
PreTransforms = {&.AnthropometricScaling};
Points0 = .TSeg2ScaleFrame(.P0);

```

```

Points1 = .P1;
Mode = VTK_LANDMARK_AFFINE;
};

AnyFunTransform3DRBF rbf = {
  PreTransforms = {&.reg};
  RBFDef.Type = RBF_Triharmonic;
  PolynomDegree = 1;
  Points0 = .reg.Points0;
  Points1 = .reg.Points1;
  BoundingBoxOnOff = On;
  BoundingBox.Type = BB_Cartesian;
  BoundingBox.ScaleXYZ = {1,1,1}*2;
  BoundingBox.DivisionFactorXYZ = {1,1,1}*5;
};

AnyFunTransform3DLin2 inv = {
  Points0=.reg.Points1;
  Points1=.reg.Points0;
  Mode = VTK_LANDMARK_RIGIDBODY;
};

AnyFunTransform3DLin2 RegistrationTransform = {
  Points0 = Main.Studies.HumanModel.SubjectSpecificScaling.Left.Thigh.distal_femur_landmarks_target; // without
the fake points (same for points1)
  Points1 =
Main.Studies.HumanModel.BodyModel.Left.Leg.Seg.Thigh.Scale(Main.Studies.HumanModel.SubjectSpecificScaling.Left.Thigh.di
stal_femur_landmarks_source);
  Mode = VTK_LANDMARK_RIGIDBODY;
};

AnyFunTransform3DIdentity ScaleFunction = {
  PreTransforms = {&.rbf, &.inv};
};

AnyFolder Patella = {
  AnyMatrix AMirroring = {
    {1,0,0},
    {0,1,0},
    {0,0,-1}
  };
};

#if STL_VERTICES_BASED_AFFINE_TRANSFORM == 0
AnyFunTransform3DLin2 AffineTransform =
{
  Points0 =

```

```

{
  { -1.6161, 15.6771, 2.1432}*0.001*.AMirroring ,
  {2.7866, -20.7290, 0.5057}*0.001*.AMirroring,
  { 1.2818, 1.8216, 22.4619}*0.001*.AMirroring,
  { 5.4503,2.2603, -19.4518}*0.001*.AMirroring,
  { 9.3115, -0.1980, 0.3074}*0.001*.AMirroring,
  { -8.9995, 16.7536, -8.1021}*0.001*.AMirroring,
  {-7.0651,16.4740,11.3233}*0.001*.AMirroring,
  {-7.5038, -11.8735, -11.0086}*0.001*.AMirroring,
  {-3.0860, -12.6480, 11.8364}*0.001*.AMirroring
};

Points1 =
{
  { 0.4197,-14.7245, -11.2685}*0.001*.AMirroring,
  {6.2192, 13.5610, 14.8240}*0.001*.AMirroring,
  {-4.7543, 16.9626, -17.5548}*0.001*.AMirroring,
  {5.9572, -11.4507, 19.9053}*0.001*.AMirroring,
  {12.2253, 0.0409,0.0052}*0.001*.AMirroring,
  { -5.4724,-22.0833, 1.3320}*0.001*.AMirroring,
  {-8.6438,-8.0622,-21.5758}*0.001*.AMirroring,
  { -8.7171, -0.9614, 19.4212}*0.001*.AMirroring,
  { -7.1259, 16.8070, -0.6811}*0.001*.AMirroring
};
Mode = VTK_LANDMARK_AFFINE;
};
#else
AnyFunTransform3Dlin2 AffineTransform = {
  AnyFileVar SourceSTL = FilePathCompleteOf(...Source.Right.FileNamePatella) + ".stl";
  AnyFileVar TargetSTL = FilePathCompleteOf(...Target.Right.FileNamePatella) + ".stl";
  Points0 = STL_Vertices(SourceSTL, iarr(0, floor(NumPoints0/NumPoints), NumPoints0 - 1), 1)*0.001*.AMirroring;
  Points1 = STL_Vertices(TargetSTL, iarr(0, floor(NumPoints1/NumPoints), NumPoints1 - 1), 1)*0.001*.AMirroring;
  AnyInt NumPoints0 = STL_Size(SourceSTL, 1)[0];
  AnyInt NumPoints1 = STL_Size(TargetSTL, 1)[0];
  AnyVar NumPoints = ...NumPointsAffine;
  Mode = VTK_LANDMARK_AFFINE;
};
#endif

AnyFunTransform3Dlin2 ReverseTransform = {
  Points0 = .AffineTransform.Points1;
  Points1 = .AffineTransform.Points0;
  Mode = VTK_LANDMARK_RIGIDBODY;
};
AnyFunTransform3Dlin2 RegistrationTransform = {
  Points0 = .AffineTransform.Points1;
  Points1 = Main.Studies.HumanModel.BodyModel.Left.Leg.Seg.Patella.Scale(.AffineTransform.Points0);
  Mode = VTK_LANDMARK_RIGIDBODY;
};

```



```
};

AnyFunTransform3DRBF RBF=
{
  PreTransforms = {&.AffineTransform};
  RBFDef.Type = RBF_Triharmonic;
  PolynomDegree = 1;
  Points0 = .AffineTransform.Points0;
  Points1 = .AffineTransform.Points1;
  BoundingBoxOnOff = On;
  BoundingBox.Type = BB_Cartesian;
  BoundingBox.ScaleXYZ = {2,2,2}*2;
  BoundingBox.DivisionFactorXYZ = {1,1,1}*3;
};

AnyFunTransform3DLin ScaleFunction = {
  ScaleMat = {{1,0,0},{0,1,0},{0,0,1}};
  Offset = {0,0,0};
  PreTransforms = {&.RBF, &.ReverseTransform};
};

};

}; // Left
```

2. Redefining reference frames (Tracking frames)

This part of the workflow is used to measure the secondary kinematics (translations and rotations) of the knee eventually. The changes were made to SubjectSpecificJoints.any file.

- Redefining reference frame of the femur:

Step	Explanation
<p>Replaced the femur nodes that are used to redefine the reference frame in FemurData.any file with the following block of code. Please note that a mirroring matrix was defined. This is because these landmarks were selected on the femur STL file (using MeshLab PickPoints feature) on the right knee (because it is the one scanned with the MRI).</p>	<pre>AnyMatrix Mir = { {1,0,0}, {0,1,0}, {0,0,-1} }; AnyRefNode FemurLateralEpicondyleNode = { AnyVec3 sRel_us = {-84.081, 16.1488, 23.6214}*0.001*Main.Studies.HumanModel.BodyModel.Left.Leg.Seg.Thigh.Mir; DEF_REFNODE_CUSTOM_SCALING_1arg(sRel_us) // AnyDrawNode dr={ScaleXYZ={1,1,1}*0.01}; }; AnyRefNode FemurMedialEpicondyleNode = { AnyVec3 sRel_us = {-6.39888, 21.1749, 22.4136}*0.001*Main.Studies.HumanModel.BodyModel.Left.Leg.Seg.Thigh.Mir; DEF_REFNODE_CUSTOM_SCALING_1arg(sRel_us) // AnyDrawNode dr={ScaleXYZ={1,1,1}*0.01}; };</pre>
<p>Within AnyFolder SubjectSpecificJCS, replaced the thigh block of code with the following. Please note that HipJoint.sRel represents the generic bone hip centre. It was used because the proximal femur was not scanned.</p>	<pre>Main.Studies.HumanModel.BodyModel.Left.Leg.Seg.Thigh = { #include "..\..\..\..\..\JCSData\FemurData.any" AnyRefNode JointCoordinateSystem = { AnyVec3 O = 0.5*(.FemurMedialEpicondyleNode.sRel + .FemurLateralEpicondyleNode.sRel); AnyVec3 EpicondylarAxis = .FemurMedialEpicondyleNode.sRel - .FemurLateralEpicondyleNode.sRel; AnyVec3 MechAxis = Main.Studies.HumanModel.BodyModel.Left.Leg.Seg.Thigh.HipJoint.sRel- O; AnyVec3 MLAxis = cross(cross(MechAxis, EpicondylarAxis), MechAxis); AnyVec3 APAxis = cross(MechAxis, MLAxis); sRel = O; ARel = {APAxis/vnorm(APAxis), MechAxis/vnorm(MechAxis), MLAxis/vnorm(MLAxis)}'; // AnyDrawRefFrame drw = {RGB = {0,1,0};ScaleXYZ=0.09*{1,1,1}}; }; };</pre>

- Redefining reference frame of the shank:

Step	Explanation
<p>Replaced the shank nodes that are used to redefine the reference frame in shank_nodes.any file with the following block of code. Please note that a mirroring matrix was defined. This is because these landmarks were selected on the femur STL file (using MeshLab PickPoints feature) on the right knee (because it is the one scanned with the MRI). Additionally, the location of the malleoli markers from the static trial were used. For these two coordinates, the mirroring was not applied because they were obtained from the markers that were placed on the left ankle.</p>	<pre>AnyMatrix Mir = { {1,0,0}, {0,1,0}, {0,0,-1} }; AnyRefNode MostLatNodeBL = { AnyVec3 sRel_us = {-87.7091, 23.1791, - 10.374}*0.001*Main.Studies.HumanModel.BodyModel.Left.Leg.Seg.Shank.Mir; DEF_REFNODE_CUSTOM_SCALING_larg(sRel_us) // AnyDrawRefFrame drw = {}; }; AnyRefNode MostMedNodeBL = { AnyVec3 sRel_us = {-17.4816,36.884, - 14.6473}*0.001*Main.Studies.HumanModel.BodyModel.Left.Leg.Seg.Shank.Mir; DEF_REFNODE_CUSTOM_SCALING_larg(sRel_us) // AnyDrawRefFrame drw = {}; }; AnyRefNode LatAnkle = { AnyVec3 sRel_us = {-0.0322082359508, 0.010916165654, -0.049980193751}; sRel = sRel_us; // AnyDrawRefFrame drw = {}; }; AnyRefNode MedAnkle = { AnyVec3 sRel_us = {0.006075, 0.0121882565, 0.02781135046859094e-02}; sRel = sRel_us; // AnyDrawRefFrame drw = {}; };</pre>
<p>Within AnyFolder SubjectSpecificJCS, replaced the shank block of code with the following. Please note that AnkleJoint.sRel of the generic model was not used because MedAnkle and LatAnkle were considered as they represent the subject's malleoli locations. Based on these two markers coordinates, ankle centre was defined (mid-point between them).</p>	<pre>Main.Studies.HumanModel.BodyModel.Left.Leg.Seg.Shank = { #include "<FDK_KNEE_MODEL_PATH>BonyLandmarksPnts\shank_nodes.any" AnyRefNode JointCoordinateSystem = { AnyVec3 O = 0.5*(.MostLatNodeBL.sRel + .MostMedNodeBL.sRel); AnyVec3 MLAxis = .MostMedNodeBL.sRel - .MostLatNodeBL.sRel; AnyVec3 APAxis = cross((O - 0.5*(.LatAnkle.sRel+.MedAnkle.sRel)),MLAxis); AnyVec3 MechAxis = cross(MLAxis,APAxis); sRel = O; ARel = {APAxis/vnorm(APAxis), MechAxis/vnorm(MechAxis), MLAxis/vnorm(MLAxis)}'; AnyDrawRefFrame drw = {RGB = {1,0,0};ScaleXYZ=0.09*{1,1,1}}; }; };</pre>

- Redefining reference frame of the patella:

Step	Explanation
<p>Replaced the shank nodes that are used to redefine the reference frame in patella_nodes.any file with the following block of code. Note that there is no mirroring matrix applied. This is because the patella of the left knee was used. In case when Linda's patella was obtained, please make sure you apply a mirroring matrix because her patella is of the right knee.</p>	<pre>AnyRefNode InfNodeBL = { AnyVec3 sRel_us = {2.02051,15.3968,-14.5062}*0.001; DEF_REFNODE_CUSTOM_SCALING_1arg(sRel_us) }; AnyRefNode SupNodeBL = { AnyVec3 sRel_us = {2.07486,-14.4136,9.46809}*0.001; DEF_REFNODE_CUSTOM_SCALING_1arg(sRel_us) }; AnyRefNode LatNodeBL = { AnyVec3 sRel_us = {1.93199,11.7092,16.3913}*0.001; DEF_REFNODE_CUSTOM_SCALING_1arg(sRel_us) };</pre>
<p>Within AnyFolder SubjectSpecificJCSLianne, replaced the patella block of code with the following.</p>	<pre>Patella = { AnyRefNode JCSLianne = { AnyVec3 O = 0.5*(.SupNodeBL.sRel_us + .InfNodeBL.sRel_us); AnyVec3 MechAxis = (.SupNodeBL.sRel_us - .InfNodeBL.sRel_us); AnyVec3 APAxis = cross(.LatNodeBL.sRel_us - O,MechAxis); AnyVec3 MLAxis = cross(APAxis,MechAxis); AnyVec3 sRel_us = 0; AnyMat33 ARel_us = {APAxis/vnorm(APAxis), MechAxis/vnorm(MechAxis), MLAxis/vnorm(MLAxis)}'; DEF_REFNODE_CUSTOM_SCALING_1arg(sRel_us) DEF_REFNODE_CUSTOM_SCALING_Arel(ARel_us) // AnyDrawRefFrame drw = {RGB = {0,0,1}}; }; };</pre>

3. Motion capture configuration:

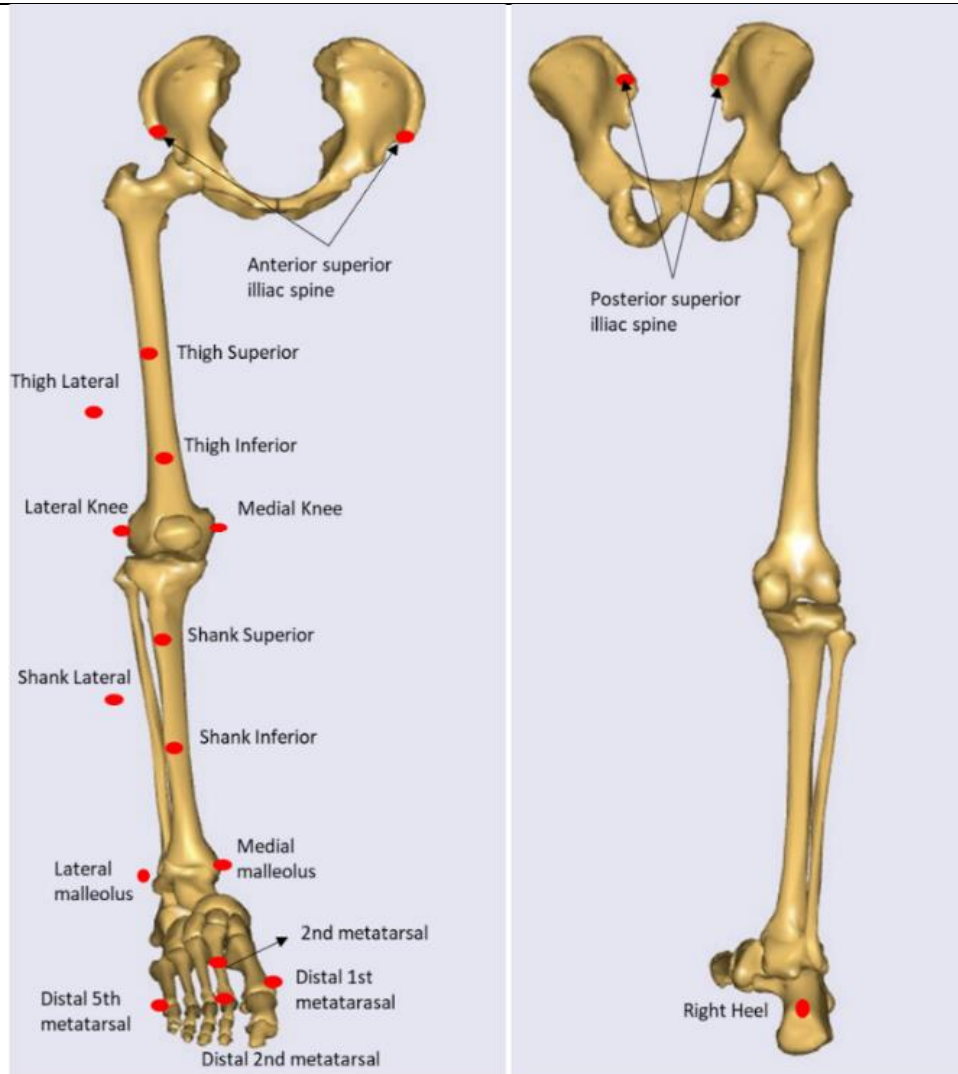
In this, the C3D markers data recorded in RRD company were utilized to drive the model. There are two sub-models that should be configured.

The static model was mainly used to optimized segment lengths and save the marker locations of the markers with respect to the body segments. You can find the model in " Grand Challenge model\AMMRV1.6TLEMSafe\AMMR-public\Application\MyModels\MoCapModel GC5\Input\Subjects\PS\Static Trials\PS_staticfor2" folder.

The dynamic model, on the other hand, was used to drive the model and obtain joints (hip, knee, and ankle) joints to be used in the inverse dynamic model. You can find the model in " Grand Challenge model\AMMRV1.6TLEMSafe\AMMR-public\Application\MyModels\MoCapModel GC5\Input\Subjects\PS_PreOp\Overground Gait Trials\PS_ngait_og_ss1" folder.

- Before using the c3d files, a preparatory step is required. This step involves renaming the markers labels of the c3d file to the marker's labels of AnyBody marker protocol. The c3d markers were attached (in the lab) to the locations explained in the figure below. In the figure, the general location is shown. In c3d file, you will have R/L letter prefixed to the name. Whatever the label of the marker in the c3d file given to these locations, please rename them to the marker labels on the right column. This step ensures that you do not have to change the name of the markers in all referenced scripts. Instead, AnyBody software will recognize the labels automatically in ModelSetup.any under "../Input/MarkersMSATest.any" and drive the model instantly.

Marker's location



Marker location and the name it should be assigned to

Marker location	Label it should be assigned to
Right anterior superior iliac spine	RAsis
Left anterior superior iliac spine	LAsis
Right posterior superior iliac spine	RPsis
Left posterior superior iliac spine	RPsis
Right Thigh superior	RThighSuperior
Right Thigh lateral	RThighLateral
Right Thigh inferior	RThighInferior
Right Medial knee	RKneeMedial
Right Lateral knee	RKneeLateral
Right Shank superior	RShankSuperior
Right Shank lateral	RShankLateral
Right Shank inferior	RShankInferior
Right Medial malleolus	RAnkleMedial
Right Lateral malleolus	RAnkleLateral
Right Distal 1 st metatarsal	RToeMedial
Right Distal 2 nd metatarsal	RToe
Right Distal 5 th metatarsal	RToeLateral
Right 2 nd metatarsal	RMidfootSuperior
Right heel	RHeel
Left Thigh superior	LThighSuperior
Left Thigh lateral	LThighLateral
Left Thigh inferior	LThighInferior
Left Medial knee	LKneeMedial
Left Lateral knee	LKneeLateral
Left Shank superior	LShankSuperior
Left Shank lateral	LShankLateral
Left Shank inferior	LShankInferior
Left Medial malleolus	LAnkleMedial
Left Lateral malleolus	LAnkleLateral

	Left Distal 1 st metatarsal	LToeMedial
	Left Distal 2 nd metatarsal	LToe
	Left Distal 5 th metatarsal	LToeLateral
	Left 2 nd metatarsal	LMidfootSuperior
	Left heel	LHeel

○ Static model:

Please follow the steps in the table below to configure this model. This model can be located in the following directory:

...\Application\MyModels\MoCapModel GC5\Input\Subjects\PS\Static Trials. However, make sure that the c3d file of the static trial is added in the folder of this model.

Step	Explanation
<p>Add the static trial in TrialSepcificData.any</p> <p>Replaced the TrialName based on your Trial name.</p>	<pre>// Name of the C3D file to be analysed AnyString TrialName = "LindaStaticPSlabels"; //Trialname specifies naming of output files (The name of my static trial (Omar)) AnyString C3DFile = TrialName + ".c3d"; // If named or placed differently then specify relative path and name o</pre>
<p>Add the calibration trial in SubjectSpecificData.any</p> <p>Make sure you add the path to the static trial within this code.</p> <p>Add the subject's weight and height</p> <p>Define the body segment's lengths/ width based on the height of the subject</p>	<pre>AnyString CalibrationTrialName = "..\\..\\..\\..\\Application\\MyModels\\MoCapModel GC5\\Input\\Subjects\\PS\\Static Trials\\PS_staticfor2\\LindaStaticPSlabels"; AnyFolder Anthropometrics={ // Subject's weight and height: AnyVar BodyMass=73; //the mass is automatically distributed to the segments AnyVar BodyHeight=1.76; //heigh AnyVar PelvisWidth =0.176*BodyHeight/1.75; //distance between hip joints</pre>

	<pre> AnyVar HeadHeight = 0.14*BodyHeight/1.75;//height in neutral position from C1HatNode to top of head AnyVar TrunkHeight = 0.620233*BodyHeight/1.75;//height in neutral position from C1HatNode to L5SacrumJnt AnyVar UpperArmLength = 0.340079*BodyHeight/1.75; AnyVar LowerArmLength = 0.2690167*BodyHeight/1.75; AnyVar HandLength = 0.182*BodyHeight/1.75; AnyVar HandBreadth = 0.085*BodyHeight/1.75; // AnyFolder Right = { // AnyVar ThighLength = 0.4234534; //righth and left side is mirrored // AnyVar ShankLength = 0.4120814; // AnyVar FootLength =0.21; // }; AnyFolder Right = { AnyVar ThighLength = 0.4098364*.BodyHeight/1.75; //righth and left side is mirrored in AnyMan.any script AnyVar ShankLength = 0.4210448*.BodyHeight/1.75; AnyVar FootLength = 0.22; //0.2571425*.BodyHeight/1.75; }; </pre>
<p>Control the optimization process in ModelSetup.any Switch on and off the parameters to be optimized. Since upper extremities are excluded, make sure you use the one where UseUpperExtremities == 0. You can find that VarusValgus is defined there. Switch on if you want to optimize the respective parameter or switch it off if you want to exclude it from the optimization.</p>	<pre> #if UseUpperExtremities == 0 OptimizeAnthropometricsOnOff OptimizeOnOff (PelvisWidthOnOff = "On", // Turn it on ThighLengthOnOff = "On", // Turn it on ShankLengthOnOff = "On", // Turn it on FootLengthOnOff = "Off", // Turn it on/off HeadHeightOnOff = "Off", // Turn it off TrunkHeightOnOff = "Off", // Turn it off UpperArmLengthOnOff = "Off", //Turn it off LowerArmLengthOnOff = "Off", // Turn it off VarusValgusOnOff = "On", Model1 = MotionAndParameterOptimizationModel, Model2 = InverseDynamicModel) = {}; </pre>

	#endif
<p>Computing markers location based on C3D with respect to each segment:</p> <p>In Kinematics.any there is #include"ComputeMarkerPositions.any" subscript. In it, you can define the location the cluster markers can be computed. There is a class called ComputeLocalMarkerPos which extracts the marker location from the respective segment.</p> <p>You can configure more landmarks based on which location you want.</p>	<pre> #endif //s Right thigh ComputeLocalMarkerPos RThighLateral (MarkerName = RThighLateral, MarkerPlacement = Right.Leg.Seg.Thigh) = {}; ComputeLocalMarkerPos RThighSuperior (MarkerName = RThighSuperior, MarkerPlacement = Right.Leg.Seg.Thigh) = {}; ComputeLocalMarkerPos RThighInferior (MarkerName = RThighInferior, MarkerPlacement = Right.Leg.Seg.Thigh) = {}; ComputeLocalMarkerPos RShankLateral (MarkerName = RShankLateral, MarkerPlacement = Right.Leg.Seg.Shank) = {}; ComputeLocalMarkerPos RShankSuperior (MarkerName = RShankSuperior, MarkerPlacement = Right.Leg.Seg.Shank) = {}; ComputeLocalMarkerPos RShankInferior (MarkerName = RShankInferior, MarkerPlacement = Right.Leg.Seg.Shank) = {}; // Left thigh ComputeLocalMarkerPos LThighLateral (MarkerName = LThighLateral, MarkerPlacement = Left.Leg.Seg.Thigh) = {}; ComputeLocalMarkerPos LThighSuperior (MarkerName = LThighSuperior, MarkerPlacement = Left.Leg.Seg.Thigh </pre>

```
) = {};  
ComputeLocalMarkerPos LThighInferior (  
  MarkerName = LThighInferior,  
  MarkerPlacement = Left.Leg.Seg.Thigh  
) = {};  
  
ComputeLocalMarkerPos LShankLateral (  
  MarkerName = LShankLateral,  
  MarkerPlacement = Left.Leg.Seg.Shank  
) = {};  
ComputeLocalMarkerPos LShankSuperior (  
  MarkerName = LShankSuperior,  
  MarkerPlacement = Left.Leg.Seg.Shank  
) = {};  
ComputeLocalMarkerPos LShankInferior (  
  MarkerName = LShankInferior,  
  MarkerPlacement = Left.Leg.Seg.Shank  
) = {};
```

- Dynamic model:
Please follow the steps in the table below to configure this model. This model can be located in the following directory:
...\\Application\\MyModels\\MoCapModel GC5\\Input\\Subjects\\PS_PreOp\\Overground Gait Trials\\ PS_ngait_og_ss1. However, make sure that the c3d file of the dynamic trial is added in the folder of this model.

Step	Explanation
<p>Add the dynamic trial in TrialSepsificData.any</p> <p>Note that here, the walking trial is defined and called from the folder of the model.</p> <p>Here you can also configure the force plate and the foot that come in contact with. Make sure that the corresponding foot is defined with the respective forceplate. For instance, the left foot is defined here as the footOnForcePlate1. You can visualize which foot comes in contact with which forceplate in Mokka software.</p> <p>You can also activate or deactivate soft drivers. Note that segments without markers attachments should be driven by soft drivers. In this protocol, Head, trunk, scapula/Clavicle segments were driven by the soft drivers by setting them to 0 which indicates that there were no markers attached to these segments and a soft driver should be used. The foot segment was set to 1 because we have 3 markers attached to the foot during the gait lab.</p>	<pre data-bbox="1115 507 2029 1331"> // Name of the C3D file to be analysed AnyString TrialName = "LindaWalking_PSLabels"; //Trialname specifies naming of output files // AnyString TrialName = "LindaWalking"; //Trialname specifies naming of output files AnyString C3DFile = TrialName + ".c3d"; // If named or placed differently then specify relative path and name o #ifndef NO_MARKER_DRIVERS #define FootOnForcePlate1 .BodyModelRef.Left.Leg.Seg.Foot #define FootOnForcePlate2 .BodyModelRef.Right.Leg.Seg.Foot #define FootOnForcePlate3 .BodyModelRef.Right.Leg.Seg.Foot #else #define EXCLUDE_FORCEPLATES #endif // ***** Extra Drivers ***** // Some Gait Labs protocols do not record sufficient markers to create a full body model. // In particular, markers on the head, trunk and a third marker on the foot are not standard. // Therefore, additionl drivers have been added to the model (fix the head, drive the trunk // above the pelvis and fix subtalar eversio). You can switch them on for your own C3D files: </pre>

	<pre> // Do you have markers on the head? If not turn on following switch: 0 means there is no marker and soft drivers will be implemented // Set it to 0 if you do not have markers (Omar): #ifndef HeadMarkersOnOff #define HeadMarkersOnOff 0 #endif // Do you have markers on the Trunk? If not turn on following switch: #ifndef TrunkMarkersOnOff #define TrunkMarkersOnOff 0 #endif // Do you have three markers on the Foot? If not turn on following switch: set to 1 if you have markers and do not need soft drivers (Omar): #ifndef ThreeFootMarkersOnOff #define ThreeFootMarkersOnOff 1 #endif // Do you have markers on the Scapula/Clavicle? If not turn on following switch: #ifndef SCMarkersOnOff #define SCMarkersOnOff 0 #endif #ifndef UseDetailNeckModel #define UseDetailNeckModel 0 #endif </pre>
<p>Force plate configuration in Environment.any file. Within this file, there is #include "../Input/ForcePlates.any" where you can define the forces, moments and the type of the force plate.</p> <p>ForcePlateType 2 refers to the type of the force plate used. You can find the type of your force plate within the model tree at the following directory: Main.ModelSetup.C3DFileData.Groups.FORCE_PLATFORM.TYPE.D ata</p>	<pre> #ifndef EXCLUDE_FORCEPLATE1 ForcePlateType2 Plate1 (PlateName = Plate1, Folder =Main.ModelSetup.C3DFileData, Limb= FootOnForcePlate1, //This must be configured (e.g., if the left foot segment is on the force plate 1): check the definition of FootOnForcePlate1 No=0, // This configures the force plate (It corresponds to force plate 1 in the experiment) </pre>

<p>Limb recalls the configuration of the force plate and the foot it comes in contact with.</p> <p>Fx, Fy, Fz and Mx, My and Mz are the forces and moments recorded on the force plate. The names of these parameters should match the ones of the force plate. You can find them in Main.ModelSetup.C3DFileData.Analog.DataFiltered.</p>	<pre> Fx=Main.ModelSetup.C3DFileData.Analog.DataFiltered.Force_46_Fx 1, Fy=Main.ModelSetup.C3DFileData.Analog.DataFiltered.Force_46_Fy 1, Fz=Main.ModelSetup.C3DFileData.Analog.DataFiltered.Force_46_Fz 1, Mx=Main.ModelSetup.C3DFileData.Analog.DataFiltered.Moment_46_M x1, My=Main.ModelSetup.C3DFileData.Analog.DataFiltered.Moment_46_M y1, Mz=Main.ModelSetup.C3DFileData.Analog.DataFiltered.Moment_46_M z1) ={ Switch_DrawForceVectorFromCOP = Off; Switch_DrawForcePlateCorners = Main.DrawSettings.ForcePlate.Visible; Switch_DrawTransducerLocation = Main.DrawSettings.ForcePlate.Visible; Switch_DrawForcePlateBox = Main.DrawSettings.ForcePlate.Visible; Switch_DrawForcePlateForceAndMoment = Off; Switch_DrawForcePlateCOPball = Off; }; #endif </pre>
<p>Reading the thigh and shank cluster markers' location: Within ModelSetup.any, there is a subscript called #include "../Input/MarkersMSATest.any". In there, you can find CreateMarkerDriverEx class. Make sure that Thigh and shank cluster markers are defined based on this class. This class reads these markers location obtained from static sub-model.</p> <p>Make sure that ReadsRelOptFromFile is On.</p>	<p>For instance, superior thigh marker should be configured with the class as follows for the right leg:</p> <pre> //Right thigh and shank cluster markers: #ifndef EXCLUDE_MARKER_RTHIGHSUPERIOR CreateMarkerDriverEx RThighSuperior (MarkerName= RThighSuperior, MarkerPlacement =Right.Leg.Seg.Thigh, OptX="Off",OptY="Off",OptZ="Off", WeightX=1.0,WeightY=1.0,WeightZ=1.0, </pre>

```

Model1=MotionAndParameterOptimizationModel, Model2=
InverseDynamicModel,
sRelOptScalingOnOff="Off",
ReadsRelOptFromFile = "On",
sRelCustomScalingOnOff = "Off"
)= {
    sRelOpt = {0.0, 0.0, 0.0}; // This is ignored when
ReadsRelOptFromFile = "On"
};
#endif

#if STATIC_DRIVERSET == 0
#ifndef EXCLUDE_MARKER_RTHIGHLATERAL
// Marker on the Right Lateral Thigh: RTHL (Omar)
CreateMarkerDriverEx RThighLateral (
MarkerName= RThighLateral,
MarkerPlacement =Right.Leg.Seg.Thigh,
OptX="Off",OptY="Off",OptZ="Off",
WeightX=1.0,WeightY=1.0,WeightZ=1.0,
Model1=MotionAndParameterOptimizationModel, Model2=
InverseDynamicModel,
sRelOptScalingOnOff="Off",
ReadsRelOptFromFile = "On",
sRelCustomScalingOnOff = "Off"
)= {
    sRelOpt = {0.0, 0.0, 0.0}; // This is ignored when
ReadsRelOptFromFile = "On"
};
#endif

// Marker on the Right Inferior Thigh: RTIn (Omar)
#ifndef EXCLUDE_MARKER_RTHIGHINFERIOR
CreateMarkerDriverEx RThighInferior (
MarkerName= RThighInferior,
MarkerPlacement =Right.Leg.Seg.Thigh,
OptX="Off",OptY="Off",OptZ="Off",
WeightX=1.0,WeightY=1.0,WeightZ=1.0,

```

```

Model1=MotionAndParameterOptimizationModel, Model2=
InverseDynamicModel,
sRelOptScalingOnOff="Off",
ReadsRelOptFromFile = "On",
sRelCustomScalingOnOff = "Off"
)= {
    sRelOpt = {0.0, 0.0, 0.0}; // This is ignored when
ReadsRelOptFromFile = "On"
};
#endif

// Marker on the Right Superior Shank: RTiS (Omar)
CreateMarkerDriverEx RShankSuperior (
MarkerName= RShankSuperior,
MarkerPlacement=Right.Leg.Seg.Shank,
OptX="Off",OptY="Off",OptZ="Off",
WeightX=1.0,WeightY=1.0,WeightZ=1.0,
Model1=MotionAndParameterOptimizationModel, Model2=
InverseDynamicModel,
sRelOptScalingOnOff="Off",
ReadsRelOptFromFile = "On",
sRelCustomScalingOnOff = "Off"
) = {
    sRelOpt = {0.0, 0.0, 0.0}; // This is ignored when
ReadsRelOptFromFile = "On"
};
#endif EXCLUDE_MARKER_RSHANKLATERAL
CreateMarkerDriverEx RShankLateral (
MarkerName= RShankLateral,
MarkerPlacement=Right.Leg.Seg.Shank,
OptX="Off",OptY="Off",OptZ="Off",
WeightX=1.0,WeightY=1.0,WeightZ=1.0,
Model1=MotionAndParameterOptimizationModel, Model2=
InverseDynamicModel,
sRelOptScalingOnOff="Off",
ReadsRelOptFromFile = "On",
sRelCustomScalingOnOff = "Off"

```

```

) = {
    sRelOpt = {0.0, 0.0, 0.0}; // This is ignored when
ReadsRelOptFromFile = "On"
};
#endif
// Marker on the Right Inferior Shank: RTiI (Omar)
CreateMarkerDriverEx RShankInferior (
MarkerName= RShankInferior,
MarkerPlacement=Right.Leg.Seg.Shank,
OptX="Off",OptY="Off",OptZ="Off",
WeightX=1.0,WeightY=1.0,WeightZ=1.0,
Model1=MotionAndParameterOptimizationModel, Model2=
InverseDynamicModel,
sRelOptScalingOnOff="Off",
ReadsRelOptFromFile = "On",
sRelCustomScalingOnOff = "Off"
) = {
    sRelOpt = {0.0, 0.0, 0.0}; // This is ignored when
ReadsRelOptFromFile = "On"
};

// Left thigh and shank cluster markers:
// Marker on the Left Superior Thigh: LTHAP
#ifndef EXCLUDE_MARKER_LTHIGHSUPERIOR
CreateMarkerDriverEx LThighSuperior (
MarkerName= LThighSuperior,
MarkerPlacement =Left.Leg.Seg.Thigh,
OptX="Off",OptY="Off",OptZ="Off",
WeightX=1.0,WeightY=1.0,WeightZ=1.0,
Model1=MotionAndParameterOptimizationModel, Model2=
InverseDynamicModel,
sRelOptScalingOnOff="On",
ReadsRelOptFromFile = "On",
sRelCustomScalingOnOff = "Off"
)= {
    sRelOpt = {0.0, 0.0, 0.0}; // This is ignored when
ReadsRelOptFromFile = "On"
}

```



```

};
#endif
CreateMarkerDriverEx LThighLateral (
MarkerName= LThighLateral,
MarkerPlacement =Left.Leg.Seg.Thigh,
OptX="Off",OptY="Off",OptZ="Off",
WeightX=1.0,WeightY=1.0,WeightZ=1.0,
Model1=MotionAndParameterOptimizationModel, Model2=
InverseDynamicModel,
sRelOptScalingOnOff="Off",
ReadsRelOptFromFile = "On",
sRelCustomScalingOnOff = "Off"
)= {
    sRelOpt = {0.0, 0.0, 0.0}; // This is ignored when
ReadsRelOptFromFile = "On"
};
CreateMarkerDriverEx LThighInferior (
MarkerName= LThighInferior,
MarkerPlacement =Left.Leg.Seg.Thigh,
OptX="Off",OptY="Off",OptZ="Off",
WeightX=1.0,WeightY=1.0,WeightZ=1.0,
Model1=MotionAndParameterOptimizationModel, Model2=
InverseDynamicModel,
sRelOptScalingOnOff="Off",
ReadsRelOptFromFile = "On",
sRelCustomScalingOnOff = "Off"
)= {
    sRelOpt = {0.0, 0.0, 0.0}; // This is ignored when
ReadsRelOptFromFile = "On"
};

#ifndef EXCLUDE_MARKER_LSHANKSUPERIOR
CreateMarkerDriverEx LShankSuperior (
MarkerName= LShankSuperior,
MarkerPlacement=Left.Leg.Seg.Shank,
OptX="Off",OptY="Off",OptZ="Off",
WeightX=1.0,WeightY=1.0,WeightZ=1.0,

```

```

Model1=MotionAndParameterOptimizationModel, Model2=
InverseDynamicModel,
sRelOptScalingOnOff="On",
ReadsRelOptFromFile = "On",
sRelCustomScalingOnOff = "Off"
) = {
    sRelOpt = {0.0, 0.0, 0.0}; // This is ignored when
ReadsRelOptFromFile = "On"
};
#endif

CreateMarkerDriverEx LShankLateral (
MarkerName= LShankLateral,
MarkerPlacement=Left.Leg.Seg.Shank,
OptX="Off",OptY="Off",OptZ="Off",
WeightX=1.0,WeightY=1.0,WeightZ=1.0,
Model1=MotionAndParameterOptimizationModel, Model2=
InverseDynamicModel,
sRelOptScalingOnOff="Off",
ReadsRelOptFromFile = "On",
sRelCustomScalingOnOff = "Off"
) = {
    sRelOpt = {0.0, 0.0, 0.0}; // This is ignored when
ReadsRelOptFromFile = "On"
};

CreateMarkerDriverEx LShankInferior (
MarkerName= LShankInferior,
MarkerPlacement=Left.Leg.Seg.Shank,
OptX="Off",OptY="Off",OptZ="Off",
WeightX=1.0,WeightY=1.0,WeightZ=1.0,
Model1=MotionAndParameterOptimizationModel, Model2=
InverseDynamicModel,
sRelOptScalingOnOff="Off",
ReadsRelOptFromFile = "On",
sRelCustomScalingOnOff = "Off"
) = {

```

	<pre>sRelOpt = {0.0, 0.0, 0.0}; // This is ignored when ReadsRelOptFromFile = "On" };</pre>
--	---

4. Contact Model:

For this model, three files are configured in sequence (1) ContactSurfacesPreOp.any, (2) ContactForcePreOp.any, (3) ReactionForces.any

Step	Explanation
Defining the contact surface using bone/ cartilage surfaces in ContactSurfacesPreOp: In PreOpSTLNode for the thigh, define the following:	<pre>Thigh = { AnyRefNode PreOpSTLNode = { //Cartilage: AnySurfSTL FemurContactSurf2 = { FileName = "STLs for contacts\Linda_FemCart.stl"; AnyFunTransform3D &scale = ..CustomMarkerScaling; ScaleXYZ = {1,1,-1}/1000; AnyDrawSurf drwSTL = { Visible = On; ScaleXYZ = .ScaleXYZ; FileName = .FileName; AnyFunTransform3D &scale = .scale; RGB = {0, 1.0, 1.0}; }; }; }; };</pre>

```

//Bone offset:
AnySurfSTL FemurContactSurf = {
  FileName = "STLs for contacts\Linda_femur"; //STL contact surface
  ScaleXYZ = {1,1,-1}*1e-3;

  AnyFunTransform3DIdentity Scale = {
    PreTransforms = {&RemoveOffset, &Scale, &AddOffset,
&...CustomMarkerScaling};

    AnyFunTransform3DLin RemoveOffset = {
      ScaleMat =
Main.Studies.HumanModel.BodyModel.Left.Leg.Seg.Thigh.JCSLianne.ARel_us';
      Offset = -
Main.Studies.HumanModel.BodyModel.Left.Leg.Seg.Thigh.JCSLianne.sRel_us;
    };
    AnyFunTransform3DLin Scale = {
      AnyFloatVar Factor = 0.05;
      AnyFloatVar Thickness = 2.14e-3; // the mean *femoral cartilage*
thickness = 2.14 mm, from Cohen et al. (1999)
      ScaleMat = {{1.0 + Factor, 0.0, 0.0}, {0.0, 1.0 + Factor, 0.0},
{0.0, 0.0, 1.0 + Factor*0}};
      Offset = {0.0, 0.0, 0.0};
    };
    AnyFunTransform3DLin AddOffset = {
      ScaleMat = .RemoveOffset.ScaleMat';
      Offset = -.RemoveOffset.Offset*ScaleMat;
    };
  };

  AnyDrawSurf drw = {
    AnyFunTransform3D &Scale = .Scale; //Applying the transformations
above to the contact stl
    FileName = .FileName;
    ScaleXYZ = {1, 1, 1}/1000;
    Opacity = 0.5;
    RGB = {0, 1.0, 1.0}}; }; };

```

Defining the contact surface using bone/ cartilage surfaces in ContactSurfacesPreOp:

In PreOpSTLNode for the lateral and medial shank, define the following:

//Lateral medial contact surface:

```
Shank = {  
  AnyRefNode PreOpSTLNode = {
```

//Cartilage:

```
  AnySurfSTL TibiaLateralContactSurf2 = {  
    FileName = "STLs for contacts\Linda_TibCart_Lateral.stl"; //cut  
    remeshed  
    AnyFunTransform3D &scale = ..CustomMarkerScaling;  
    ScaleXYZ = {1,1,-1}/1000;  
  
    AnyDrawSurf drwSTL = {  
      Visible = On;  
      ScaleXYZ = .ScaleXYZ;  
      FileName = .FileName;  
      AnyFunTransform3D &scale = .scale;  
      RGB = {0.35, 0.35, 0.8};  
    };  
  };  
};
```

//Bone offset:

```
AnySurfSTL TibiaLateralContactSurf = {  
  FileName = "STLs for contacts\Linda_Tibia_LatContact.stl";  
  ScaleXYZ = {1,1,-1}*1e-3;  
  AnyFunTransform3DIdentity Scale = {  
    PreTransforms = {&RemoveOffset, &Scale, &AddOffset,  
&...CustomMarkerScaling};  
    AnyFunTransform3DLin RemoveOffset = {  
      ScaleMat =  
Main.Studies.HumanModel.BodyModel.Left.Leg.Seg.Shank.JCSLianne.ARel_us';  
      Offset = -  
Main.Studies.HumanModel.BodyModel.Left.Leg.Seg.Shank.JCSLianne.sRel_us;  
    };  
    AnyFunTransform3DLin Scale = {  
      AnyFloatVar Factor = 0.1;  
      // AnyFloatVar Thickness = 1.6e-3; // lateral thickness of varus  
      osteoarthritis, from Burgkart R et al. (2001)
```

```
//      AnyFloatVar Thickness = 1.5e-3; // lateral thickness of
mediolateral osteoarthritis, from Burgkart R et al. (2001)
      AnyFloatVar Thickness = 3.13e-3; // lateral thickness of
healthy, from Burgkart R et al. (2001)
      ScaleMat = {{1.0, 0.0, 0.0}, {0.0, 1.0, 0.0}, {0.0, 0.0, 1.0}};
      Offset = {0.0, Thickness, 0.0};
    };
    AnyFunTransform3Dlin AddOffset = {
      ScaleMat = .RemoveOffset.ScaleMat';
      Offset = -.RemoveOffset.Offset*ScaleMat;
    };
  };
  AnyDrawSurf drw = {
    AnyFunTransform3D &Scale = .Scale;
    FileName = .FileName;
    ScaleXYZ = .ScaleXYZ;
    Opacity = 0.5;
    RGB = {0, 0, 1.0};
  };
};
```

//Medial medial contact surface:

//Cartilage:

```
AnySurfSTL TibiaMedialContactSurf2 = {
  FileName = "STLs for contacts\Linda_TibCart_Medial.stl"; //cut
  remeshed
  AnyFunTransform3D &scale = ..CustomMarkerScaling;
  ScaleXYZ = {1,1,-1}/1000;

  AnyDrawSurf drwSTL = {
    Visible = On;
    ScaleXYZ = .ScaleXYZ;
    FileName = .FileName;
    AnyFunTransform3D &scale = .scale;
    RGB = {1.0, 0, 0};
  };
};
```

//Bone offsets;

```
AnySurfSTL TibiaMedialContactSurf = {
  FileName = "STLs for contacts\Linda_Tibia_MedContact.stl";
  ScaleXYZ = {1,1,-1}*1e-3;
  AnyFunTransform3DIdentity Scale = {
    PreTransforms = {&RemoveOffset, &Scale, &AddOffset,
&...CustomMarkerScaling};
    AnyFunTransform3DLin RemoveOffset = {
      ScaleMat =
Main.Studies.HumanModel.BodyModel.Left.Leg.Seg.Shank.JCSLianne.ARel_us';
      Offset = -
Main.Studies.HumanModel.BodyModel.Left.Leg.Seg.Shank.JCSLianne.sRel_us;
    };
    AnyFunTransform3DLin Scale = {
      AnyFloatVar Factor = 0.1;
//      AnyFloatVar Thickness = 1.2e-3; // medial thickness of varus
//      osteoarthritis, from Burgkart R et al. (2001)
//      AnyFloatVar Thickness = 1.0e-3; // medial thickness of
//      mediolateral osteoarthritis, from Burgkart R et al. (2001)
```

```
AnyFloatVar Thickness = 2.56e-3; // medial thickness of healthy,  
from Burgkart R et al. (2001)  
ScaleMat = {{1.0, 0.0, 0.0}, {0.0, 1.0, 0.0}, {0.0, 0.0, 1.0}};  
Offset = {0.0, Thickness, 0.0};  
};  
AnyFunTransform3Dlin AddOffset = {  
ScaleMat = .RemoveOffset.ScaleMat';  
Offset = -.RemoveOffset.Offset*ScaleMat;  
};  
};  
AnyDrawSurf drw = {  
AnyFunTransform3D &Scale = .Scale;  
FileName = .FileName;  
ScaleXYZ = .ScaleXYZ;  
Opacity = 0.5;  
RGB = {1.0, 0, 0};  
};  
};
```


Defining the contact surface using bone/ cartilage surfaces in ContactSurfacesPreOp:

In PreOpSTLNode for the patella, define the following:

```
Patella = {  
  //Cartilage:  
  AnySurfSTL PatellaContactSurf2 = {  
    FileName = "STLs for contacts\Linda_PatellaCartilage.stl";  
    AnyFunTransform3D &scale = ..CustomMarkerScaling;  
    ScaleXYZ = {1,1,-1}/1000;  
  
    AnyDrawSurf drwSTL = {  
      Visible = On;  
      ScaleXYZ = .ScaleXYZ;  
      FileName = .FileName;  
      AnyFunTransform3D &scale = .scale;  
      RGB = {1.0, 0, 0};  
    };  
  };  
};  
  
//Bone offset:  
AnyRefNode PreOpSTLNode = {  
  
  AnySurfSTL PatellaContactSurf = {  
    FileName = "STLs for contacts\Patella preop.stl";  
    ScaleXYZ = {1,1,1}*1e-3;  
    AnyFunTransform3DIdentity Scale = {  
      PreTransforms = {&RemoveOffset, &Scale, &AddOffset,  
&...CustomMarkerScaling};  
    AnyFunTransform3DLin RemoveOffset = {  
      ScaleMat =  
Main.Studies.HumanModel.BodyModel.Left.Leg.Seg.Patella.JCSLianne.ARel_us';  
      Offset = -  
Main.Studies.HumanModel.BodyModel.Left.Leg.Seg.Patella.JCSLianne.sRel_us;  
    };  
    AnyFunTransform3DLin Scale = {  
      AnyFloatVar Factor = 0.1;  
      AnyFloatVar Thickness = 3.08e-3; // mean patellar cartilage  
thickness from Cohen et al. (1999)  
      ScaleMat = {{1.0, 0.0, 0.0}, {0.0, 1.0, 0.0}, {0.0, 0.0, 1.0}};  
      Offset = {-Thickness, 0.0, 0.0};  
    };  
  };  
};
```

```
};  
AnyFunTransform3DLin AddOffset = {  
  ScaleMat = .RemoveOffset.ScaleMat';  
  Offset = -.RemoveOffset.Offset*ScaleMat;  
};  
};  
AnyDrawSurf drw = {  
  AnyFunTransform3D &Scale = .Scale;  
  FileName = .FileName;  
  ScaleXYZ = .ScaleXYZ;  
  Opacity = 0.5;  
  RGB = {1.0, 0, 1.0};  
};  
};  
}};
```

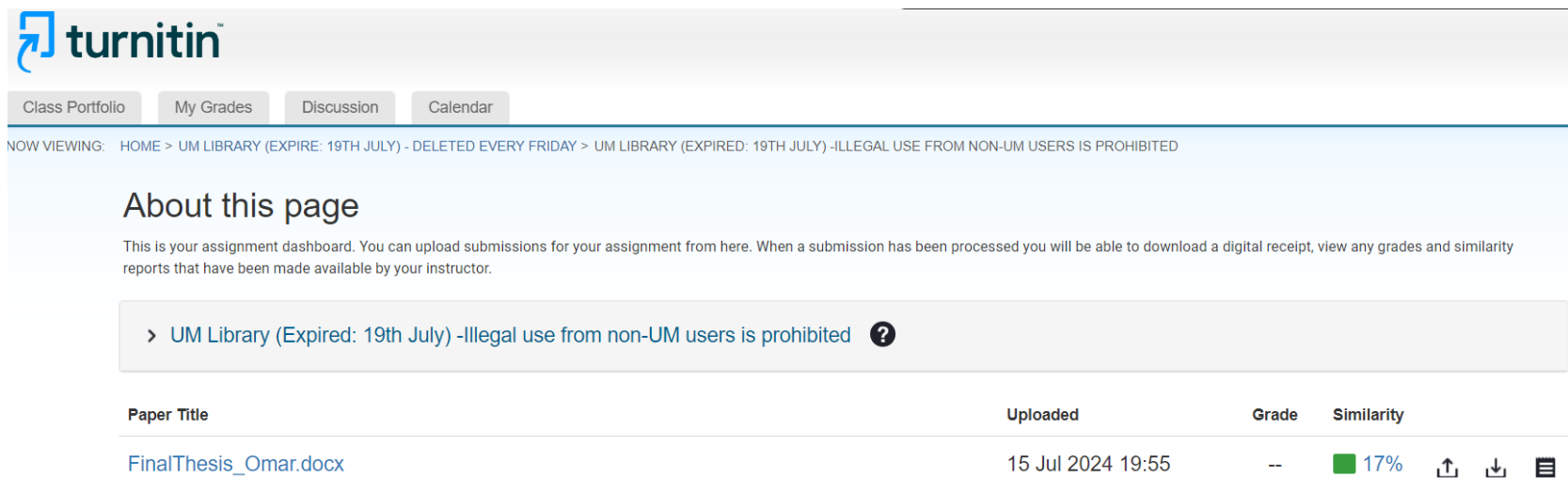
5. Ligament model:

There are four files that you can refer to:




- KneeLigamentGeometry.any
- KneeLigamentGeometry.any
- LineLigamentMeasures.any
- SheetLigamentMeasures.any

4.1 Appendix L: Similarity Index

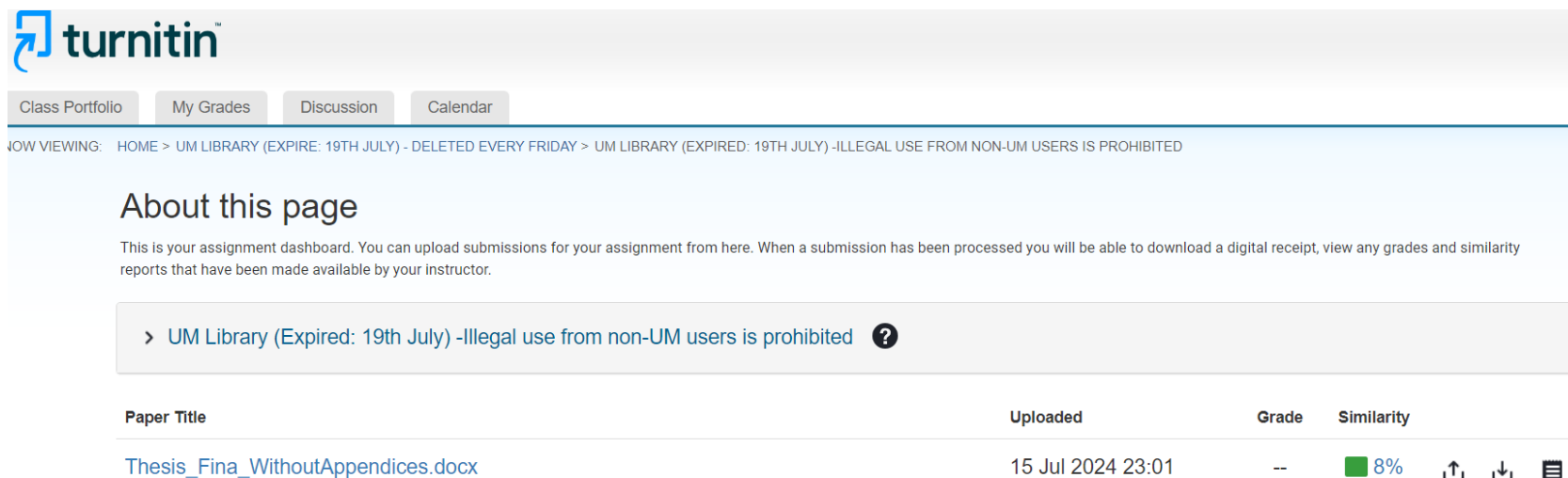
- With the appendices



The screenshot shows the Turnitin assignment dashboard. At the top is the Turnitin logo and navigation tabs: Class Portfolio, My Grades, Discussion, and Calendar. Below the navigation is a breadcrumb trail: HOME > UM LIBRARY (EXPIRE: 19TH JULY) - DELETED EVERY FRIDAY > UM LIBRARY (EXPIRED: 19TH JULY) -ILLEGAL USE FROM NON-UM USERS IS PROHIBITED. The main heading is "About this page" with a subtext: "This is your assignment dashboard. You can upload submissions for your assignment from here. When a submission has been processed you will be able to download a digital receipt, view any grades and similarity reports that have been made available by your instructor." Below this is a notification box: "> UM Library (Expired: 19th July) -Illegal use from non-UM users is prohibited ?". The submission table has the following data:

Paper Title	Uploaded	Grade	Similarity
FinalThesis_Omar.docx	15 Jul 2024 19:55	--	■ 17%   

- Without the appendices



The screenshot shows the Turnitin assignment dashboard. At the top is the Turnitin logo and navigation tabs: Class Portfolio, My Grades, Discussion, and Calendar. Below the navigation is a breadcrumb trail: HOME > UM LIBRARY (EXPIRE: 19TH JULY) - DELETED EVERY FRIDAY > UM LIBRARY (EXPIRED: 19TH JULY) -ILLEGAL USE FROM NON-UM USERS IS PROHIBITED. The main heading is "About this page" with a subtext: "This is your assignment dashboard. You can upload submissions for your assignment from here. When a submission has been processed you will be able to download a digital receipt, view any grades and similarity reports that have been made available by your instructor." Below this is a notification box: "> UM Library (Expired: 19th July) -Illegal use from non-UM users is prohibited ?". The submission table has the following data:

Paper Title	Uploaded	Grade	Similarity
Thesis_Fina_WithoutAppendices.docx	15 Jul 2024 23:01	--	■ 8% 